

**A TIME-DOMAIN CROSS-DIFFERENTIAL  
PROTECTION ALGORITHM FOR DOUBLE  
CIRCUIT TRANSMISSION LINES**

**LETÍCIA ALMEIDA GAMA**

**PHD THESIS  
ON ELECTRICAL ENGINEERING**

**ELECTRICAL ENGINEERING DEPARTMENT**

**TECHNOLOGY FACULTY  
UNIVERSITY OF BRASILIA**

University of Brasilia  
Technology Faculty  
Electrical Engineering Department

**A Time-Domain Cross-Differential Protection Algorithm  
For Double Circuit Transmission Lines**

**Letícia Almeida Gama**

PhD thesis submitted to the Graduate Program in Electrical Engineering at the University of Brasilia, as part of the necessary requirements to obtain the degree of PhD in Electrical Engineering.

APPROVED BY:

---

Prof. Kleber Melo e Silva, D.Sc. (ENE - UnB)  
(Advisor)

---

Prof. José Carlos de Melo Vieira Júnior, D.Sc. (USP - S. Carlos)  
(External Examiner)

---

Prof. Felipe Vigolvino Lopes, D.Sc. (UFPB)  
(External Examiner)

---

Prof. Fernando Cardoso Melo, D.Sc. (ENE - UnB)  
(Internal Examiner)

Brasilia/DF, September 1<sup>st</sup> 2023.

## FICHA CATALOGRÁFICA

GAMA, LETÍCIA ALMEIDA

A Time-Domain Cross-Differential Protection Algorithm For Double Circuit Transmission Lines. [Brasília/Distrito Federal] 2023.

xi, 80p., 210 x 297 mm (ENE/FT/UnB, Doutora, Tese de Doutorado, 2023).

Universidade de Brasília, Faculdade de Tecnologia, Departamento de Engenharia Elétrica.

Departamento de Engenharia Elétrica

- |   |                                       |
|---|---------------------------------------|
| 1. Double-circuit transmission line       | 2. ATP/EMTP                           |
| 3. Time-domain algorithm                  | 4. Electromagnetic transient analysis |
| 5. Cross-differential protection function |                                       |

I. ENE/FT/UnB

II. Título (série)

## REFERÊNCIA BIBLIOGRÁFICA

GAMA, L. A. (2023). A Time-Domain Cross-Differential Protection Algorithm For Double Circuit Transmission Lines. Tese de Doutorado em Engenharia Elétrica, Publicação PPGE 200/23, Departamento de Engenharia Elétrica, Universidade de Brasília, Brasília, DF, 80p.

## CESSÃO DE DIREITOS


AUTORA: Letícia Almeida Gama

TÍTULO: A Time-Domain Cross-Differential Protection Algorithm For Double Circuit Transmission Lines.

GRAU: Doutora em Engenharia Elétrica

ANO: 2023

É concedida à Universidade de Brasília permissão para reproduzir cópias desta tese de doutorado e para emprestar ou vender tais cópias somente para propósitos acadêmicos e científicos. A autora reserva outros direitos de publicação e nenhuma parte desta tese de doutorado pode ser reproduzida sem autorização por escrito da autora.



Letícia Almeida Gama

Departamento de Eng. Elétrica (ENE)

Faculdade de Tecnologia (FT)

Universidade de Brasília (UnB)

Campus Darcy Ribeiro

Brasília - DF CEP 70919-970

## ACKNOWLEDGMENTS

I would like to thank my advisor Professor Kleber M. e Silva for his guidance and long term collaboration through my Masters and PhD journey. All your professional and personal lessons were greatly appreciated professor. Thank you for the friendship.

And to Professor Felipe Vigolvino Lopes, thank you so much for always stimulating me and others at the lab to do more and more research, and helping us see how qualified we are.

I also want to express my gratitude to the members of the thesis defense committee, Professor Jose Carlos de Melo Vieira Junior and Professor Fernando Cardoso Melo, for accepting the invitation to participate in this thesis defense.

I'm very thankful for the immense support provided by my friends and colleagues at Power Systems Protection Lab (LAPSE).

This thesis was part of a program with University of Toronto (UofT) and it was financially supported through a scholarship granted by the Brazilian Coordination for Improvement of Higher Education Personnel - (CAPES). All financial support promoted by CAPES throughout the development of this thesis is greatly acknowledged.

I would like to thank Professor Ali Hooshyar for hosting me at his laboratory, Centre for Applied Power Electronics (CAPE), at UofT, from October 2021 to March 2022.

Lastly, I want to deeply thank my family and friends for being with me through both good and bad times, consistently offering their love and support. I know that without their presence, I wouldn't be where I am at today.

## ABSTRACT

Zero-sequence mutual coupling in double-circuit transmission lines leads to challenges related to protection systems dependability and security. When it comes to protecting double circuit lines, differential and distance protection functions present disadvantages such as the requirement of communication channel and data synchronization, which increases the complexity and cost of the protection scheme implementation, and the presence of underreaching elements, caused by zero-sequence coupling. The solution presented by the cross-protection function is based on only one terminal and it is immune to the effects of zero-sequence coupling. However, its operation is limited by the inherent delay regarding phasor estimation. Thus, this thesis proposes a new cross-differential time domain-based protection algorithm for double circuit transmission lines. For this purpose, concepts of time domain-based incremental elements are combined with the principle of phasor-based cross-differential protection. Incremental replica currents are used for each phase of both circuits of the evaluated double circuit line. Then, operating and restraining currents are obtained similarly to the cross-differential protection function. The ATP/EMTP software was used to simulate a real 200 km 500 kV transmission line subjected to different fault scenarios. The simulated cases were experimentally evaluated using real commercially available relays. In this manner, the performance of the proposed algorithm could be compared with native functions of the relays under analysis. The use of the proposed algorithm results in secure, wide-ranging and fast operations. Thus, adoption of the proposed cross-differential time domain-based algorithm alongside readily available device-embedded protection functions represents a promising and appropriate alternative for protecting double circuit transmission lines.

**Keywords:** Double circuit transmission line, ATP/EMTP, cross-differential protection, time domain protection, incremental replica currents.

## RESUMO

**Título da Tese: Um algoritmo de proteção diferencial transversal no domínio do tempo para linhas de transmissão de circuito duplo.**

A disponibilidade de energia elétrica está ligada ao desenvolvimento socioeconômico da sociedade. No Brasil, o consumo de energia elétrica cresceu 10% em uma década, devido ao progresso tecnológico, além disso, a previsão média de crescimento de carga no Brasil de 2023 a 2027 é de 3,3%. A operação coletiva eficiente dos equipamentos que compõem os sistemas de energia elétrica é essencial para garantir níveis de energia confiáveis e seguros para os consumidores. No entanto, para garantir a continuidade na entrega desse serviço os sistemas de energia elétrica são conduzidos a se expandir, o que geralmente implica num aumento na complexidade do sistema de transmissão, devido à inevitabilidade da construção de linhas de transmissão adicionais. Por contribuírem para aumentar a segurança e a confiabilidade do sistema, há interesse em linhas de transmissão de circuito duplo. No entanto, a proximidade dos circuitos gera acoplamento mútuo, desafiando os esquemas de proteção. Devido à sua grande extensão e exposição climática, as linhas de transmissão são suscetíveis a defeitos. Portanto, sistemas de proteção eficientes são vitais para garantir a integridade dos equipamentos, a estabilidade do sistema e evitar apagões generalizados. A proteção de linhas de transmissão de circuito duplo é crucial para garantir a confiabilidade do sistema elétrico. As abordagens tradicionais, como esquemas de teleproteção e proteção diferencial, dependem da existência de canais de comunicação e sincronização de dados, o que pode aumentar os custos e a complexidade do sistema. Uma alternativa eficaz é a proteção de distância, que opera com base em um único terminal, não depende de comunicações entre terminais, mas pode ter atrasos na detecção de faltas. Uma solução promissora que está sendo investigada é a proteção diferencial cruzada, a qual elimina a dependência de canal de comunicação, mas por necessitar da estimação fasorial pode refletir em atrasos na sua atuação. Dada a crescente demanda por eletricidade, há uma busca contínua por elementos de proteção mais rápidos, como os fundamentados no domínio

do tempo, com o objetivo de assegurar tempos de eliminação de faltas mais curtos e, assim, preservar a estabilidade do sistema elétrico. Nesse contexto, o algoritmo proposto representa uma solução inovadora para a proteção de linhas de circuito duplo. Ele combina a eficácia da proteção diferencial cruzada, conhecida por sua alta cobertura instantânea de proteção, com a agilidade do domínio do tempo, caracterizado por tempos de operação rápidos. O conjunto de entrada do algoritmo proposto é composto por correntes secundárias provenientes do TCS instalado em cada fase, no mesmo terminal, para ambos os circuitos da linha de transmissão do circuito duplo em análise. Esses sinais são normalizados na mesma base, a fim de eliminar as diferenças na relação de transformação dos TCS e nos parâmetros da linha, para os casos em que os circuitos não compartilham a mesma torre de transmissão. Após a normalização, novos sinais de corrente são inseridos diretamente no bloco de cálculo de valor incremental, geralmente chamado de filtro delta. Para eliminar os efeitos da componente CC de decaimento exponencial, são calculadas correntes de réplica incremental. Após esse procedimento, as correntes de operação e restrição são obtidas de maneira analogada à função de proteção diferencial cruzada e condições de operação são avaliadas. Para facilitar isso, as condições examinadas são integradas e referidas como energias operacionais dos circuitos 1 e 2. Ao mesmo tempo, um sinal senoidal, que representa a corrente de *pickup* escolhida, também é integrado. Finalmente, o bloco que representa a lógica de *trip* usa as quantidades integradas como entrada, para que o elemento diferencial proposto determine se um comando de *trip* deve ser emitido ou não. Dos resultados percebe-se que o desempenho do algoritmo proposto não é afetado pela variação da intensidade do acoplamento de sequência zero entre os circuitos. O algoritmo proposto exibiu também um desempenho superior em relação ao tempo de operação e à cobertura de proteção instantânea da linha de transmissão, mesmo em cenários com variações na localização da falta e na força das fontes. Além disso, o algoritmo não tem seu desempenho prejudicado pela variação da resistência de falta, ao considerar a faixa de avaliação avaliada, e opera corretamente para todos os casos simulados. Notavelmente, sua operação não requer comunicação entre os terminais da linha de transmissão nem a utilização de sinal GPS e sincronização de dados, por utilizar dados provenientes de um único terminal.

**Palavras-chave:** Linha de transmissão de circuito duplo, ATP/EMTP, proteção diferencial cruzada, proteção no domínio do tempo, corrente réplica incremental.

# CONTENTS

<b>Table of contents</b>	i
<b>List of figures</b>	iv
<b>List of tables</b>	vii
<b>List of symbols</b>	viii
<b>Glossary</b>	xi
<b>Chapter 1 – Introduction</b>	1
1.1 Background . . . . .	1
1.2 Motivation . . . . .	2
1.3 Objectives and Contributions . . . . .	3
1.4 Publications . . . . .	4
1.5 Thesis Structure . . . . .	6
<b>Chapter 2 – Fundamentals</b>	7
2.1 Parallel Transmission Line . . . . .	7
2.1.1 Zero Sequence Mutual Coupling Effect . . . . .	8
2.2 Phasor-Based Transmission Line Protection . . . . .	12
2.2.1 Cross-Differential Protection . . . . .	12
2.2.2 Cross-Differential Protection Numerical Example . . . . .	15
2.3 Time-Domain-Based Transmission Line Protection . . . . .	22
2.3.1 Incremental Quantities . . . . .	23
2.3.2 Replica Current Concept . . . . .	24
2.3.3 Integrated Torque for Overcurrent Supervision Element . . . . .	26
2.4 Evaluated Functions . . . . .	27
2.4.1 Phasor Domain Distance Protection Function . . . . .	27
2.4.2 Time Domain Distance Protection Function . . . . .	29



<b>Chapter 3 – State of the Art</b>	<b>31</b>
3.1 Protection of Double Circuit Transmission Lines . . . . .	31
3.2 Time Domain Protection . . . . .	35
3.3 Chapter Summary . . . . .	37
<b>Chapter 4 – Proposed Algorithm</b>	<b>39</b>
4.1 Proposed Formulation . . . . .	39
4.1.1 Currents Normalization . . . . .	40
4.1.2 Incremental Currents . . . . .	41
4.1.3 Incremental Replica Currents . . . . .	42
4.1.4 Operating and Restraining Currents . . . . .	42
4.1.5 Operating Torque . . . . .	43
4.1.6 Starting Unit . . . . .	43
4.1.7 Integrated Operating Conditions . . . . .	44
4.1.8 Trip Logic . . . . .	44
4.1.9 General Description of the Proposed Algorithm . . . . .	45
<b>Chapter 5 – Results and Discussions</b>	<b>47</b>
5.1 Test Power System . . . . .	47
5.2 Test Infrastructure . . . . .	49
5.3 Adaptations Employed During Testing Procedures . . . . .	50
5.4 Experimental Evaluations . . . . .	51
5.4.1 Transient Short-Circuit Analysis . . . . .	51
5.4.2 Zero-sequence Mutual Coupling Variation Analysis . . . . .	55
5.4.2.1 Mutual Coupling Variation for Faults in 50% of Circuit 1 . . . . .	55
5.4.2.2 Mutual Coupling Variation for Faults in 70% of Circuit 1 . . . . .	56
5.4.3 Parametric Sensitivity Fault Analysis . . . . .	58
5.4.3.1 Case 01: Fault Location Variation - Considering Strong Local Source and Weak Remote Source . . . . .	60
5.4.3.2 Case 02 - Fault Location Variation - Considering Strong Local Source and Weaker Remote Source . . . . .	62
5.4.3.3 Case 03: Fault Location Variation - Considering Local and Re- mote Sources as Strong . . . . .	63
5.4.3.4 Case 04: Fault Location Variation - Considering Local and Re- mote Sources as Strong and Fault Resistance . . . . .	64
5.4.3.5 Case 05: Fault Resistance Variation - Solid SLG Phase A Fault in 1% of Circuit 1 . . . . .	66

---

5.4.3.6	Case 06: Fault Resistance Variation - Solid SLG Phase A Fault in 50% of Circuit 1 . . . . .	67
5.4.3.7	Case 07: Fault Resistance Variation - Solid SLG Phase A Fault in 30% of Circuit 1 . . . . .	68
5.4.3.8	Case 08: Fault Resistance Variation - Solid SLG Phase A Fault in 30% of Circuit 1 . . . . .	69
5.5	Additional Remarks . . . . .	71
<b>Chapter 6 – Conclusions and Future Investigations</b>		<b>73</b>
<b>References</b>		<b>75</b>

## LIST OF FIGURES

2.1	Zero-sequence mutual coupling presence on double circuit transmission lines. . .	10
2.2	Cross-differential relay connection. . . . .	12
2.3	Test system for exemplification of cross-differential operating modes. . . . .	16
2.4	Superposition theorem. . . . .	23
2.5	Pure fault circuit. . . . .	25
2.6	Incremental replica - correction of inductive characteristic. . . . .	26
2.7	Overcurrent supervision. . . . .	27
2.8	Impedance trajectory on R-X diagram for mho and quadrilateral characteristics.	29
2.9	Operation principle of the time-domain distance protection function. . . . .	30
4.1	Proposed algorithm's integrated operating condition comparison. . . . .	45
4.2	Proposed time domain cross-differential protection algorithm flowchart. . . . .	46
5.1	Test System. . . . .	47
5.2	Setup implemented for simulation procedures. . . . .	49
5.3	Local terminal without CT saturation. . . . .	52
	(a) Circuit 1 . . . . .	52
	(b) Circuit 2 . . . . .	52
5.4	Remote terminal without CT saturation. . . . .	53
	(a) Circuit 1 . . . . .	53
	(b) Circuit 2 . . . . .	53

5.5	Remote terminal without CT saturation. . . . .	54
(a)	Circuit 1 . . . . .	54
(b)	Circuit 2 . . . . .	54
5.6	Operation time of evaluated functions in comparison with the proposed algorithm.	54
(a)	Local terminal . . . . .	54
(b)	Remote terminal . . . . .	54
5.7	Position and distance between cables on the evaluated transmission tower. . . .	55
5.8	Zero-sequence mutual coupling variation for solid faults on circuit 1 at 50% of the line. . . . .	56
5.9	Zero-sequence mutual coupling variation for faults on circuit 1 at 50% of the line, considering 25 $\Omega$ resistance. . . . .	57
5.10	Zero-sequence mutual coupling variation for faults on circuit 1 at 50% of the line, considering 50 $\Omega$ resistance. . . . .	57
5.11	Transient analysis of SLG fault on circuit 1 at 50% of the line, considering 25 $\Omega$ resistance. . . . .	58
5.12	Zero-sequence mutual coupling variation for solid faults on circuit 1 at 70% of the line. . . . .	58
5.13	Zero-sequence mutual coupling variation for faults on circuit 1 at 70% of the line, considering 25 $\Omega$ resistance. . . . .	59
5.14	Zero-sequence mutual coupling variation for faults on circuit 1 at 70% of the line, considering 50 $\Omega$ resistance. . . . .	59
5.15	Transient analysis of SLG fault on circuit 1 at 70% of the line, considering 25 $\Omega$ resistance. . . . .	60
5.16	Case 01 - Fault location variation for a solid SLG fault on phase A of circuit 1, considering $F_L = 1.0$ and $F_R = 2.5$ . . . . .	61
5.17	Case 02 - Fault location variation for a solid SLG fault on phase A of circuit 1, considering $F_L = 1.0$ and $F_R = 5.0$ . . . . .	62

---

5.18	Case 03 - Fault location variation for a solid SLG fault on phase A of circuit 1, considering $F_L = 1.5$ and $F_R = 1.5$ . . . . .	64
5.19	Case 04 - Fault location variation for a SLG fault on phase A of circuit 1 with fault resistance of $50 \Omega$ , considering $F_L = 1.5$ and $F_R = 1.5$ . . . . .	65
5.20	Case 05 - Fault resistance variation for a SLG fault on phase A of circuit 1 with fault location of 1%, considering $F_L = 1.5$ and $F_R = 1.5$ - Local terminal results.	66
5.21	Case 06 - Fault resistance variation for a SLG fault on phase A of circuit 1 with fault location of 50%, considering $F_L = 1.0$ and $F_R = 5.0$ - Local terminal results.	67
5.22	Case 06 - Fault resistance variation for a SLG fault on phase A of circuit 1 with fault location of 50%, considering $F_L = 1.0$ and $F_R = 5.0$ - Remote terminal results. . . . .	67
5.23	Case 07 - Fault resistance variation for a SLG fault on phase A of circuit 1 with fault location of 30%, considering $F_L = 1.5$ and $F_R = 1.5$ - Local terminal results.	68
5.24	Case 07 - Fault resistance variation for a SLG fault on phase A of circuit 1 with fault location of 30%, considering $F_L = 1.5$ and $F_R = 1.5$ - Remote terminal results. . . . .	69
5.25	Case 08 - Fault resistance variation for a SLG fault on phase A of circuit 1 with fault location of 30%, considering $F_L = 1.0$ and $F_R = 5.0$ - Local terminal results.	70
5.26	Case 08 - Fault resistance variation for a SLG fault on phase A of circuit 1 with fault location of 30%, considering $F_L = 1.0$ and $F_R = 5.0$ - Remote terminal results. . . . .	70

## LIST OF TABLES

3.1	Summary of literature review topics of research and comparison with the ones covered by the proposed algorithm. . . . .	38
4.1	Advantages of the proposed algorithm. . . . .	40
5.1	Considered cases for the transient analysis evaluation. . . . .	51
5.2	Considered cases for the zero-sequence coupling variation analysis. . . . .	56
5.3	Considered cases for the parametric sensitivity analysis evaluation. . . . .	59

## LIST OF SYMBOLS

$a$	Symmetrical components transformation operator.
$\Delta i$	Instantaneous incremental current.
$\Delta i_{L1}$	Circuit 1 instantaneous incremental current.
$\Delta i_{L2}$	Circuit 2 instantaneous incremental current.
$\Delta i_{opL1}$	Circuit 1 incremental operating current.
$\Delta i_{opL2}$	Circuit 2 incremental operating current.
$\Delta i_{resL1}$	Circuit 1 incremental restraining current.
$\Delta i_{resL2}$	Circuit 2 incremental restraining current.
$\Delta i_z$	Instantaneous replica incremental current.
$\Delta i_{zL1}$	Circuit 1 instantaneous replica incremental current.
$\Delta i_{zL2}$	Circuit 2 instantaneous replica incremental current.
$\Delta \hat{I}_1$	Circuit 1 superimposed current phasor.
$\Delta \hat{I}_2$	Circuit 2 superimposed current phasor.
$\Delta s$	Instantaneous incremental element.
$\Delta v$	Instantaneous incremental voltage.
$\mathbf{A}$	Fortescue transformation matrix.
$E_{opL1}$	Circuit 1 operating energy.
$E_{opL2}$	Circuit 2 operating energy.
$E_{pk}$	Energy pickup.
$F_L$	Source strength at local terminal of the transmission line.

---

$F_R$	Source strength at remote terminal of the transmission line.
$G_1$	Circuit 1 compensation factor.
$G_2$	Circuit 2 compensation factor.
$\hat{I}_{0M}$	Parallel circuit zero-sequence current phasor.
$i_{L1}$	Circuit 1 normalized instantaneous current.
$i_{L2}$	Circuit 2 normalized instantaneous current.
$i_{pri1}$	Circuit 1 instantaneous primary current.
$i_{pri2}$	Circuit 2 instantaneous primary current.
$i_{TC1}$	Circuit 1 instantaneous secondary current.
$i_{TC2}$	Circuit 2 instantaneous secondary current.
$I_{op}$	Operating current.
$I_{res}$	Restraining current.
$I_{pickup}$	Pickup current.
$\hat{I}_1$	Circuit 1 current phasor.
$\hat{I}_2$	Circuit 2 current phasor.
$\hat{I}_{1,pre}$	Circuit 1 pre-fault current phasor.
$\hat{I}_{2,pre}$	Circuit 2 pre-fault current phasor.
$L_L$	Inspected line local equivalent positive-sequence inductance.
$m$	Distance protection reach.
$N$	Number of samples per cycle.
$p$	Number of cycles chosen for incremental element duration.
$R_L$	Inspected line local equivalent positive-sequence resistance.
$SLP$	Slope value.
$s$	Instantaneous measured signal.



$T$	Fundamental period of the measured signal.
$T_{opL1}$	Circuit 1 operating torque.
$T_{opL2}$	Circuit 2 operating torque.
$TAP_1$	Circuit 1 current normalization tap.
$TAP_2$	Circuit 2 current normalization tap.
$\hat{V}_{0M}$	Zero-sequence mutual coupling induced voltage.
$\hat{V}_{A,expected}$	Phase A voltage measured at single circuit.
$\hat{V}_{A,measured}$	Phase A voltage measured at faulty double circuit.
$K$	Cross-differential percentage sensitivity coefficient.
$Z_{\phi\gamma}$	Phase element positive-sequence impedance.
$Z_{\phi T}$	Ground element positive-sequence impedance.
$\mathbf{Z}_{012}$	Sequence impedance matrix of the transmission line.
$Z_{0M}$	Zero-sequence mutual coupling impedance.
$\mathbf{Z}_{ABC}$	Phase impedance matrix of the transmission line.
$Z_G$	Ground mode impedance.
$Z_{IL}$	Inter-line mode impedance.
$Z_L$	Line mode impedance.
$Z_m$	Mutual impedance between conductors.
$Z_p$	Inter-circuit coupling impedance.
$Z_s$	Self impedance of a conductor.
$Z_{L1}$	Circuit 1 positive-sequence impedance.
$Z_{L2}$	Circuit 2 positive-sequence impedance.
$Z_{TL,0}$	Transmission line zero-sequence impedance.
$Z_{TL,1}$	Transmission line positive-sequence impedance.

## GLOSSARY

21TD	Time domain distance protection function
21PD	Phasor distance protection function
87L	Line differential protection function
87CD	Cross-differential protection function
ATP	Alternative transients program
COMTRADE	Common format for transient data exchange
CT	Current transformer
CTR	Current transformer ratio
CVT	Capacitive voltage transformer
DC	Direct current
DTT	Direct transfer trip
EMTP	Electromagnetic transients program
EPE	Energy research company
LCC	Line/Cable Constants
RTDS	Real time digital simulator
TL	Transmission line
UnB	University of Brasilia

### 1.1 BACKGROUND

Electrical energy availability and consumption are closely related to technological and socioeconomic development of the human society (ANEEL, 2008). According to the Energy Research Company (EPE), the consumption of electrical power in Brazil in the last 10 years has grown by approximately 10%, resulting from the constant technological development of society (EPE, 2023). Despite the 4.5% decline detected on primary energy consumption in 2020 during lockdown imposition all over the world, renewable energy has had its demand increased significantly (BP, 2021; BP, 2022). Additionally, the average annual load growth forecast for the 2023-2027 period in Brazil is at 3.3% (ONS, 2023).

Electrical power systems are described as large interconnected systems that combine different electrical equipment to generate, transfer and consume electrical energy. Efficient collective operation of those equipment is necessary to ensure reliable and safe energy levels for consumers. However, in order to guarantee continuity of power supply, in view of significant load growth, electric power systems are driven to expand.

Among the elements that the electrical power system consists of, transmission lines portray the fundamental purpose of connecting power generation plants to load centers. Furthermore, considering the need to expand the electrical system, development of new projects commonly implies an increase in the complexity of the transmission system, due to the inevitability of constructing additional lines (ZIEGLER, 2012). Therefore, ensuring the continuous and reliable operation of this equipment is essential to preserve the electrical system functionality. In this sense, there is interest in double circuit transmission lines, since they contribute to increasing safety and reliability of the system (HOROWITZ; PHADKE, 2008; SANAYE-PASAND; JAFARIAN, 2011).

Double circuit transmission lines provide advantages related to high electrical power transfer capacity, lower environmental impact and implementation cost, since there are two circuits sharing the same tower (BO *et al.*, 2003; SANTOS, 2008; SANAYE-PASAND; JAFARIAN, 2011). On the other hand, the proximity between circuits leads to the arising of mutual coupling and its effects, which bring challenges to protection schemes (APOSTOLOV *et al.*, 2007). In addition, as a result of its large extent and consequently greater exposure to adverse climatic conditions, transmission lines are highly susceptible to failures. Therefore, it is essential to have efficient and reliable double circuit transmission line protection schemes, capable of clearing and isolating faults rapidly, to ensure equipment integrity, stability of the electrical system and to avoid widespread blackouts (BO *et al.*, 2003; APOSTOLOV *et al.*, 2007).

## 1.2 MOTIVATION

Considering double circuit transmission line unit protection, distance elements associated with pilot schemes and line differential protection schemes are frequently employed. Despite being bold, their operation depend on the availability of communication channel and data synchronization. If these requirements are not met, data loss and time delay can be experienced. This drawback indicates an increase in cost and complexity of the protection scheme. Therefore, the employment of a protection function that does not require information exchanges between line terminals is desirable.

In this sense, double circuit transmission lines must be protected by non-unity functions, among which distance elements are frequently selected. As a single terminal based scheme, distance protection is inherently non-dependent of communication channel and data synchronization. However, its instantaneous operation, i.e operation with no intentional time delay, can only take place when a fault is detected within its first zone, usually set as 70% of the line (SEL, 2015). Therefore, fault clearing time increases because the first relay detects the fault in the first distance zone while the relay on the other line terminal detects the fault only within the second distance zone, specially due to zero-sequence coupling between circuits which causes underreaching (APOSTOLOV *et al.*, 2007; ZIEGLER, 2006). Also, under and overreach results in a smaller overlapped operating area, considering inputs from both line ends relays.

Therefore, despite not being readily available in commercial relays so far, cross-differential protection is introduced as a promising solution for protecting double circuit transmission lines and meeting demands of a growing electrical system. Since it was created to overcome drawbacks presented by most commonly used protection functions, it does not depend on communication channels availability, GPS or data synchronization and it is immune to zero-sequence mutual coupling effects (MCLAREN *et al.*, 1997; ROBERTS *et al.*, 2001). Cross-differential protection's basic principle of operation is to compare currents measured from both circuits at a single terminal of the double circuit line. If the difference between magnitudes is greater than a pre-set threshold, a fault is detected.

Regardless of advantages brought by cross-differential protection, its operation is limited by phasor estimation and its inherent delay. Moreover, constant electricity demand increase created challenges for power systems operation. Transmission lines often need to operate closer to their stability limits in order to meet the load increase (ANDERSON; FOUAD, 2008). Since power transfer capacity is directly related to fault clearing time, and consequently to electrical systems stability, there is a demand for faster protection elements (EASTVEDT, 1976). In this sense, time domain protection elements have become an alternative to speed up fault clearing times.

### 1.3 OBJECTIVES AND CONTRIBUTIONS

The primary objective of this thesis is to introduce a novel time domain cross-differential protection algorithm for double-circuit transmission lines, developed considering current market trends, that demonstrate a promising performance when compared to existing alternatives. Therefore, the following elements are outlined as specific objectives:

- Develop a protection algorithm that combines communication channel independency and zero-sequence coupling immunity with short operating times by using incremental replica currents and by adapting cross-differential protection operating and restraining formulation to the time domain.
- Conduct a comprehensive comparative assessment between commercially available protection functions and the proposed algorithm. This analysis includes the identification of

benefits and drawbacks related to each approach, thereby supporting the interest behind the developed method's significance.

The contributions of this thesis are equivalent to advantages that the proposed algorithm has when compared to functions usually employed to protect double circuit transmission lines, and are listed below:

- Safe and fast performance – compatible with the expectations of protection functions in the time domain – obtained through the use of the proposed algorithm's operating conditions;
- Greater sensitivity in the detection of short-circuits considering different fault resistance values – consistent with the use of incremental elements – as well as robustness considering the correct operation for different source strengths;
- Greater instantaneous coverage of the protected double circuit transmission line – in line with the principle of cross-differential protection without needing data synchronization and exchange through communication channels between line terminals.

## 1.4 PUBLICATIONS

With respect to publications made during the development of this thesis research, the following papers are listed.

### **Journal papers directly related to the thesis research:**

- GAMA, L.A.; ALMEIDA, M. L. S.; HONORATO, T. R.; SERPA, V. R.; SILVA, K. M. "Mathematical and experimental evaluation of an incremental differential protection function embedded in a real transmission line relay", in *Electric Power Systems Research*, vol. 196, pp. 1-8, 2021. ISSN 0378-7796. DOI 10.1016/j.epsr.2021.107158.

**Other publications:**

- DANTAS, K. M. C.; LOPES, F. V.; SILVA, K.M.; COSTA, F. B.; RIBEIRO, N. S. S.; **GAMA, L. A.** "Leveraging existing relays to improve single phase auto-reclosing", in *Electric Power Systems Research*, vol. 212, pp. 1-8, 2022. ISSN 0378-7796. DOI 10.1016/j.epsr.2022.108457.
- LOPES, F. V.; COSTA, J. S.; HONORATO, T. R.; TOLEDO, R. T.; **GAMA, L. A.**; PEREIRA, P. S. et al. "Busbar capacitance modeling effects during relay testing procedures for transmission lines interconnecting wind power plants", in *J Control Autom Electr Syst*, vol. 33, pp. 541-549, 2022. ISSN 2195-3899. DOI 10.1007/s40313-021-00831-9.
- COSTA, J. S.; **GAMA, L. A.**; TOLEDO, R. T.; SANTOS, G. B.; LOPES, F. V.; PEREIRA, P. S. et al., "Análise de transitórios de falta em linha de transmissão considerando conexão de parque eólico interfaceado por conversores", in *12th Seminar on Power Electronics and Control (SEPOC)*, Natal - Brazil, 2019. pp. 1-4.
- COSTA, J. S.; TOLEDO, R. T. ; **GAMA, L. A.**; SANTOS, G. B.; LOPES, F. V.; PEREIRA, P. S. et al., "Investigation on full-converter-based wind power plant behavior during short-circuits", in *2019 Workshop on Communication Networks and Power Systems (WCNPS)*, Brasilia - Brazil, IEEE Xplore, 2019, pp. 1-4. DOI 10.1109/WCNPS.2019.8896241.
- LOPES, F. V.; COSTA, J. S.; HONORATO, T. R.; TOLEDO, R. T.; **GAMA, L. A.**; PEREIRA, P. S. et al., "Transmission line protection performance in the presence of wind power plants: Study on the busbar capacitance modeling during relay testing procedures", in *VIII Simpósio Brasileiro de Sistemas Elétricos (SBSE)*, Santo André - Brazil: SBA, 2020, pp. 1-4. DOI 10.48011/sbse.v1i1.2184.
- COSTA, J. S.; TOLEDO, R. T.; **GAMA, L. A.**; HONORATO, T. R.; LOPES, F. V.; PEREIRA, P. S. et al., "Phasor-based and time-domain Transmission line protection considering wind power integration", in *15th International Conference on Developments in Power System Protection (DPSP)*, Liverpool - England: IEEE Xplore, 2020, pp. 1-6. DOI 10.1049/cp.2020.0012.

The paper titled “Mathematical and experimental evaluation of an incremental differential protection function embedded in a real transmission line relay” was the winner of Best Young Researcher Award at the 14th International Conference on Power Systems Transients (IPST) in June 2021.

## 1.5 THESIS STRUCTURE

The organization of this thesis is carried out according to the following structure.

**Chapter 2** portrays concepts and problems of double circuit lines, alongside cross-differential protection and time domain protection principles. In addition, distance elements, later depicted for performance evaluation, are briefly presented.

**Chapter 3** presents a literature review carried out considering two separate topics: cross-differential protection of double circuit transmission lines and evolution of time domain protection techniques.

**Chapter 4** details the proposed algorithms procedures and displays it as a flowchart for better understanding.

**Chapter 5** presents the results and analyzes of experimental tests carried out and implemented in real devices using suitable equipment for testing.

**Chapter 6** discloses the final considerations and proposals for future researches related to the continuity of this topic’s research.



This chapter introduces concepts related to double circuit transmission line, as well as problems associated with its operation. Phasor and time domain-based protection theory and aspects are presented in order to support important formulations considered in the development of this thesis. In addition, phasor domain and time domain distance protection functions were chosen for performance evaluation comparison since they are commonly employed for transmission lines protection. In this sense, basics of both functions in question are also presented.

### 2.1 PARALLEL TRANSMISSION LINE

In literature, concepts of parallel lines and double circuit lines can sometimes be mistaken, so it is important to highlight the definition adopted in this work. It is common to notice the presence of double circuit tower transmission lines in the electrical system. However, other configurations can also be found, such as two single circuit tower transmission lines which can share the same right of way partially or entirely. Both are examples of parallel lines that suffer from effects of mutual coupling.

Parallel transmission lines are employed to meet the growing electrical energy demand, considering space limitations, while maintaining its security and reliability (HU *et al.*, 2009). Depending on the connections chosen at both line ends and the system topology, parallel transmission lines can have the following configurations (APOSTOLOV *et al.*, 2007):

- Share the same bus at both line ends;
- Share the same bus at just one of the line ends;
- Do not share the same bus at either line ends.

In cases where circuits operate at different voltage levels, there are more possible configurations for parallel lines, which are transmission lines considering circuits connected at the same substation for both line terminals, for only one of the terminals or for none of the terminals (APOSTOLOV *et al.*, 2007). Among all possible arrangements, double circuit transmission line represents the most discussed and examined, so for that reason it is the one considered in this thesis (CALERO, 2007).

### 2.1.1 Zero Sequence Mutual Coupling Effect

Although they have already proven to be an efficient way to guarantee high levels of electrical power transfer, in addition to decreasing environmental impacts and implementation costs, double circuit transmission lines still bring challenges and add complexity for protection systems (BO *et al.*, 2003; SANTOS, 2008; SANAYE-PASAND; JAFARIAN, 2011). Double circuit lines are subject to the effects of magnetic mutual induction between its circuits. Depending on the transposition scheme adopted, positive- and negative-sequence mutual coupling values verified in the double circuit line are very small and therefore usually neglected. However, for zero-sequence mutual coupling, values commonly range from 50% to 70% of the transmission line self impedance (APOSTOLOV *et al.*, 2007). Having significantly high mutual coupling value influences the ground elements of protection functions, considering its relation to zero-sequence quantities (TZIOUVARAS *et al.*, 2014; CALERO, 2007).

The impedance matrix portrays self and mutual coupling effects detected in the transmission network. Mathematically, the phase impedance matrix,  $\mathbf{Z}_{ABC}$ , of a double circuit line or two parallel single circuit lines, considering any arrangement of conductors, is given by (CALERO, 2007):

$$\mathbf{Z}_{ABC} = \begin{bmatrix} Z_{aa} & Z_{ab} & Z_{ca} & Z_{aa'} & Z_{ab'} & Z_{c'a} \\ Z_{ab} & Z_{bb} & Z_{bc} & Z_{ba'} & Z_{bb'} & Z_{bc'} \\ Z_{ca} & Z_{bc} & Z_{cc} & Z_{ca'} & Z_{b'c} & Z_{cc'} \\ Z_{aa'} & Z_{a'b} & Z_{ca'} & Z_{a'a'} & Z_{a'b'} & Z_{c'a'} \\ Z_{ab'} & Z_{bb'} & Z_{b'c} & Z_{a'b'} & Z_{b'b'} & Z_{b'c'} \\ Z_{c'a} & Z_{bc'} & Z_{cc'} & Z_{c'a'} & Z_{b'c'} & Z_{c'c'} \end{bmatrix} \quad (2.1)$$

where, self and mutual impedance between conductors  $i$  and  $j$  are represented by  $Z_{ii}$  and  $Z_{ij}$ , considering phases a, b, c for circuit 1 and a', b', c' for circuit 2.

Transmission lines are mainly described and analyzed through their sequence elements.

For balanced transmission lines, using symmetrical components is simpler because equations that represent the transmission network, and are coupled in the phase domain, can become decoupled after transformation. Phase impedance values are transformed and sequence domain matrix,  $\mathbf{Z}_{012}$ , is obtained according to the formulation outlined in (2.2)-(2.6) (DOMMEL; BHATTACHARYA, 1992; TZIOUVARAS *et al.*, 2014; CALERO, 2007).

$$\begin{bmatrix} V_{ABC} \\ V_{ABC'} \end{bmatrix} = \mathbf{Z}_{ABC} \cdot \begin{bmatrix} I_{ABC} \\ I_{ABC'} \end{bmatrix} \quad (2.2)$$

$$\begin{bmatrix} \mathbf{A} & [0] \\ [0] & \mathbf{A} \end{bmatrix} \cdot \begin{bmatrix} V_{012} \\ V_{012'} \end{bmatrix} = \mathbf{Z}_{ABC} \cdot \begin{bmatrix} \mathbf{A} & [0] \\ [0] & \mathbf{A} \end{bmatrix} \cdot \begin{bmatrix} I_{012} \\ I_{012'} \end{bmatrix} \quad (2.3)$$

$$\begin{bmatrix} V_{012} \\ V_{012'} \end{bmatrix} = \begin{bmatrix} \mathbf{A} & [0] \\ [0] & \mathbf{A} \end{bmatrix}^{-1} \cdot \mathbf{Z}_{ABC} \cdot \begin{bmatrix} \mathbf{A} & [0] \\ [0] & \mathbf{A} \end{bmatrix} \cdot \begin{bmatrix} I_{012} \\ I_{012'} \end{bmatrix} \quad (2.4)$$

$$\begin{bmatrix} V_{012} \\ V_{012'} \end{bmatrix} = \mathbf{Z}_{012} \cdot \begin{bmatrix} I_{012} \\ I_{012'} \end{bmatrix} \quad (2.5)$$

$$\mathbf{Z}_{012} = \begin{bmatrix} \mathbf{A} & [0] \\ [0] & \mathbf{A} \end{bmatrix}^{-1} \cdot \mathbf{Z}_{ABC} \cdot \begin{bmatrix} \mathbf{A} & [0] \\ [0] & \mathbf{A} \end{bmatrix}, \quad (2.6)$$

in which,  $\mathbf{A}$  is the Fortescue matrix considering the ABC 3-phase sequence,  $[0]$  the null matrix and  $a$  the complex operator, defined by:

$$\mathbf{A} = \begin{bmatrix} 1 & 1 & 1 \\ 1 & a^2 & a \\ 1 & a & a^2 \end{bmatrix}, \quad [0] = \begin{bmatrix} 0 & 0 & 0 \\ 0 & 0 & 0 \\ 0 & 0 & 0 \end{bmatrix}, \quad \text{and} \quad a = e^{j120^\circ} \quad (2.7)$$

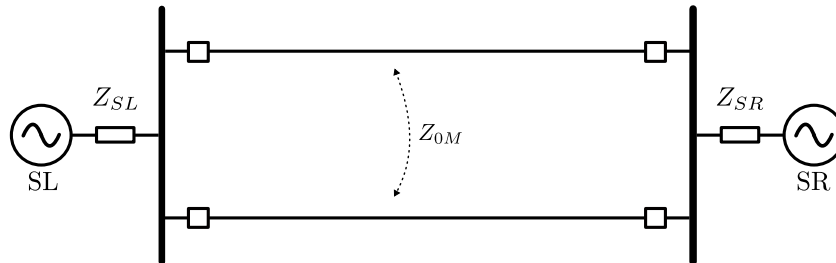
Different phase arrangements affect transmission line impedance values, which can result in imbalances, causing the self-impedance elements of the impedance matrix to differ as well as the mutual impedance elements (CALERO, 2007). Transposition schemes are employed to attain a more balanced network. A transmission line is considered transposed when phase conductors positions are rearranged in a regular sequence and at a specific interval. Conductors physical position should be altered at the same distance for  $3^n$  times, considering  $n$  the number of circuits, for a transmission line to be totally transposed. Thus, for a double circuit line there must be 9 transposition sections (DOMMEL; BHATTACHARYA, 1992; ANDERSON, 1999; CALERO, 2007). The sequence impedance matrix  $\mathbf{Z}_{012}$  for a double circuit transmission line

after a nine-section transposition scheme, is obtained by using the domain transformation of (2.6).

$$\mathbf{Z}_{012} = \begin{bmatrix} Z_{00} & 0 & 0 & Z_{0M} & 0 & 0 \\ 0 & Z_{11} & 0 & 0 & 0 & 0 \\ 0 & 0 & Z_{22} & 0 & 0 & 0 \\ Z_{0M} & 0 & 0 & Z_{00'} & 0 & 0 \\ 0 & 0 & 0 & 0 & Z_{11'} & 0 \\ 0 & 0 & 0 & 0 & 0 & Z_{22'} \end{bmatrix} \quad (2.8)$$

It is seen in (2.8) that both positive- and negative-sequence mutual coupling elements are eliminated. However, zero-sequence mutual coupling between circuits,  $Z_{0M}$ , displayed in Figure 2.1, is still present in the transposed double circuit line sequence impedance matrix. Therefore, regardless of the number of transpositions performed on the transmission line, (2.8) indicates that the zero-sequence mutual coupling term cannot be eliminated. Its magnitude can change according to adopted transposition schemes, conductors characteristics and tower geometry. Depending on the case, element  $Z_{0M}$  magnitude can be similar to the positive-sequence impedance of the transmission line  $Z_{11}$  (CALERO, 2007; TZIOUVARAS *et al.*, 2014).

**Figure 2.1.** Zero-sequence mutual coupling presence on double circuit transmission lines.



**Source:** Own authorship.

Within a double circuit transmission line, zero-sequence magnetic flux interconnection can be substantial, with its magnitude demonstrating an inverse relationship with the distance between conductors. Accordingly, zero-sequence voltage induction on one of the line's circuit is caused by the zero-sequence current flowing on the other circuit. Hence, on the event of a ground fault, the voltage measured in the faulted circuit embodies an induced zero-sequence voltage, which is proportional to the zero-sequence current in the parallel circuit, that is, the healthy circuit. This behavior poses a challenge to the protection system, as the current measurements obtained from protective relays do not encompass the impact of mutual coupling (CALERO, 2007; APOSTOLOV *et al.*, 2007).

Distance elements, widely used to protect transmission lines, might have their performance compromised due to impedance measurement errors caused by induced zero-sequence current. Distance elements could underreach or overreach, depending on the direction of zero-sequence current flow in the healthy circuit. Therefore, for more accurate measurements, zero-sequence compensation is required (JONGEPIER; SLUIS, 1994; APOSTOLOV *et al.*, 2007; TZIOUVARAS *et al.*, 2014).

For instance, considering a ground fault in phase A, the following equation expresses the voltage measured at one of the faulted circuit's terminal (TZIOUVARAS *et al.*, 2014):

$$\hat{V}_{A,measured} = \underbrace{mZ_{1TL}(\hat{I}_A + k_0\hat{I}_r)}_{\hat{V}_{A,expected}} + \underbrace{mZ_{0M}\hat{I}_{0M}}_{\hat{V}_{0M}}, \quad (2.9)$$

in which,  $\hat{V}_{A,measured}$  is the phase A voltage measured on the faulted circuit,  $\hat{V}_{A,expected}$  is the voltage that would be measured on a single-circuit transmission line, and  $\hat{V}_{0M}$  is the induced zero-sequence mutual coupling voltage. Also,  $m$  is the percentage of the line where the fault took place,  $Z_{1TL}$  is the positive-sequence impedance of the protected circuit,  $\hat{I}_A + k_0\hat{I}_r$  represents the current with zero-sequence compensation,  $Z_{0M}$  is the zero-sequence mutual impedance between the two circuits and  $\hat{I}_{0M}$  represents the induced zero-sequence current.

As indicated in (2.9), the induced voltage is obtained by multiplying the zero-sequence current measured in the healthy parallel circuit to the zero-sequence mutual impedance of the transmission line. Depending on the direction of current flow in the healthy circuit, the induced voltage  $\hat{V}_{0M}$  exhibits either positive or negative value, causing an increase or decrease on the total voltage measured in the faulted circuit (APOSTOLOV *et al.*, 2007). Fault contribution deriving out of adjacent systems connected at the double circuit transmission line terminals holds a significant influence on determining the direction of current flow within the healthy circuit. With an increase on the difference between equivalent impedances of neighboring systems, there is also an increase on the healthy circuit current and, therefore, the zero-sequence coupling induced voltage. Thus, considering that the voltage behavior directly influences protection elements that rely on their measurements, during certain operating scenarios the systems reliability can be compromised (HONORATO *et al.*, 2020).

## 2.2 PHASOR-BASED TRANSMISSION LINE PROTECTION

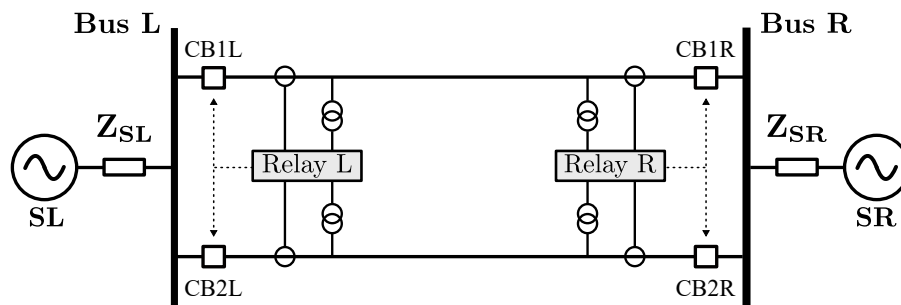
Concerning transmission line protection in general, it is possible to find numerous publications evaluating the differential protections performance under several operating conditions and power system arrangements, besides proposing improvements to it.

Differential protection's basic principle for any electrical device is to compare currents measured at both terminals of the protected equipment in order to detect faults in it. Considering longitudinal differential protection of transmission lines, ANSI code 87L, it is known that during normal operating conditions and external faults, the currents measured at both terminals should ideally be equal in magnitude and with opposite directions, considering the polarity of current transformers (CTs), unless there are intrinsic errors that can influence the relays sensitivity. However, during an internal fault, the directions of currents in both terminals must be the same, considering the polarity of CTs, and the magnitudes may or may not be the same, depending on the system configuration (ROBERTS *et al.*, 2001).

### 2.2.1 Cross-Differential Protection

Cross-differential protection function, addressed as 87CD in this thesis, was specifically developed for the protection of double circuit transmission lines and it operates based on the comparison of measured current magnitudes, at the same terminal, from both circuits of the analyzed line. Correct connection of cross-differential relay in a double circuit transmission line system can be seen in Figure 2.2 (WANG *et al.*, 2005b).

**Figure 2.2.** Cross-differential relay connection.



Source: Own authorship.

Cross-differential protection operation includes instantaneous and successive modes, which are directly related to fault clearance speed.

For the instantaneous operating mode, currents read by relays installed at both line terminals present values sufficiently high for the fault to be detected simultaneously. In this condition, both relays send trip commands to their respective circuit breakers which are opened instantaneously and independently.

The successive operating mode occurs mainly for faults located far from the evaluated line terminal. For these conditions, currents magnitudes in both circuits are similar and, consequently, the operating current value does not surpass the pickup current value. Therefore, only the relay installed closer to the fault is capable of instantaneously detecting the fault and trip its circuit breaker. Meanwhile, the fault continues to be fed by the opposite end of the transmission line. After opening the first circuit breaker, there is a following change in the system topology and the fault current contribution changes so that current magnitudes are not similar and the operating value becomes significant, which allows fault detection by the second relay and a trip command to the circuit breaker (WANG *et al.*, 2005c).

Since the complete fault clearance depends on a remote operation, the successive operating mode is linked to both circuit breakers' opening time, which can vary from one and a half cycles to three cycles (SCHWEITZER *et al.*, 2015).

Within literature, the conventional and percentage elements, described below, are usually adopted for cross-differential protection.

The conventional element of the cross-differential function compares magnitudes from currents flowing in each of the circuits, both measured at the same terminal, with a pre-established operating threshold value, called pickup current. The inequalities (2.10) and (2.11) represent operating conditions in circuits 1 and 2, respectively.

$$|\hat{I}_1| - |\hat{I}_2| > I_{pickup}, \quad (2.10)$$

$$|\hat{I}_2| - |\hat{I}_1| > I_{pickup}, \quad (2.11)$$

with  $\hat{I}_1$  and  $\hat{I}_2$  being the current phasors from circuit 1 and 2 in the same line terminal, respectively, and  $I_{pickup}$  a pre-established threshold of operation, represented by the pickup current.

During external faults, or normal operating conditions, currents  $\hat{I}_1$  and  $\hat{I}_2$  have similar magnitudes and, consequently, the conditions presented in (2.10) and (2.11) are not satisfied. On the other hand, during internal faults operating conditions are met and the protection function is able to detect the fault. However, this will depend on the value defined for the operating threshold, which must consider the maximum load current under single-circuit operation, the differential current of healthy phase in the successive operating mode for SLG fault, and unbalanced current for external fault condition (WANG *et al.*, 2005b).

To comply with these requirements, the pre-established operating threshold,  $I_{pickup}$ , must be set to a very high value, and consequently sensitivity decreases, mainly considering heavy loading conditions. That is, the line coverage under instantaneous operating mode decreases and more faults are cleared through the successive operating mode (WANG *et al.*, 2005b).

To overcome this drawback, a percentage element was developed to improve the performance of conventional cross-differential protection and increase sensitivity. The percentage cross-differential element introduces the calculation of two new quantities, the operating and restraining currents described on (2.12) and (2.13) (WANG *et al.*, 2005c).

$$I_{op} = |\hat{I}_1| - |\hat{I}_2|, \quad \text{and} \quad I_{res} = |\hat{I}_1| + |\hat{I}_2|, \quad (2.12)$$

$$I_{op} = |\hat{I}_2| - |\hat{I}_1|, \quad \text{and} \quad I_{res} = |\hat{I}_1| + |\hat{I}_2|, \quad (2.13)$$

where (2.12) refers to circuit 1 and (2.13) to circuit 2.

The inequalities presented in (2.14) denote the operating conditions that must be satisfied for the percentage cross-differential element to operate (WANG *et al.*, 2005c).

$$I_{op} > K I_{res}, \quad \text{and} \quad I_{op} > I_{pickup}, \quad (2.14)$$

in which,  $K$  represents a protection sensitivity coefficient.

It is important to highlight that the percentage of the transmission line operating in instantaneous or successive mode depends directly on factors such as the strength of equivalent sources connected at line ends, fault impedance and system loading angle. The challenge, therefore, is to increase the region in which the cross-differential protection operates in instantaneous mode, promoting an improvement in its performance (LI *et al.*, 2017).

Although the use of percentage cross-differential element ensures an increase in the relay's sensitivity, it is still strongly influenced by the loading current that flows in the double circuit



line, mainly after opening only one of the line terminals circuit breaker. When the loading angle is high, outfeed situations may occur, since the fault current contribution may be insufficient to reverse the flow of pre-fault current present in the system. Also, cross-differential protection operating logic may not result in correct operations if one of the circuits is out of service. Furthermore, in situations of considerable difference between sources strengths connected at transmission line ends, the magnitudes from currents measured at both circuits in the weakest terminal of the line are similar and the performance of cross-differential relays can be compromised. To avoid these disadvantages, the superimposed method is adopted (WANG *et al.*, 2005a; SERPA, 2020).

The method of superimposed currents, or incremental, makes use of pure fault currents, which are defined as the difference between the currents measured after the fault and their respective pre-fault currents (WANG *et al.*, 2005a). In this way, the influence of loading in the protection function's performance is decreased.

Formulations of the operating and restraining currents are now defined as:

$$I_{op} = |\Delta\hat{I}_1| - |\Delta\hat{I}_2|, \quad \text{and} \quad I_{res} = |\Delta\hat{I}_1| + |\Delta\hat{I}_2|, \quad (2.15)$$

$$I_{op} = |\Delta\hat{I}_2| - |\Delta\hat{I}_1|, \quad \text{and} \quad I_{res} = |\Delta\hat{I}_1| + |\Delta\hat{I}_2|, \quad (2.16)$$

where (2.15) refers to circuit 1 and (2.16) to circuit 2. Furthermore,  $\Delta\hat{I}_1$  and  $\Delta\hat{I}_2$  characterize the incremental current phasors of circuits 1 and 2, respectively.

$$\Delta\hat{I}_1 = \hat{I}_1 - \hat{I}_{1,pre}, \quad \text{and} \quad \Delta\hat{I}_2 = \hat{I}_2 - \hat{I}_{2,pre}, \quad (2.17)$$

in which,  $\hat{I}_{1,pre}$  and  $\hat{I}_{2,pre}$  represent the pre-fault phasors for circuits 1 and 2.

The inequalities representing operating conditions are in accordance with (2.18).

$$I_{op} > SLP \cdot I_{res}, \quad \text{and} \quad I_{op} > I_{pickup}, \quad (2.18)$$

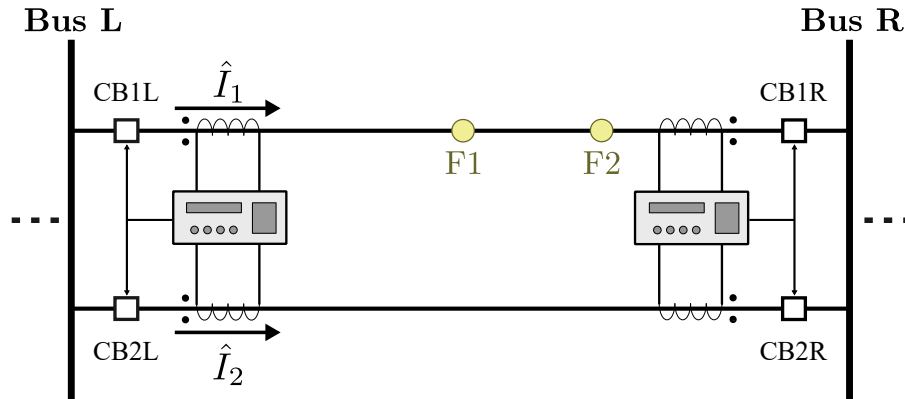
where  $SLP$  represents the slope, protection sensitivity coefficient and  $I_{pickup}$  the pickup current, defined based on the greatest asymmetry in steady state (WANG *et al.*, 2005a).

### 2.2.2 Cross-Differential Protection Numerical Example

Two numerical examples are presented bellow to elucidate operating principles of the superimposed current method applied to cross-differential protection. Faults were simulated in

a test system implemented via Alternative Transients Program (ATP) and through numerical results it is possible to analytically demonstrate the cross-differential protection performance in its instantaneous and successive operating modes.

**Figure 2.3.** Test system for exemplification of cross-differential operating modes.



**Source:** Own authorship.

The system represented in Figure 2.3, has a nominal voltage of 500 kV and it is composed of a 200 km double-circuit transmission line. There are two fault application points represented in the figure by F1 and F2, which will be use for the analysis presented in this section.

◦ **Fault at F1: 50% of the transmission line**

For the numerical analysis of the instantaneous operating mode, a SLG fault is applied to point F1 in Figure 2.3. The current values acquired at each terminal of the double circuit line were obtained using the ATP software through simulations in permanent fault conditions. As the short-circuit is applied at the middle of the transmission line, currents measured at both terminals have sufficiently high values for the cross-differential protection to operate in the instantaneous mode. Therefore, both relays detect the fault simultaneously, and circuit breakers at both line ends are issued a trip command. Thus, it is possible to verify the operation logic of the protection numerically.

**Pre Fault Currents Circuit 01**

$$\hat{I}_{L1a} = 1364.1981 \angle 8.9695^\circ A$$

$$\hat{I}_{R1a} = 1336.1998 \angle 167.1446^\circ A$$

**Pre Fault Currents Circuit 02**

$$\hat{I}_{L2a} = 1364.1981 \angle 8.9695^\circ A$$

$$\hat{I}_{R2a} = 1336.1998 \angle 167.1446^\circ A$$

**Fault Currents Circuit 01**

$$\hat{I}_{L1a} = 2262.2780 \angle -31.6919^\circ A$$

$$\hat{I}_{R1a} = 1545.8855 \angle -105.5094^\circ A$$

**Fault Currents Circuit 02**

$$\hat{I}_{L2a} = 1528.9045 \angle -13.5223^\circ A$$

$$\hat{I}_{R2a} = 1356.4177 \angle -175.7792^\circ A$$

As a result, local and remote incremental currents for both circuits are:

**Incremental Local Current Circuit 01**

$$\Delta \hat{I}_{L1a} = \hat{I}_{L1a, fault} - \hat{I}_{L1a, pre fault}$$

$$\Delta \hat{I}_{L1a} = 2262.2780 \angle -31.6919^\circ - 1364.1981 \angle 8.9695^\circ$$

$$\Delta \hat{I}_{L1a} = 1515.4954 \angle -67.6036^\circ$$

**Incremental Remote Current Circuit 01**

$$\Delta \hat{I}_{R1a} = \hat{I}_{R1a, fault} - \hat{I}_{R1a, pre fault}$$

$$\Delta \hat{I}_{R1a} = 1545.8855 \angle -105.5094^\circ - 1336.1998 \angle 167.1446^\circ$$

$$\Delta \hat{I}_{R1a} = 1995.9704 \angle -63.5402^\circ$$

**Incremental Local Current Circuit 02**

$$\Delta \hat{I}_{L2a} = \hat{I}_{L2a, fault} - \hat{I}_{L2a, pre fault}$$

$$\Delta \hat{I}_{L2a} = 1528.9045 \angle -13.5223^\circ - 1364.1981 \angle 8.9695^\circ$$

$$\Delta \hat{I}_{L2a} = 586.8842 \angle -76.2991^\circ$$

### Incremental Remote Current Circuit 02

$$\Delta \hat{I}_{R2a} = \hat{I}_{R2a, fault} - \hat{I}_{R2a, pre fault}$$

$$\Delta \hat{I}_{R2a} = 1356.4177 \angle -175.7792^\circ - 1336.1998 \angle 167.1446^\circ$$

$$\Delta \hat{I}_{R2a} = 400.2646 \angle -97.1805^\circ$$

Considering the slope,  $SLP$  in Equation (2.18), equals to 0.3, the operating conditions can be determined as it follows.

### Operating Condition for Local Circuit Breaker CB1L

$$|\Delta \hat{I}_{L1a}| - |\Delta \hat{I}_{L2a}| > SLP \times (|\Delta \hat{I}_{L1a}| + |\Delta \hat{I}_{L2a}|)$$

$$1515.4954 - 586.8842 > 0.3 \times (1515.4954 + 586.8842)$$

$$\mathbf{928.6112 > 630.7139}$$

### Operating Condition for Remote Circuit Breaker CB1R

$$|\Delta \hat{I}_{R1a}| - |\Delta \hat{I}_{R2a}| > SLP \times (|\Delta \hat{I}_{R1a}| + |\Delta \hat{I}_{R2a}|)$$

$$1995.9704 - 400.2646 > 0.3 \times (1995.9704 + 400.2646)$$

$$\mathbf{1595.7057 > 718.8705}$$

### Operating Condition for Local Circuit Breaker CB2L

$$|\Delta \hat{I}_{L2a}| - |\Delta \hat{I}_{L1a}| > SLP \times (|\Delta \hat{I}_{L2a}| + |\Delta \hat{I}_{L1a}|)$$

$$586.8842 - 1515.4954 > 0.3 \times (586.8842 + 1515.4954)$$

$$\mathbf{-928.6112 > 630.7139}$$

### Operating Condition for Remote Circuit Breaker CB2R

$$|\Delta \hat{I}_{R2a}| - |\Delta \hat{I}_{R1a}| > SLP \times (|\Delta \hat{I}_{R2a}| + |\Delta \hat{I}_{R1a}|)$$

$$400.2646 - 1995.9704 > 0.3 \times (400.2646 + 1995.9704)$$

$$\mathbf{-1595.7057 > 718.8705}$$

#### ◦ Fault at F2: 85% of the transmission line

Now, the same SLG fault is applied to point F2 in Figure 2.3. For this situation, the fault located close to the remote terminal of the double circuit line produces a fault current distribu-

tion through both circuits that cause only the remote relay to detect the fault instantaneously and open its corresponding circuit breaker. Thus, after opening the first circuit breaker, the systems topology change. New calculations are made while the fault is fed only by the local line terminal. As a result, the local current becomes large enough for its relay to detect a fault and issue a trip command to the second circuit breaker. Therefore, it is possible to numerically verify the successive operating mode for the evaluated protection function.

### Fault Currents Circuit 01

$$\hat{I}_{L1a} = 1912.3640 \angle -26.3394^\circ A$$

$$\hat{I}_{R1a} = 2839.2927 \angle -95.1703^\circ A$$

### Fault Currents Circuit 02

$$\hat{I}_{L2a} = 1696.3581 \angle -11.7050^\circ A$$

$$\hat{I}_{R2a} = 1598.2711 \angle 148.9177^\circ A$$

As a result, local and remote incremental currents for both circuits are calculated as:

### Incremental Local Current Circuit 01

$$\Delta \hat{I}_{L1a} = \hat{I}_{L1a, fault} - \hat{I}_{L1a, pre fault}$$

$$\Delta \hat{I}_{L1a} = 1912.3640 \angle -26.3394^\circ - 1364.1981 \angle 8.9695^\circ$$

$$\Delta \hat{I}_{L1a} = 1122.6267 \angle -70.9558^\circ$$

### Incremental Remote Current Circuit 01

$$\Delta \hat{I}_{R1a} = \hat{I}_{R1a, fault} - \hat{I}_{R1a, pre fault}$$

$$\Delta \hat{I}_{R1a} = 2839.2927 \angle -95.1703^\circ - 1336.1998 \angle 167.1446^\circ$$

$$\Delta \hat{I}_{R1a} = 3295.7105 \angle -71.4799^\circ$$

### Incremental Local Current Circuit 02

$$\Delta \hat{I}_{L2a} = \hat{I}_{L2a, fault} - \hat{I}_{L2a, pre fault}$$

$$\Delta \hat{I}_{L2a} = 1696.3581 \angle -11.7050^\circ - 1364.1981 \angle 8.9695^\circ$$

$$\Delta \hat{I}_{L2a} = 639.0535 \angle -60.6151^\circ$$

### Incremental Remote Current Circuit 02

$$\Delta \hat{I}_{R2a} = \hat{I}_{R2a, fault} - \hat{I}_{R2a, prefault}$$

$$\Delta \hat{I}_{R2a} = 1598.2711 \angle 148.9177^\circ - 1336.1998 \angle 167.1446^\circ$$

$$\Delta \hat{I}_{R2a} = 531.9666 \angle 97.1372^\circ$$

Considering the slope,  $SLP$  in Equation (2.18), equals to 0.3, the operating conditions that will trip each circuit breaker (CB) connected to the line terminals can be determined as it follows.

#### Operating Condition for Local Relay Circuit 01 - CB1L

$$|\Delta \hat{I}_{L1a}| - |\Delta \hat{I}_{L2a}| > SLP \times (|\Delta \hat{I}_{L1a}| + |\Delta \hat{I}_{L2a}|)$$

$$1122.6267 - 639.0535 > 0.3 \times (1122.6267 + 639.0535)$$

$$\mathbf{483.5732 > 528.5041}$$

#### Operating Condition for Remote Relay Circuit 01 - CB1R

$$|\Delta \hat{I}_{R1a}| - |\Delta \hat{I}_{R2a}| > SLP \times (|\Delta \hat{I}_{R1a}| + |\Delta \hat{I}_{R2a}|)$$

$$3295.7105 - 531.9666 > 0.3 \times (3295.7105 + 531.9666)$$

$$\mathbf{2763.7439 > 1148.3031}$$

#### Operating Condition for Local Relay Circuit 02 - CB2L

$$|\Delta \hat{I}_{L2a}| - |\Delta \hat{I}_{L1a}| > SLP \times (|\Delta \hat{I}_{L2a}| + |\Delta \hat{I}_{L1a}|)$$

$$639.0535 - 1122.6267 > 0.3 \times (639.0535 + 1122.6267)$$

$$\mathbf{-483.5732 > 528.5041}$$

#### Operating Condition for Remote Relay Circuit 02 - CB2R

$$|\Delta \hat{I}_{R2a}| - |\Delta \hat{I}_{R1a}| > SLP \times (|\Delta \hat{I}_{R2a}| + |\Delta \hat{I}_{R1a}|)$$

$$531.9666 - 3295.7105 > 0.3 \times (531.9666 + 3295.7105)$$

$$\mathbf{-2763.7439 > 1148.3031}$$

The operating condition for the local CB of the faulted circuit was not achieved. But, after the opening of CB1R, the system presents a new configuration and fault current values at each terminal are obtained again via ATP software.

**Fault Currents Circuit 01**

$$\hat{I}_{L1a} = 3413.4258 \angle -77.0844^\circ A$$

$$\hat{I}_{R1a} = 0 A$$

**Fault Currents Circuit 02**

$$\hat{I}_{L2a} = 2422.4770 \angle 36.8285^\circ A$$

$$\hat{I}_{R2a} = 2305.1621 \angle -150.2856^\circ A$$

Local and remote incremental currents for both circuits are calculated as:

**Incremental Local Current Circuit 01**

$$\Delta \hat{I}_{L1a} = \hat{I}_{L1a, fault} - \hat{I}_{L1a, pre fault}$$

$$\Delta \hat{I}_{L1a} = 3413.4258 \angle -77.0844^\circ - 1364.1981 \angle 8.9695^\circ$$

$$\Delta \hat{I}_{L1a} = 3587.7009 \angle -99.3773^\circ$$

**Incremental Remote Current Circuit 01**

$$\Delta \hat{I}_{R1a} = \hat{I}_{R1a, fault} - \hat{I}_{R1a, pre fault}$$

$$\Delta \hat{I}_{R1a} = 0 - 1336.1998 \angle 167.1446^\circ$$

$$\Delta \hat{I}_{R1a} = 1336.1998 \angle -12.8554^\circ$$

**Incremental Local Current Circuit 02**

$$\Delta \hat{I}_{L2a} = \hat{I}_{L2a, fault} - \hat{I}_{L2a, pre fault}$$

$$\Delta \hat{I}_{L2a} = 2422.4770 \angle 36.8285^\circ - 1364.1981 \angle 8.9695^\circ$$

$$\Delta \hat{I}_{L2a} = 1373.3139 \angle 64.4867^\circ$$

**Incremental Remote Current Circuit 02**

$$\Delta \hat{I}_{R2a} = \hat{I}_{R2a, fault} - \hat{I}_{R2a, pre fault}$$

$$\Delta \hat{I}_{R2a} = 2305.1621 \angle -150.2856^\circ - 1336.1998 \angle 167.1446^\circ$$

$$\Delta \hat{I}_{R2a} = 1600.7547 \angle -115.9051^\circ$$

Considering the slope,  $SLP$  in Equation (2.18), equals to 0.3, the operating conditions can be determined as it follows.

#### Operating Condition for Local Circuit Breaker CB1L

$$|\Delta \hat{I}_{L1a}| - |\Delta \hat{I}_{L2a}| > SLP \times (|\Delta \hat{I}_{L1a}| + |\Delta \hat{I}_{L2a}|)$$

$$3587.7009 - 1373.3139 > 0.3 \times (3587.7009 + 1373.3139)$$

$$\mathbf{2214.3870 > 1488.3044}$$

#### Operating Condition for Remote Circuit Breaker CB1R

$$|\Delta \hat{I}_{R1a}| - |\Delta \hat{I}_{R2a}| > SLP \times (|\Delta \hat{I}_{R1a}| + |\Delta \hat{I}_{R2a}|)$$

$$1336.1998 - 1600.7547 > 0.3 \times (1336.1998 + 1600.7547)$$

$$\mathbf{-264.5549 > 881.0863}$$

#### Operating Condition for Local Circuit Breaker CB2L

$$|\Delta \hat{I}_{L2a}| - |\Delta \hat{I}_{L1a}| > SLP \times (|\Delta \hat{I}_{L2a}| + |\Delta \hat{I}_{L1a}|)$$

$$1373.3139 - 3587.7009 > 0.3 \times (1373.3139 + 3587.7009)$$

$$\mathbf{-2214.3870 > 1488.3044}$$

#### Operating Condition for Remote Circuit Breaker CB2R

$$|\Delta \hat{I}_{R2a}| - |\Delta \hat{I}_{R1a}| > SLP \times (|\Delta \hat{I}_{R2a}| + |\Delta \hat{I}_{R1a}|)$$

$$1600.7547 - 1336.1998 > 0.3 \times (1600.7547 + 1336.1998)$$

$$\mathbf{264.5549 > 881.0863}$$

The operating condition for the remote CB of the faulted circuit is met, and the remote relay issues a trip command to CB1L.

## 2.3 TIME-DOMAIN-BASED TRANSMISSION LINE PROTECTION

Fault clearance time in an electrical system influences the stability margin, the power transfer limit and the integrity of equipment (EASTVEDT, 1976). Thus, in the search for faster protection functions, those based on the time domain have stood out.

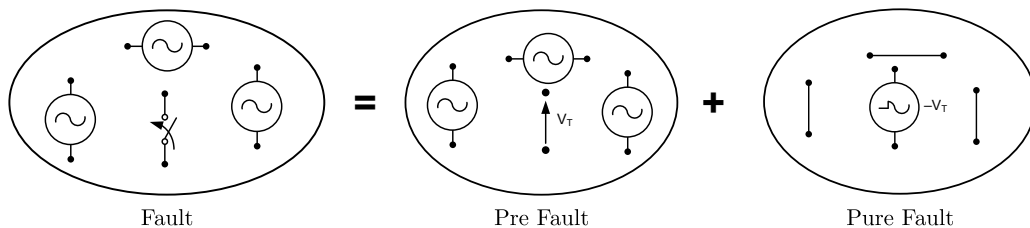


Transient quantities utilization to extract information related to disturbances present in the system has been reported in the literature for years. But, its implementation in real devices proved to be challenging for economic and technological reasons (CHAMIA; LIBERMAN, 1978; DOMMEL, 1978; GREENWOOD, 1991). However, microprocessor-based relays are currently able to provide high sampling rates and, consequently, guarantee the correct operation of protection functions based on incremental quantities and traveling waves. Therefore, the development and use of real devices, whose protection functions are based on the time domain, became feasible (SCHWEITZER *et al.*, 2015).

### 2.3.1 Incremental Quantities

The superposition theorem states that, in a linear electrical system with more than one independent source, the resulting voltage or current at any point in the system is equal to the algebraic sum of the individual voltage or current contributions from each independent source (BOYLESTAD, 2009). When applied to a faulted system, it can be analyzed through two independent circuits, these are: pre-fault circuit and pure fault circuit, which represent the voltage and current signals during pre-fault steady state and the signals solely caused by the fault, respectively. As observed in Figure 2.4, the circuit representing the faulted system is equal to the sum of the pre-fault circuit and the pure fault circuit (SCHWEITZER *et al.*, 2015).

**Figure 2.4.** Superposition theorem.



**Source:** Adapted from Schweitzer *et al.* (2015).

For protection techniques based on incremental quantities, the superposition theorem is essential because pure fault circuit signals can be calculated according to (2.19) (SCHWEITZER

*et al.*, 2015).

$$\Delta s(t) = s(t) - s(t - pT), \quad (2.19)$$

where  $\Delta s$  is the instantaneous incremental quantity,  $s$  the instantaneous measured signal,  $T$  the fundamental period of the measured signal and  $p$  the number of cycles chosen for the duration of the incremental element.

It is worth mentioning that voltage and current signals generated solely from the occurrence of faults are independent of the pre-fault loading conditions of the system, for the first milliseconds after the fault takes place. Thus, protection elements based on incremental values must continue to operate correctly regardless of the load imposed on the analyzed system.

In reality, signals from the monitored system are constantly measured and stored by the protection device. After a system disturbance occurs, the relay instantaneous measurements represent the superposition of the pre-fault and pure fault signals. In this sense, by subtracting the stored pre-fault signal from the current measured signal, pure fault circuit signals are obtained. Since the memory, of  $n$  cycles, of the previously measured signals is used to calculate the incremental quantity, it is worth mentioning that after this period the protection function must be blocked because the incremental element becomes invalid, since the memory samples are in the fault period and no longer represent the pre-fault period (SCHWEITZER *et al.*, 2015; HENSLER *et al.*, 2017).

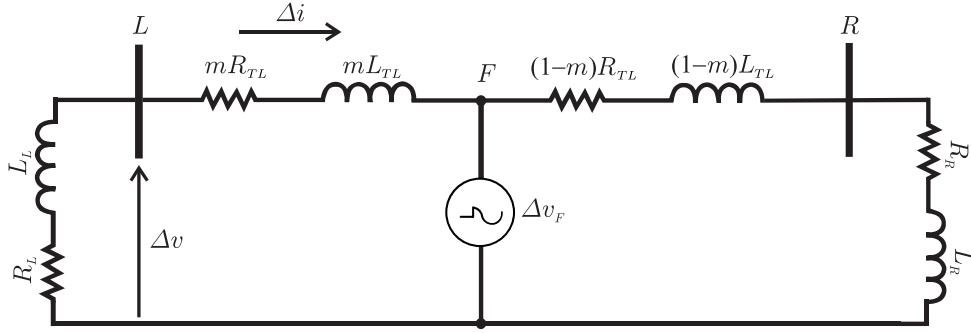
### 2.3.2 Replica Current Concept

Figure 2.5 illustrates the pure fault circuit for a single-phase RL transmission system with a fault applied at a certain percentage of the line, represented by the variable  $m$ . It is assumed that the equivalent Thévenin impedances connected at the local and remote terminals,  $L$  and  $R$ , of the transmission line represent the systems adjacent to it.

Considering the relay installed at the local terminal, incremental voltage and current values are related through:

$$\Delta v = - \left( R_L \cdot \Delta i + L_L \cdot \frac{d}{dt} \Delta i \right). \quad (2.20)$$

Simplifying (2.20) with its normalization by the equivalent impedance of the source con-

**Figure 2.5.** Pure fault circuit.

**Source:** Adapted from Schweitzer *et al.* (2015).

nected to the local terminal, that is, multiplying and dividing the equation by  $Z_L$ , we have:

$$\Delta v = -|Z_L| \left( \frac{R_L}{|Z_L|} \cdot \Delta i + \frac{L_L}{|Z_L|} \cdot \frac{d}{dt} \Delta i \right). \quad (2.21)$$

Note that (2.21) presents a new current signal which is the combination of the instantaneous incremental current and its derivative. This signal was named incremental replica current,  $\Delta i_Z$  (SCHWEITZER *et al.*, 2015; SEL, 2019):

$$\Delta i_Z = \left( \frac{R_L}{|Z_L|} \cdot \Delta i + \frac{L_L}{|Z_L|} \cdot \frac{d}{dt} \Delta i \right) = D_0 \cdot \Delta i + D_1 \cdot \frac{d}{dt} \Delta i, \quad (2.22)$$

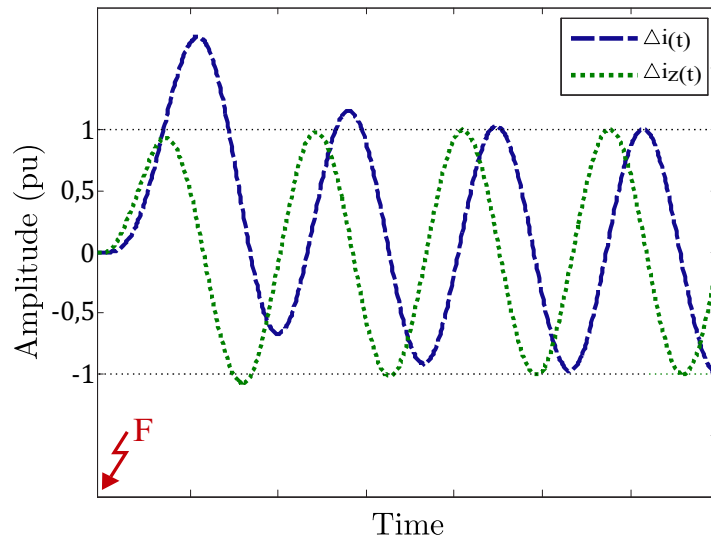
in which:

$$D_0 = \frac{R_L}{|Z_L|}, \quad \text{and} \quad D_1 = \frac{L_L}{|Z_L|}. \quad (2.23)$$

Through this mathematical manipulation, it is possible to simplify the equation that relates instantaneous values of incremental current and voltage, according to (2.24).

$$\Delta v = -|Z_L| \cdot \Delta i_Z. \quad (2.24)$$

The replica current is employed in order to compensate the angular lag, imposed by the systems RL characteristic, allowing the analysis of the fault as if the monitored circuit was resistive. Furthermore, the use of replica current guarantees unitary gain at the fundamental frequency of the system and reduces the effect of inductive impedance, as seen in Figure 2.6 (KASZTENNY *et al.*, 2016).

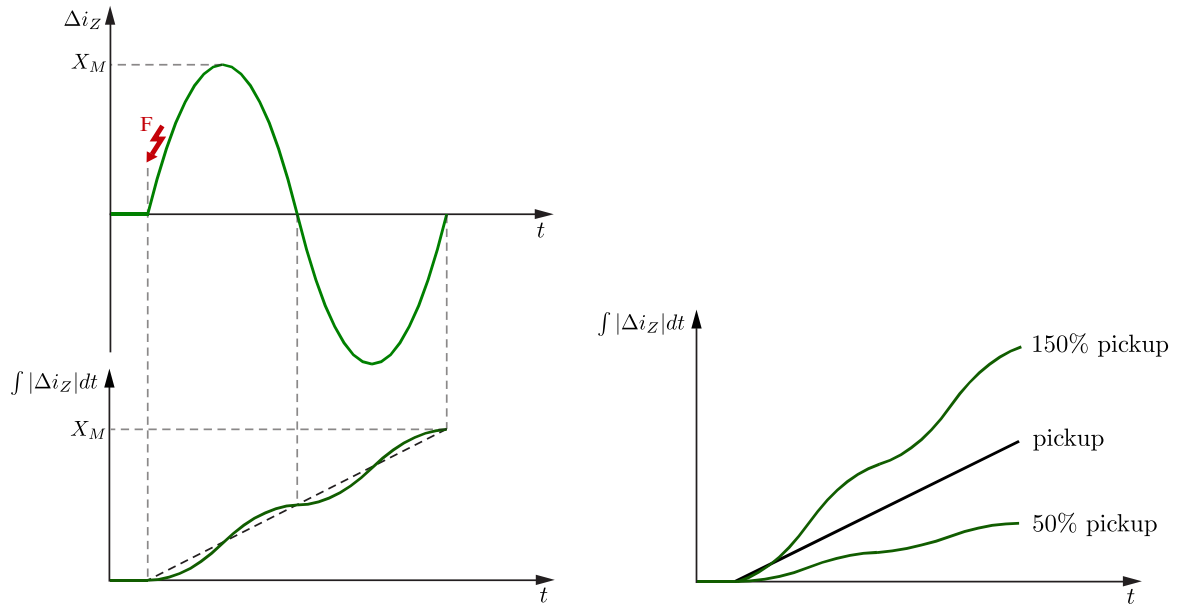
**Figure 2.6.** Incremental replica - correction of inductive characteristic.

Source: Adapted from Ribeiro (2019).

### 2.3.3 Integrated Torque for Overcurrent Supervision Element

To ensure safety of the protection algorithm during switches that can generate high frequency transients in the system, overcurrent supervision is applied. By monitoring the incremental replica current, it can be verified whether the event contains relevant energy levels to be considered a fault, so that the protection element can issue a trip command (SCHWEITZER *et al.*, 2015; SEL, 2019). The incremental replica is employed because of its ideally null value prior to the power system disturbance and its theoretical immunity to the DC exponential decaying component (RIBEIRO *et al.*, 2016). As these are time-domain signals, that is, magnitudes whose values are constantly changing over time, the incremental replica current signals are integrated in order to obtain a stable comparison of their operating conditions. The integral of a signal with such characteristics resembles a straight line, with a slope proportional to the magnitude of the integrated signal itself, as shown in Figure 2.7.

The overcurrent supervision element compares the integrated incremental replica current with the integral of the pickup current, which is determined from short-circuit studies on the monitored line. As shown in Figure 2.7, if the integrated incremental replica current crosses the pickup line, the disturbance is classified as an internal fault. Otherwise, it is understood that a short-circuit has not occurred within the protection zone (SEL, 2019).

**Figure 2.7.** Overcurrent supervision.

Source: Adapted from Schweitzer *et al.* (2015).

## 2.4 EVALUATED FUNCTIONS

To ensure a comprehensive evaluation of the proposed algorithm's performance, it's essential to use a time-domain device. And, as recommended by the manufacturer, employment of a companion relay equipped with phasor-based functions is required. Therefore, focusing solely on single terminal protection functions, a comparative evaluation was carried out between phasor-based and time-domain distance protection elements. To provide context, a brief conceptual overview of the fundamentals of these protection methods is necessary.

### 2.4.1 Phasor Domain Distance Protection Function

Traditional phasor-based distance protection elements, referred to here as 21PD, estimate the fault distance by calculating the apparent positive sequence impedance, measured between the relay and the fault point. The sensitivity of the function depends on the reach set, which is based on the positive sequence impedance of the transmission line. As illustrated in (2.25) and (2.26) both phase-to-ground and phase-to-phase elements depend on current and voltage

phasors provided by the relay (COOK, 1985; ZIEGLER, 2006):

$$Z_{\phi T} = \frac{\hat{V}_{\phi}}{\hat{I}_{\phi} + \frac{Z_{TL,0} - Z_{TL,1}}{Z_{TL,1}} \hat{I}_0}, \quad (2.25)$$

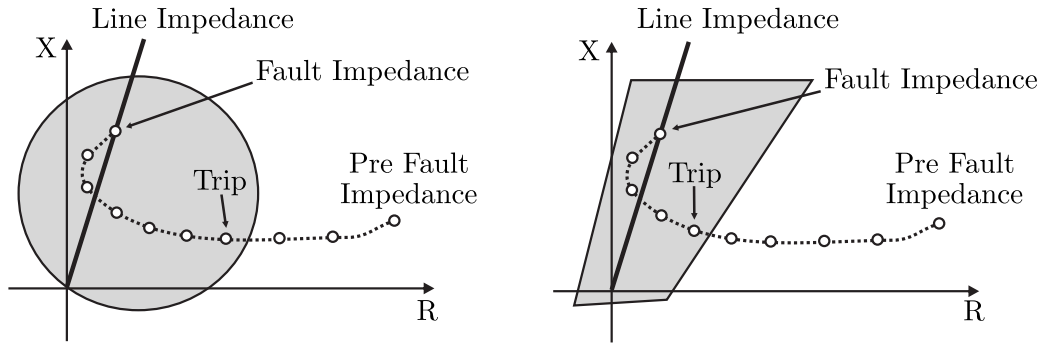
$$Z_{\phi\gamma} = \frac{\hat{V}_{\phi} - \hat{V}_{\gamma}}{\hat{I}_{\phi} - \hat{I}_{\gamma}}, \quad (2.26)$$

where  $Z_{\phi T}$  represents the positive sequence impedance estimated by the phase-to-ground impedance element that encompasses the phase  $\phi$ , while  $Z_{\phi\gamma}$  represents the positive sequence impedance estimated by the phase-phase element that encompasses the phases  $\phi$  and  $\gamma$ .  $\hat{I}_{\phi}$ ,  $\hat{I}_{\gamma}$ ,  $\hat{V}_{\phi}$  and  $\hat{V}_{\gamma}$  represent current and voltage phasors of phases  $\phi$  and  $\gamma$ . The zero-sequence current phasor is symbolized by  $\hat{I}_0$ , and the zero and positive-sequence transmission line impedance by  $Z_{TL,0}$  and  $Z_{TL,1}$ , respectively.

The evaluation of distance protection can be performed using impedance diagrams, as shown in Figure 2.8. By means of these R-X diagrams, the apparent positive sequence impedance calculated by the relay as well as the operating characteristic set for the 21PD function can be visually represented and analyzed. Regarding the operating characteristics of the distance protection, Figure 2.8 presents the two most commonly implemented, mho and quadrilateral characteristics. In both features, two regions can be observed: the operating region, in gray, and the restriction region, external to the highlighted areas (ZIEGLER, 2006).

Also through Figure 2.8, it is possible to examine that during an internal fault, the impedance calculated by the relay moves from the pre fault position in the restriction area to the operating region. As a result, trip commands are issued to its circuit breaker, signaling that the calculated impedance is positioned inside the operating region. It is important to mention that, in order to obtain the preliminary results, the relay was adjusted considering the mho characteristic in addition to the quadrilateral characteristic for phase-to-ground elements, and only the mho characteristic for phase-to-phase elements.

Distance protection elements offer multiple protection zones, with different ranges and intentional delays. The first zone is usually used instantaneously, protecting without intentional delay between 80% and 85% of the transmission line. The other zones are generally implemented as backup protection, going beyond the protected line and also intentionally delayed (ZIEGLER, 2006). In addition, as the first zone does not cover the entire line, for security reasons, in order to provide instant protection across the line it is necessary to associate distance

**Figure 2.8.** Impedance trajectory on R-X diagram for mho and quadrilateral characteristics.

**Source:** Adapted from Silva (2009).

elements with pilot schemes (COOK, 1985; HOROWITZ; PHADKE, 2008). It should be noted that in this thesis, the relay was adjusted considering the first zone at 80%, second zone at 120% and reversed third zone, with an adjustment of 50%. With respective time delays of 0, 24 and 90 cycles.

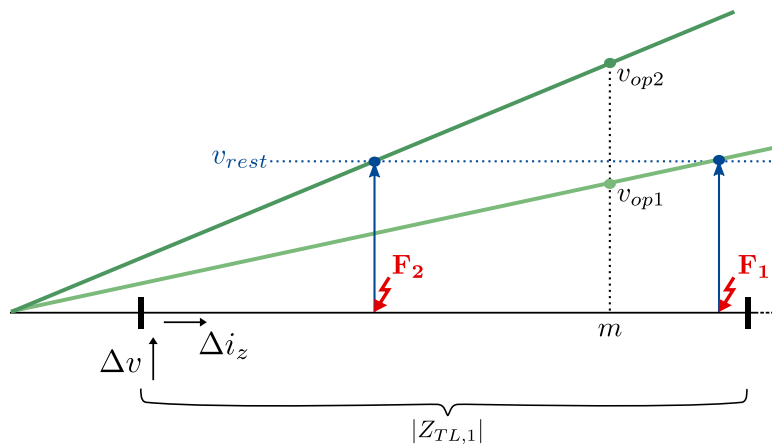
#### 2.4.2 Time Domain Distance Protection Function

Unlike traditional distance protection elements, the time domain distance protection, 21TD, uses incremental quantities and impedance parameters of the protected line to assess voltage variation at the defined reach point. For this, the voltage profile along the line is estimated and its magnitude at the reach point is evaluated in order to define whether the fault is inside or outside the protected zone. The voltage at reach point is calculated as follows (SCHWEITZER *et al.*, 2015):

$$v_{reach} = v - m \cdot |Z_{TL,1}| \cdot i_z, \quad (2.27)$$

where  $v$  is the pre-fault voltage measured by the relay,  $m$  is the reach setting,  $|Z_{TL,1}|$  is the module of positive-sequence impedance of the line, and  $i_z$  is the replica current measured in the relay.

The maximum voltage variation occurs during solid short circuits, since in these cases the pre-fault voltage theoretically drops to zero at the fault point. Thus, the pre-fault voltage at the reach point, given by (2.27), is used as a restraining quantity, while the operating signal is

**Figure 2.9.** Operation principle of the time-domain distance protection function.

**Source:** Adapted from SEL (2019).

the voltage variation at the reach point, as shown in (2.28) (SEL, 2019).

$$v_{op} = \Delta v - m \cdot |Z_{TL,1}| \cdot \Delta i_z, \quad (2.28)$$

considering  $\Delta v$  and  $\Delta i_z$  respectively as incremental voltage and incremental replica current.

Operating principles of the time domain distance protection function are shown in Figure 2.9. As previously explained, the 21TD operating conditions use voltage as a comparison parameter. Thus, if  $v_{op} \geq v_{rest}$  an in-zone fault is detected ( $F_2$ ), otherwise with  $v_{op} < v_{rest}$  an out-zone fault is declared ( $F_1$ ).

The 21TD does not offer other operating zones, unlike the 21PD function for example, as it would defeat its purpose of detecting severe faults in a few milliseconds (SCHWEITZER *et al.*, 2015). Furthermore, considering that the 21TD function has overreach control and depends on data coming from only one end of the transmission line, it can be implemented autonomously, as a stand-alone scheme. However, for the 21PD function, the range of elements is not adjusted to provide 100% of transmission line coverage. The manufacturers recommendation, and the setting chosen for the experimental tests presented in this thesis project, is 70% (SEL, 2019).



# STATE OF THE ART

Aiming to highlight the context in which this thesis is inserted, with regards to cross-differential protection of double circuit transmission lines, this chapter presents a state of the art review. This was achieved firstly considering cross-differential protection, and later introducing studies related to time domain-based strategies for protecting transmission lines.

### 3.1 PROTECTION OF DOUBLE CIRCUIT TRANSMISSION LINES

Gilany *et al.* (1992) present a protection technique for double circuit transmission lines based on the use of only one relay at each end of the protected transmission line. The algorithm is based on a recursive method to calculate a measure proportional to the average of current samples. This method, called average component, is calculated by summing the magnitudes of each cycle of the current samples. To minimize effects of high frequency components on current signals, the author makes use of a Butterworth filter. In this way, a fault is detected when the difference between the average components of the faulted circuit and the circuit exceeds a pre-set value, if the average component is also higher than another pre-defined value. The authors evaluate the performance of the algorithm by analyzing several fault scenarios in a system of parallel lines with a length of 300 km, voltage rate of 500 kV, with and without series compensation, modeled on distributed parameters in an Electromagnetic Transients Program (EMTP)-based software. From the results, authors found that in addition to providing fast operating times, the proposed algorithm is stable during switching conditions.

Wang *et al.* (2005b) and Wang *et al.* (2005c) investigate percentage cross-differential element usage to increase the performance of conventional cross-differential relay. Cross differential protection provides fast operations and is independent of communication channels. However, the fact that the differential current must be greater than the maximum load current during single-

circuit operation, in addition to being greater than the differential current in healthy phase for single-line-to-ground (SLG) faults during successive operating mode, makes the adjustments of the conventional cross-differential protection to be set with very high values. Consequently, the relays sensitivity, especially under high load conditions, is affected. Therefore, to improve stability of the proposed percentage differential element in distinguishing between open circuit and fault situations, and in identifying faults at healthy phases during the successive operating mode, the authors introduce voltage pick-up and phase selection elements, respectively. Through the use of EMTP type software and the RTDS (Real time digital simulator), the authors were able to evaluate the performance of percentage solution presented for computational purposes and via implementation through the platform programmable relay rating. According to the results, percentage cross-differential element provided an increase in the instantaneous operation zone and in the relay's sensitivity to internal faults, in addition to improving its stability during external short-circuits.

Wang *et al.* (2005a) present a cross-differential element based on superimposed currents, defined as the current phasors, measured at each transmission line terminal, subtracted from their respective pre-fault current phasors. The authors state that despite the use of the percentage cross-differential element previously presented to improve the sensitivity of the differential relay, it is still influenced by the load current. Also, during situations where the difference between the strengths of the sources at the two ends of the transmission line is very large, the amplitudes of currents measured in each circuit at the terminal referring to the weak source are similar, so that the differential relay may not operate. Therefore, the use of the overlapping current technique benefits the performance of the differential relay. In order to demonstrate the performance of the cross-differential protection element based on overlapping currents, the authors conducted several tests on a 500 kV and 400 km transmission system through EMTP type software. The short-circuit contribution from the line terminals were varied, as well as the fault type and its location. By comparing it with the conventional method, the authors show that the proposed cross-differential element is, in addition to being more sensitive, capable of operating correctly in the presence of strong and weak sources at the terminals of the analyzed line. In addition, the superimposed current method presented guarantees instantaneous and successive operation for all fault configurations portrayed.

Sanaye-Pasand & Jafarian (2011) propose a logical decision algorithm based on a state diagram with the objective of combining the outputs obtained through the cross- and impedance-based differential functions. The algorithm aims to protect double circuit transmission lines through a cross-differential protection method that compares the currents in phases of both circuits in a two-dimensional space segmented into six specific regions of operation. Thus, the algorithm is able to discriminate between normal operating and short-circuit conditions, by comparing the differential current calculated between the parallel circuits and the threshold usually established for the cross-differential protection. Furthermore, through the use of an additional algorithm, based on impedance, the proposed method is able to compensate for the mutual coupling effect, according to the location of phase currents in the implemented two-dimensional space, thus avoiding the problem of overreaching the conventional distance relay. Using an EMTP type software, several fault scenarios were performed in order to evaluate the performance of the proposed algorithm. The results revealed the ability of the evaluated method to correctly classify the faulted phases. Through the algorithm based on the state diagram, the sequences of transitions between different defined states are used to recognize the operation scenarios and correctly make the final decision of the relay. Furthermore, the authors exposed the operation of the proposed algorithm with operating times of less than one cycle, due to the high sensitivity of the cross-differential technique used.

Gomes & Silva (2014) present the analysis of the performance of the cross-differential protection applied in double circuit lines. The authors evaluated the performance of the percentage differential element associated with the use of the overlapping currents method, when compared to the traditional method. To do so, several fault conditions and protection operation modes were examined, in a 230 kV test system, modeled in EMTP type software. Based on the results, authors proved a greater sensitivity and safety for the overlapping currents method, in relation to the traditional method.

Neves & Silva (2018) describe a comparative evaluation of longitudinal and cross-differential protections applied to double circuit transmission lines. Protections are analyzed via a complex representation plane of current ratio, known as alpha plane. The authors used a 230 kV and 200 km system, modeled on an EMTP type software. Transient analyses and parametric sensitivity analyses are employed to examine the performance of protection elements in question.

Through these, it was verified that the cross-differential protection is little affected by fault resistance and system loading, but it is sensitive to the effects of source strength and fault location. Longitudinal differential protection was shown to be significantly affected by all parameters analyzed, and may not be sensitized, depending on the load and fault resistance values adopted.

Serpa *et al.* (2019) experimentally evaluated the performance of cross-differential function in the protection of double circuit transmission lines. For this, the authors implemented in a real device, through the free programming platform of customized logics, the cross-differential protection algorithm based on the method of superimposed currents. The authors modeled, in EMTP type software, a double circuit line with distributed parameters, with mutual coupling between two identical three-phase lines individually transposed and with a voltage level of 230 kV. From this model, transient and parametric sensitivity analyses were performed for different fault scenarios. The representation plane chosen to present the results was the alpha plane. According to the results obtained experimentally, it was found that the cross-differential protection has high coverage in instantaneous mode, high sensitivity to resistive faults and it is not affected by the line loading.

Continuing the studies carried out in Serpa *et al.* (2019), Serpa *et al.* (2020) examine the performance of cross-differential protection for cross-country faults. Given the arrangement and proximity of conductors in a double circuit topology, the possibility of faults occurring between circuits becomes high and, as this is a critical phenomenon, it must be carefully considered in the employed protection scheme. Based on the relevance of the topic, the authors carried out studies considering fault scenarios in which the fault location and fault resistance are varied, in order to assess the instantaneous coverage of the protection function. In addition, the trajectory traversed by the cross-differential element is analyzed in the alpha plane. Finally, the authors conclude that the cross-differential protection is capable of detecting faults between two different phases, for the two existing circuits, in addition to having high coverage in instantaneous mode for this type of fault.

## 3.2 TIME DOMAIN PROTECTION

Chamia & Liberman (1978) introduce one of the first protective relays developed by adopting a traveling wave (TW) approach and employing the theory of incremental quantities (IQ) in the time domain. The efficacy of the proposed algorithm in determining fault direction, based on the polarity difference between calculated voltages and incremental currents, was demonstrated.

Vitins (1981) presents a directional protection methodology which detects, by analyzing elliptical paths formed by the magnitudes of incremental voltage and current, the direction of a fault applied to the monitored transmission line. Results presented by the authors highlight the rapid response exhibited by the proposed method, while also displaying its limitations and suggesting potential solutions.

Lanz *et al.* (1985), on the other hand, proposes the differentiation of incremental current using a replica impedance, which significantly impacts the trajectories traced by incremental currents and voltages. Consequently, the paper suggests the adoption of an asteroid-shaped operating characteristic, enhancing the accuracy of fault direction indication.

Despite the advances and contributions made in the 70's and 80's, with regard to protection functions in the time domain, the need for high signal processing rates limited and prevented the evolution and implementation of these concepts. However, technological advances achieved in recent years, considering microprocessor-based relays, allowed time domain functions to be reconsidered. Thus, relevant contributions to the use of fast protection functions in the time domain resurfaced (KASZTENNY *et al.*, 2006).

Schweitzer *et al.* (2015) proposed time-domain versions of widely known and traditionally used phasor-based distance and directional power protection functions. And, in 2017, the first protective device exclusively comprised of protection functions centered on the time domain, featuring incremental quantities and the traveling wave theory, was introduced and became commercially available (SEL, 2019).

Years of widespread application of incremental quantities and traveling wave techniques for fault analysis helped shift focus of protective relay developers towards high-speed protection strategies (FRANCA *et al.*, 2021).

Ultra-high-speed line protection methods capable of tripping in few milliseconds are intro-

duced with Schweitzer *et al.* (2016). The protective device presents IQ-based and TW-based directional elements, as well as IQ-based distance and TW-based differential elements. Their performance is showcased through digital simulations and real-world fault scenarios.

Dong *et al.* (2016) proposes a TW-based directional protection scheme that uses the dyadic wavelet transform to extract the polarities of voltage and current traveling waves, which are subsequently analyzed to detect faults in transmission lines.

The effectiveness of the proposed permissive overreaching transfer trip scheme, which combines IQ- and TW-based directional elements, is evaluated in Guzmán *et al.* (2017). This evaluation is made considering the presence of coupling capacitor voltage transformers, while subjected to various internal and external fault scenarios using real field data events.

A high-speed protection method for determining fault direction and distinguish internal faults from external ones is presented by Namdari & Salehi (2017). Results are achieved by comparing the polarity and arrival time of initial current TWs from both line ends using filter developed to accurately extract transient components from fault-induced signals.

With Costa *et al.* (2017), a protection function based on the initial wavefront arrival time at each line end is proposed and evaluated taking into account the influence of sampling rate and TW velocity estimation on line protection. The results indicate that traveling wave-based protection remains accurate and high-speed even at medium sampling rates.

Tang *et al.* (2017) introduces a new approach to differential protection by using reconstructed equivalent traveling waves through the application of a wavelet transform. Since this method involves the exchange of only several wavelet-transform modulus maxima between terminals, communication load is considerably reduced.

A new time domain differential protection scheme that incorporates both an energy-based algorithm and a reactive power-based algorithm is presented in Dantas *et al.* (2018). These algorithms integrate time-domain measurements and signals to establish stable quantities, which are subsequently employed for transmission line protection. The proposed solution operates effectively, providing fast operation and secure and reliable performance.

Indeed, the efficacy of time domain-based protection functions can be validated and evaluated through a combination of computational and experimental studies across various research

efforts. From a time domain-based differential protection algorithm based on the Bayes' Theorem to determine the probability of fault occurrence over time (TIFERES; MANASSERO, 2022), to a hybrid IQ and TW protection scheme for series compensated transmission lines (NAIDU *et al.*, 2022), to employing Cartesian planes of voltage and current for the development of techniques for distinction and detection between internal and external faults, fault direction and fault type identification (MOHANTY *et al.*, 2022) and to an alternative time domain-based distance protection proposed scheme, in which the fitting calculation error is utilized to create a weight matrix, and an algorithm is developed to solve time-domain differential equations, improving stability and calculation speed (HU *et al.*, 2023).

### 3.3 CHAPTER SUMMARY

The studies described in this literature review are classified in Table 3.1 according to the type of protection employed and the aspects analyzed in each cited work. It is verified that within the frequency domain, cross-differential protection is widely studied. However, in the time domain, although some papers explore alternative functions and strategies to protect the transmission line, a time domain cross-differential element for double circuit transmission lines had not yet been developed.

Considering the aforementioned points, there is a potential opportunity to bridge the current gap in double-circuit transmission line protection by achieving enhanced performance and reduced operating times. Hence, this thesis proposes a novel time domain percentage cross-differential element based on incremental replica currents. This innovative concept aims to enhance the protection of double circuit transmission lines.

**Table 3.1.** Summary of literature review topics of research and comparison with the ones covered by the proposed algorithm.

Reference	Covered Contents								
	21	87L	87CD	TD	PS	RD	PE	IE	IR
Gilany <i>et al.</i> (1992)	–	–	✓	–	–	–	–	–	–
Wang <i>et al.</i> (2005b)	–	–	✓	–	–	–	✓	–	–
Wang <i>et al.</i> (2005c)	–	–	✓	–	–	–	✓	–	–
Wang <i>et al.</i> (2005a)	–	–	✓	–	–	–	✓	✓	–
Sanaye-Pasand & Jafarian (2011)	✓	–	–	✓	–	–	–	–	–
Gomes & Silva (2014)	–	–	✓	–	✓	–	✓	✓	–
Neves & Silva (2018)	–	✓	✓	–	✓	–	–	–	–
Serpa <i>et al.</i> (2019)	–	–	✓	–	✓	✓	–	–	–
Serpa <i>et al.</i> (2020)	–	–	✓	–	✓	✓	–	–	–
Chamia & Liberman (1978)	–	–	–	✓	–	–	–	✓	–
Vitins (1981)	–	–	–	✓	–	–	–	✓	–
Lanz <i>et al.</i> (1985)	–	–	–	✓	–	–	–	✓	✓
Schweitzer <i>et al.</i> (2015)	✓	–	–	✓	–	✓	–	✓	✓
Dong <i>et al.</i> (2016)	–	–	–	✓	✓	✓	–	✓	–
Guzmán <i>et al.</i> (2017)	✓	–	–	✓	✓	✓	–	✓	✓
Namdari & Salehi (2017)	–	–	–	✓	✓	–	–	✓	–
Costa <i>et al.</i> (2017)	–	–	–	✓	✓	✓	–	–	–
Tang <i>et al.</i> (2017)	–	✓	–	✓	✓	–	–	–	–
Dantas <i>et al.</i> (2018)	–	✓	–	✓	✓	–	–	–	–
Naidu <i>et al.</i> (2022)	–	–	–	✓	✓	–	–	✓	–
Tiferes & Manassero (2022)	–	✓	–	✓	✓	–	–	–	–
Mohanty <i>et al.</i> (2022)	–	–	–	✓	✓	–	–	✓	–
Hu <i>et al.</i> (2023)	✓	✓	–	✓	✓	–	–	–	–
<b>Proposed Algorithm</b>	–	–	✓	✓	✓	✓	✓	✓	✓

**Legend:**

21: Distance Protection	RD: Real Device
87L: Differential Protection	PE: Percentage Element
87CD: Cross-Differential Protection	IE: Incremental Element
TD: Time Domain-Based	IR: Incremental Replica
PS: Parametric Sensibility	

**Source:** Own authorship.



# PROPOSED ALGORITHM

Cross-differential protection presents advantages in relation to other functions usually employed for double circuit transmission line protection, such as distance protection. Despite its typical outstanding coverage reach of 90% of the line, the performance of cross-differential function is limited by phasor estimation data window length, typically of one cycle (SCHWEITZER *et al.*, 2016; SERPA, 2020).

Seeking faster fault clearing times, to guarantee transient stability for the electrical system and provide greater power transfer capabilities, researches involving time domain protection functions have been carried out. Among them, techniques for mapping traditional functions, such as directional power and distance protection, from the frequency domain to the time domain have already been implemented in real devices (SEL, 2019).

In this sense, the proposed algorithm brings a solution for the protection of double circuit lines based on the association of cross-differential protection, recognized for its high percentage of line coverage, with time domain, characterized by its fast operating times. Therefore, the procedures involved in the implementation of the proposed algorithm are detailed in this chapter. Additionally, a diagram is presented for a better understanding of each step.

### 4.1 PROPOSED FORMULATION

In order to find a protection algorithm for double circuit transmission lines with high performance in terms of line coverage and operating time, this thesis project proposes a protection algorithm based on the mapping of traditional phasor-based 87CD function to the time domain.

As stated in Table 4.1, single-terminal protection functions do not rely upon communication channel or data synchronization for appropriate operation, which is not the case of traditional line differential protection since its operation depends on both local and terminal current mea-

surements. Regarding zero-sequence coupling, distance protection functions are affected while differential functions are immune. With respect to phasor estimation, 21PD, 87L and 87CD do rely upon it as they are phasor-based protection functions, which makes 21TD the only available function that does not depend on the estimation window. Furthermore, none of the four protection functions mentioned can fulfill all desired features. The proposed algorithm, in turn, aims to fill this gap.

**Table 4.1.** Advantages of the proposed algorithm.

<b>Protection Function</b>	Communication Channel Independency	Data Synchronization Independency	Zero-Sequence Coupling Immunity	Phasor Estimation Independency
21PD	✓	✓	✗	✗
87L	✗	✗	✓	✗
87CD	✓	✓	✓	✗
21TD	✓	✓	✗	✓
<b>Proposed</b>	✓	✓	✓	✓

**Source:** Own authorship.

The detailed description of each section of the proposed algorithm is presented next, where subscripts L1 and L2 represent circuits 1 and 2 of the double-circuit transmission line, respectively, and the subscript  $\phi$  represents phases A, B or C. Also, the equations shown below are not presented considering a specific line terminal, thus they can be applied to either local or remote terminals.

#### 4.1.1 Currents Normalization

Measurements from CTs installed on both transmission line circuits are normalized to per unit, considering maximum CT primary currents as base values. The normalization is achieved with the use of tap values  $TAP_1$  and  $TAP_2$ , defined in (4.1) and (4.2), to the secondary currents. Thereby correcting errors caused by different CT ratios.

$$TAP_1 = \frac{\max(i_{pri1}, i_{pri2})}{CTR_1}, \quad (4.1)$$

$$TAP_2 = \frac{\max(i_{pri1}, i_{pri2})}{CTR_2}, \quad (4.2)$$

where  $i_{pri1}$  and  $i_{pri2}$  are the instantaneous primary currents from CTs installed on circuits 1 and 2, respectively, and  $CTR_1$  and  $CTR_2$  the CT ratio for both circuits.

Additionally, to compensate current disparity during external faults and steady state operation for cases that circuits have different parameters or do not share the same transmission tower, the correction factors  $G_1$  and  $G_2$ , defined by (4.3) and (4.4), must be applied.

$$G_1 = \frac{|Z_{L1} + Z_{L2}|}{|Z_{L2}|}, \quad (4.3)$$

$$G_2 = \frac{|Z_{L1} + Z_{L2}|}{|Z_{L1}|}, \quad (4.4)$$

with  $Z_{L1}$  and  $Z_{L2}$  being the positive sequence impedances of circuits 1 and 2, respectively.

Thus, secondary currents of circuits 1 and 2,  $i_{CT1\phi}(k)$  and  $i_{CT2\phi}(k)$ , are normalized to  $i_{L1\phi}(k)$  and  $i_{L2\phi}(k)$ , respectively, via (4.5) and (4.6).

$$i_{L1\phi}(k) = G_1 \cdot \frac{i_{CT1\phi}(k)}{TAP_1}, \quad (4.5)$$

$$i_{L2\phi}(k) = G_2 \cdot \frac{i_{CT2\phi}(k)}{TAP_2}, \quad (4.6)$$

in which  $i_{CT1\phi}$  and  $i_{CT2\phi}$  are the secondary currents originated from CTs installed on circuits 1 and 2, respectively.

#### 4.1.2 Incremental Currents

As mentioned in Section 2.2.1, the use of superimposed, or incremental, quantities minimizes the influence of system loading in the protection function's performance. Moreover, the use of incremental currents mitigate negative effects of capacitive charging currents in the transmission line protection, such that their compensation is not required with the proposed algorithm. In this sense, for the proposed algorithm, incremental currents are calculated with (4.7) and (4.8).

$$\Delta i_{L1\phi}(k) = i_{L1\phi}(k) - i_{L1\phi}(k - pN), \quad (4.7)$$

$$\Delta i_{L2\phi}(k) = i_{L2\phi}(k) - i_{L2\phi}(k - pN), \quad (4.8)$$

where  $\Delta i_{L1\phi}$  and  $\Delta i_{L2\phi}$  are the normalized incremental currents of circuits 1 and 2,  $p$  is the number of cycles chosen for incremental quantities to stay active and  $N$  is the number of samples per cycle.

### 4.1.3 Incremental Replica Currents

The inductive characteristic of the transmission system results in angular offsets between the current and voltage signals obtained. Analysis performed in the proposed algorithm require amplitude comparisons of instantaneous values. Thus, incremental replica currents  $\Delta i_{zL1\phi}(k)$  and  $\Delta i_{zL2\phi}(k)$  of circuits 1 and 2, respectively, presented in (4.9) and (4.10), are used to compensate current and voltage signals misalignment, and to eliminate the effect of exponential decaying DC component. In this way, analysis of the pure fault circuit can be performed considering characteristic responses of a resistive circuit.

$$\Delta i_{zL1\phi}(k) = \frac{1}{|Z_{L1}|} \left\{ R_1 \Delta i_{L1\phi}(k) + L_1 \left[ \frac{\Delta i_{L1\phi}(k) - \Delta i_{L1\phi}(k-1)}{\Delta t} \right] \right\}, \quad (4.9)$$

$$\Delta i_{zL2\phi}(k) = \frac{1}{|Z_{L2}|} \left\{ R_2 \Delta i_{L2\phi}(k) + L_2 \left[ \frac{\Delta i_{L2\phi}(k) - \Delta i_{L2\phi}(k-1)}{\Delta t} \right] \right\}, \quad (4.10)$$

where  $R_1$  and  $R_2$  are the positive sequence resistance of circuits 1 and 2, whereas  $L_1$  and  $L_2$  are their positive sequence inductance, and  $\Delta t$  is the sampling interval.

The replica current proportionally reproduces the voltage measured at the terminal where the relay is installed. It is a voltage drop verified in an inductive circuit with unity gain maintained at the nominal frequency of the system. Fact made evident through the simplified equation  $\Delta v = -|Z_L| \cdot \Delta i_z$ , in which the incremental voltage and current signals are related via source impedance of the terminal to which the relay is connected.

### 4.1.4 Operating and Restraining Currents

The chosen method to determine the operating and restraining currents comes from the formulation of percentage cross-differential protection, portrayed in (2.15) and (2.16), considering incremental quantities as shown in (4.11) to (4.14) (WANG *et al.*, 2005c).

$$\Delta i_{opL1\phi}(k) = |\Delta i_{zL1\phi}(k)| - |\Delta i_{zL2\phi}(k)|, \quad (4.11)$$

$$\Delta i_{resL1\phi}(k) = |\Delta i_{zL1\phi}(k)| + |\Delta i_{zL2\phi}(k)|, \quad (4.12)$$

$$\Delta i_{opL2\phi}(k) = |\Delta i_{zL2\phi}(k)| - |\Delta i_{zL1\phi}(k)|, \quad (4.13)$$

$$\Delta i_{resL2\phi}(k) = |\Delta i_{zL1\phi}(k)| + |\Delta i_{zL2\phi}(k)|, \quad (4.14)$$

### 4.1.5 Operating Torque

Similarly, the operating conditions,  $T_{opL1\phi}$  and  $T_{opL2\phi}$ , derive from those presented in (2.18) of Section 2.2.1 and are calculated as described below (WANG *et al.*, 2005c):

$$T_{opL1\phi}(k) = \Delta i_{opL1\phi}(k) - SLP \cdot \Delta i_{resL1\phi}(k), \quad (4.15)$$

$$T_{opL2\phi}(k) = \Delta i_{opL2\phi}(k) - SLP \cdot \Delta i_{resL2\phi}(k), \quad (4.16)$$

in which, the letter  $T$  is used as an allusion to the operating torques used in time domain directional elements (SEL, 2019).

According to (4.17), if (4.15) is greater than or equal to zero, i.e.  $\Delta i_{opL1\phi} \geq SLP \cdot \Delta i_{resL1\phi}$ , the operating condition is fulfilled and the auxiliary operating conditions,  $\bar{T}_{opL1\phi}$ , receives the value of  $T_{opL1\phi}$ . Otherwise,  $\bar{T}_{opL1\phi}$  is equal to zero. The same logic applies to (4.16) when obtaining the auxiliary operating conditions for circuit 2,  $\bar{T}_{opL2\phi}$ , in (4.18).

$$\bar{T}_{opL1\phi}(k) = \begin{cases} T_{opL1\phi}(k), & \text{if } T_{opL1\phi}(k) \geq 0 \\ 0, & \text{if } T_{opL1\phi}(k) < 0 \end{cases} \quad (4.17)$$

$$\bar{T}_{opL2\phi}(k) = \begin{cases} T_{opL2\phi}(k), & \text{if } T_{opL2\phi}(k) \geq 0 \\ 0, & \text{if } T_{opL2\phi}(k) < 0 \end{cases} \quad (4.18)$$

### 4.1.6 Starting Unit

The starting unit consists of a disturbance detector and, it is important to mention that, the subsections presented from now on are dependent on the active result provided by this unit. Several detection techniques reported in the literature could be implemented along with the proposed algorithm (COSTA *et al.*, 2008; COSTA *et al.*, 2011; LOPES *et al.*, 2013). However, for the sake of simplicity and to provide a fair comparison, in this thesis the considered starting unit logic is the one provided by the evaluated time-domain-based relay. By doing so, the starting unit is used as a disturbance detection step in the proposed algorithm, which can run in an integrated way to the equipment used experimentally.

### 4.1.7 Integrated Operating Conditions

The proposed algorithm makes use of integrated operating conditions. These conditions are calculated numerically as described in (4.19) and (4.20). It should be noted that the integrated operating conditions, named  $E_{opL1\phi}$  and  $E_{opL2\phi}$ , are only calculated after a disturbance has been detected.

$$E_{opL1\phi}(k) = E_{opL1\phi}(k-1) + \bar{T}_{opL1\phi}(k) \cdot \Delta t, \quad (4.19)$$

$$E_{opL2\phi}(k) = E_{opL2\phi}(k-1) + \bar{T}_{opL2\phi}(k) \cdot \Delta t, \quad (4.20)$$

In order to determine the relay's sensitivity, a minimum operating threshold,  $I_{pickup}$ , defined as 0.1 p.u., is considered in accordance to thresholds typically employed for sequence differential elements (SEL, 2015). To adapt it to the behavior of  $E_{opL1\phi}$  and  $E_{opL2\phi}$ , this value is accumulated over time, being called  $E_{pk}$ , as shown in (4.21):

$$E_{pk}(k) = \frac{2}{\pi} \cdot I_{pickup} \cdot \Delta t, \quad (4.21)$$

considering  $E_{pk}$  being calculated after a disturbance is detected in the monitored system by the starting unit.

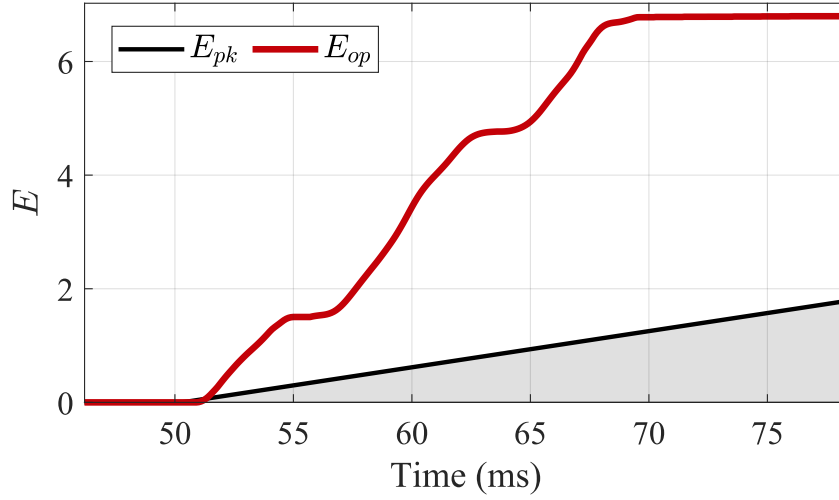
### 4.1.8 Trip Logic

The integrated operating conditions are compared with the integrated pickup threshold,  $E_{pk}$ , resulting in the operation or non operation of the proposed differential element. Phase-segregated trip signals, referring to circuits 1 or 2, are generated as soon as one of the following conditions, (4.22) and (4.23), is fulfilled.

$$E_{opL1\phi}(k) > E_{pk}(k), \quad (4.22)$$

$$E_{opL2\phi}(k) > E_{pk}(k), \quad (4.23)$$

The operation of the proposed scheme can be summarized as follows: when a disturbance is detected, the integrated operating conditions start being computed. After at least one of the trip logic conditions is fulfilled, an internal fault is declared. Otherwise, the algorithm states an external fault situation, thereby its trip command issuing is disabled. Figure 4.1 displays the operating condition in which trip is issued when  $E_{op} > E_{pk}$ .

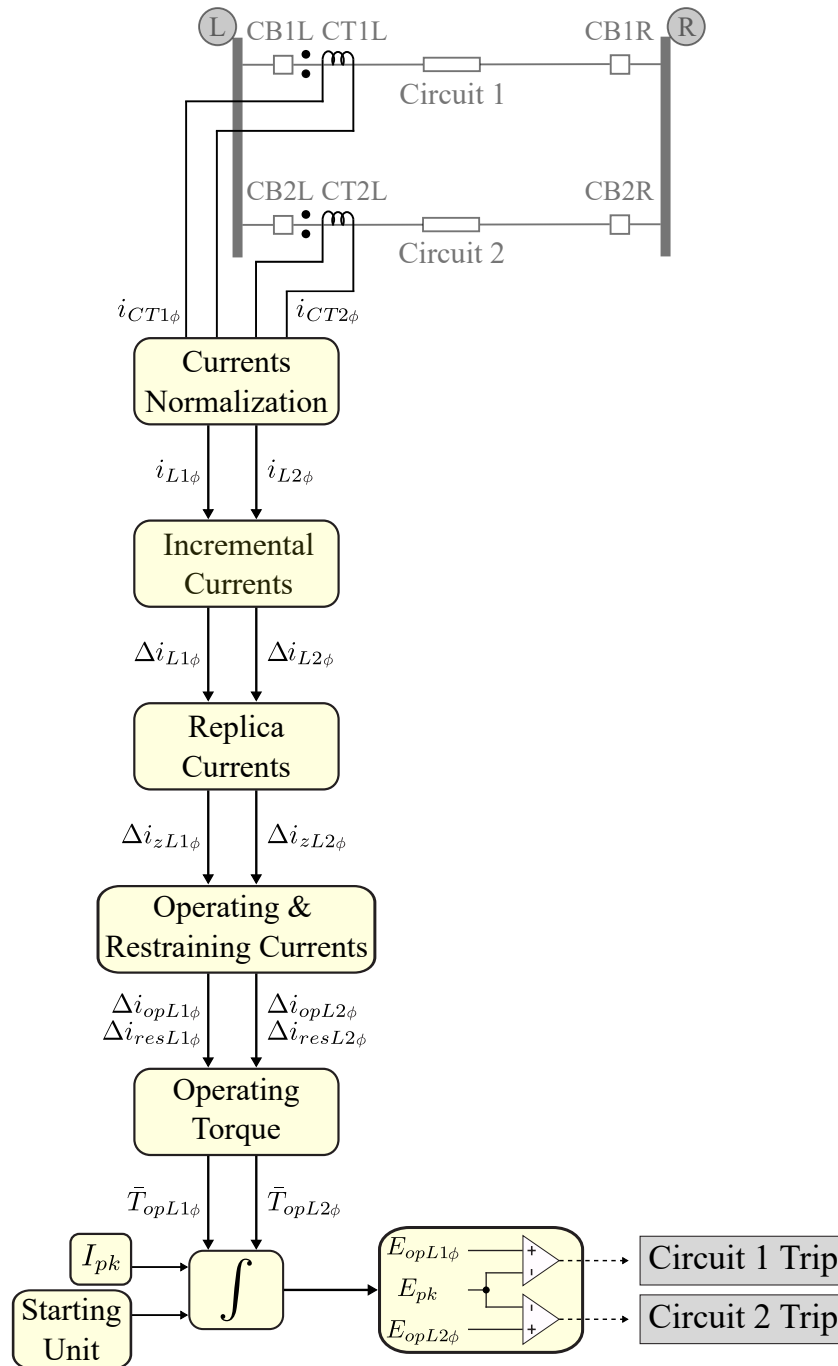
**Figure 4.1.** Proposed algorithm's integrated operating condition comparison.

Source: Own authorship.

#### 4.1.9 General Description of the Proposed Algorithm

Based on the flowchart illustrated in Figure 4.2, it is observed that the input set of the algorithm is composed of secondary currents coming from the CTs installed in each phase, at the same terminal, for both circuits of the double circuit transmission line under analysis. These signals are normalized on the same basis in order to eliminate differences in CT ratios and line parameters, for cases in which circuits do not share the same transmission tower. After normalization, new current signals are directly inserted into the incremental value computing block, often called as delta filter. In order to eliminate the effects of exponential decaying DC component, incremental replica currents  $\Delta \mathbf{i}_{zL1\phi}$  and  $\Delta \mathbf{i}_{zL2\phi}$  are calculated. After this procedure, the operating and restraining currents are obtained analogously to the cross-differential protection function and operating conditions are evaluated. To facilitate this, the examined conditions are integrated and referred to as operating energies of circuits 1 and 2,  $\mathbf{E}_{opL1\phi}$  and  $\mathbf{E}_{opL2\phi}$ , respectively. At the same time, a sinusoidal signal, which represents the adjusted pickup current, is also integrated and called  $\mathbf{E}_{pk}$ . Finally, the block that represents the trip logic uses the integrated quantities as input, so that the proposed differential element determines whether a trip command must be issued or not.

Figure 4.2. Proposed time domain cross-differential protection algorithm flowchart.



Source: Own authorship.



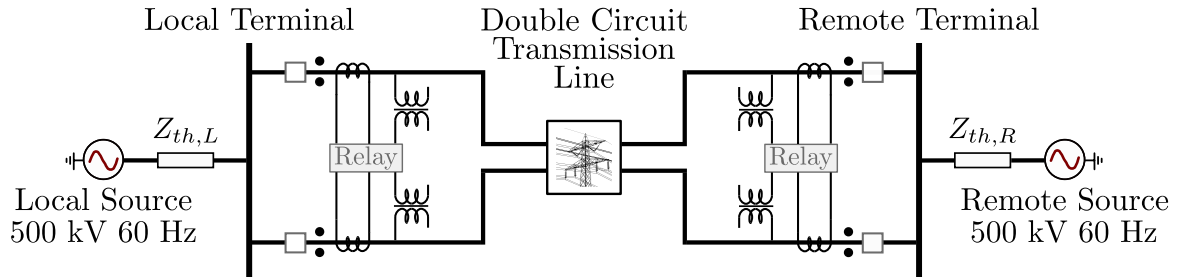
## RESULTS AND DISCUSSIONS

This chapter illustrates a description of the evaluated power system and details the infrastructure adopted for testing, along with adaptations implemented during experimental tests. Later, results considering short-circuit transient state and parametric sensitivity analyses, obtained from inspecting time domain cross-differential protections performance, are exhibit.

### 5.1 TEST POWER SYSTEM

The power system depicted in Figure 5.1 is considered for the proposed algorithm's behavior analysis.

**Figure 5.1.** Test System.



**Source:** Own authorship.

The test system employed is composed of a 200 km long double circuit transmission line and 500 kV rated voltage. Thévenin equivalents connected at both line ends represent the bordering networks associated to the system under analysis. Furthermore, CTs with ratio of 2000-5, and Capacitive Voltage Transformers (CVTs) of 500 kV/60 Hz were employed (IEEE, 2004; PAJUELO *et al.*, 2008).

Double circuit transmission line modeling was performed via Line/Cable Constants (LCC) supporting routine from ATP. Line parameters are obtained with LCC routine considering

cables' electrical characteristics and their geometric arrangement on the transmission tower. Line parameters are essential for calculating mutual coupling values between double circuit lines, and for performing electromagnetic transient studies. As a result, the evaluated line was modeled as a double circuit distributed parameter transmission line with two individually continuously transposed three-phase lines considering only zero-sequence mutual coupling between them (LEUVEN, 1987; DOMMEL; BHATTACHARYA, 1992).

The structure of the phase impedance matrix for double circuit lines with zero-sequence mutual coupling is:

$$\mathbf{Z}_{\text{ABC}} = \begin{bmatrix} Z_s & Z_m & Z_m & Z_p & Z_p & Z_p \\ Z_m & Z_s & Z_m & Z_p & Z_p & Z_p \\ Z_m & Z_m & Z_s & Z_p & Z_p & Z_p \\ Z_p & Z_p & Z_p & Z_s & Z_m & Z_m \\ Z_p & Z_p & Z_p & Z_m & Z_s & Z_m \\ Z_p & Z_p & Z_p & Z_m & Z_m & Z_s \end{bmatrix} \quad (5.1)$$

in which  $Z_s$  and  $Z_m$  represent self and mutual impedances, and  $Z_p$  the coupling between circuits.

If both circuits of the double circuit transmission line are identical, the transposed phase impedance matrix can be converted into a symmetrical component-based diagonal modal matrix by means of (DOMMEL; BHATTACHARYA, 1992; MORAES, 2023):

$$\mathbf{Z}'_{012} = \mathbf{T}^{-1} \cdot \mathbf{Z}_{\text{ABC}} \cdot \mathbf{T}, \quad (5.2)$$

in which  $\mathbf{T}$  is originated from an  $\alpha$ ,  $\beta$ , 0-transformation matrix formulation generalized to accommodate any number of phases, and defined as (DOMMEL; BHATTACHARYA, 1992):

$$\mathbf{T} = \frac{1}{\sqrt{6}} \begin{bmatrix} 1 & 1 & \sqrt{3} & 1 & 0 & 0 \\ 1 & 1 & -\sqrt{3} & 1 & 0 & 0 \\ 1 & 1 & 0 & -2 & 0 & 0 \\ 1 & -1 & 0 & 0 & \sqrt{3} & 1 \\ 1 & -1 & 0 & 0 & -\sqrt{3} & 1 \\ 1 & -1 & 0 & 0 & 0 & -2 \end{bmatrix} \quad (5.3)$$

The resulting diagonal modal matrix  $\mathbf{Z}'_{012}$  is structured as follows:

$$\mathbf{Z}'_{012} = \begin{bmatrix} Z_G & 0 & 0 & 0 & 0 & 0 \\ 0 & Z_{IL} & 0 & 0 & 0 & 0 \\ 0 & 0 & Z_L & 0 & 0 & 0 \\ 0 & 0 & 0 & Z_L & 0 & 0 \\ 0 & 0 & 0 & 0 & Z_L & 0 \\ 0 & 0 & 0 & 0 & 0 & Z_L \end{bmatrix} \quad (5.4)$$

where  $Z_G$  is the ground mode parameter,  $Z_{IL}$  is the inter-line mode associated with the zero-sequence mutual coupling effect and  $Z_L$  is the line mode parameter. These modes can be

determined via (5.5)-(5.7):

$$Z_G = Z_s + 2Z_m + 3Z_p, \quad (5.5)$$

$$Z_{IL} = Z_s + 2Z_m - 3Z_p, \quad (5.6)$$

$$Z_L = Z_s - Z_m, \quad (5.7)$$

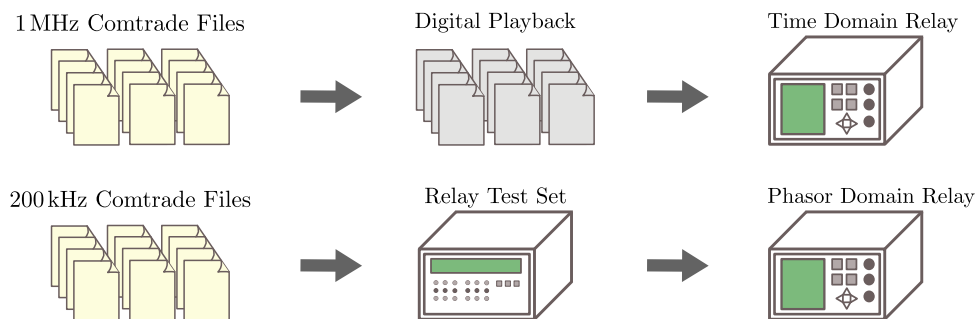
Despite appearing so, matrix (5.4) does not result in six decoupled equations representing the double circuit transmission line. Mode impedances  $Z_G$  and  $Z_{IL}$  are influenced by phase impedance  $Z_p$ , that represent mutual coupling between circuits (LEUVEN, 1987; MORAES, 2023).

Mode impedance values are used as input for the evaluated ATP block unit, named “**LINE ZT\_6**”, which represents the balanced distributed-parameter double circuit transmission line with mutual coupling between two individually transposed 3-phase lines.

## 5.2 TEST INFRASTRUCTURE

To carry out the experimental evaluation of the proposed algorithm and analyze its performance when compared with protection functions implemented in the field, 21PD and 21TD, a mass simulation procedure was carried out considering two commercially available protection relays. The implemented testing infrastructure is shown in Figure 5.2.

**Figure 5.2.** Setup implemented for simulation procedures.



**Source:** Own authorship.

The test methodology was based on the analysis of a compilation of short circuit cases, generated from a base ATP file of the chosen test system. Through routines developed in

Python, the base file was automatically altered in order to cover all fault scenarios under analysis. Subsequently, simulations of evaluated cases were also automatically carried out. Finally, PL4 oscillographic files generated via software ATP were obtained and then converted to COMTRADE format (IEEE, 2012). Thus, as shown in Figure 5.2, signals of interest were injected through different methods for each relay. Using the relay’s internal digital playback function in the time domain, digital records of the evaluated fault scenarios were loaded directly into the relays memory (GUZMÁN *et al.*, 2018). As for the phasor relay, the injection of evaluated cases took place through a traditional playback procedure, using specific relay test set devices for testing.

It is important to mention that, aside from the technical limitation of playback procedures at disposal for both relays, the different test methodologies employed were considered in order to accurately compare both devices. Time domain protection functions use high sampling rates, unlike functions existent in phasor-based relays. In this manner, through the adopted infrastructure, the devices performance could be analyzed considering appropriate conditions.

### 5.3 ADAPTATIONS EMPLOYED DURING TESTING PROCEDURES

In order to test the proposed algorithm through realistic and fair comparative analysis, adaptations were employed and variables used in the algorithm were obtained directly from the memory of the evaluated protection devices.

Incremental replica currents, presented in the section 4.1.3, can be obtained directly from the evaluated time domain-based relay. By doing so, signal processing used for the proposed algorithm are consistent with signal filtering and sampling rate employed for the real device’s native functions. Therefore, a proper comparison can be assured.

Furthermore, it is explained in the section 4.1.7 that the integration of operating conditions commences exclusively after disturbance detection. Therefore, the starting variable of the fault loops coming from the relay itself is used to release the integration of operating conditions for the proposed algorithm instead of a self-authored disturbance detector.

Considering both adaptations, after injecting fault scenarios into both devices at test, incremental replica currents and the starting variable, related to the detection of disturbances in

the system, are arranged, alongside every other variable of interest, in an oscillographic file in COMTRADE format (IEEE, 2012). After proper reading, data is obtained and applied in a computational software in order to implement the proposed algorithm.

Note that the relay stores phase incremental replica currents and zero sequence incremental replica currents. Thus, it is necessary to subtract the zero-sequence incremental replica current from the phase-incremental replica current magnitudes obtained from the protection device to guarantee the correct detection of short circuits through the phase-to-ground loop values.

## 5.4 EXPERIMENTAL EVALUATIONS

Based on what was described in section 5.2, experimental evaluations were performed. To evaluate the proposed algorithm's performance and compare it with traditional and time domain distance functions, transient and parametric sensitivity analyses were performed. Additionally, cases of zero-sequence coupling variation were examined under parametric sensitivity and transient inquiry.

### 5.4.1 Transient Short-Circuit Analysis

Transient short-circuit analyses allow the observation of operation coefficients behavior,  $E_{opL1\phi}$  and  $E_{opL2\phi}$ , from pre-fault steady state to fault steady state. Thus, it is possible to verify whether the evaluated algorithm presents oscillatory or stable behavior. In this thesis, a specific case of solid SLG fault applied in 1% of circuit one was evaluated in transient state without and with CT saturation. Load and inception angle were kept at  $10^\circ$  and  $45^\circ$ , and the local source is set to be stronger than the remote, as described in Table 5.1.

**Table 5.1.** Considered cases for the transient analysis evaluation.

Case	Fault Type	$d$ (%)	$R_F$ ( $\Omega$ )	$F_L$	$F_R$
01	SLG	1	0.0	1.0	2.5
02	SLG with CT Saturation	1	0.0	1.0	2.5

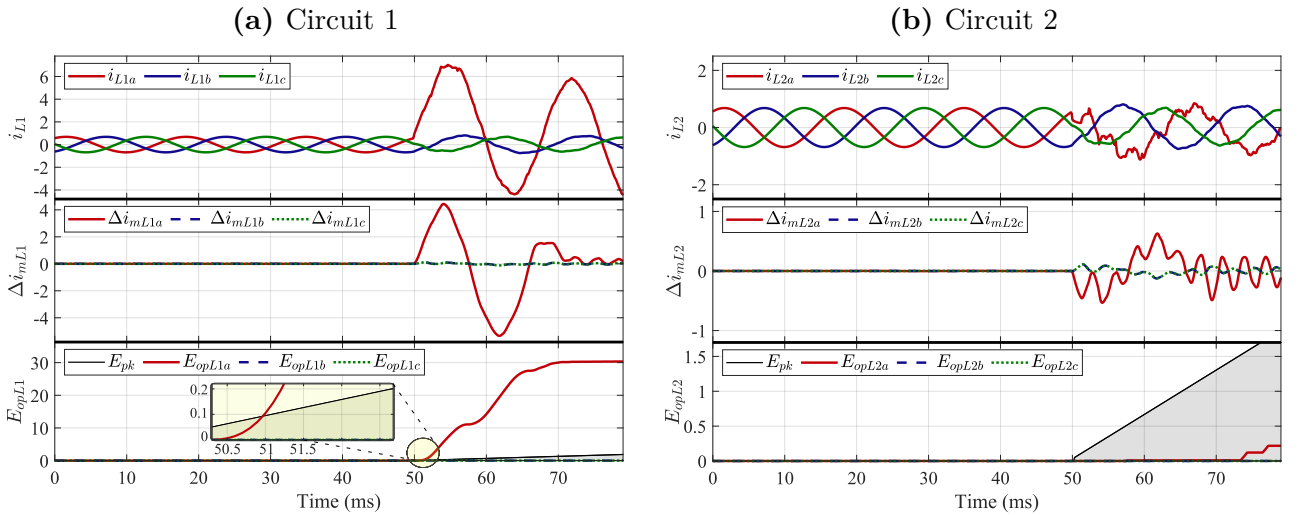
**Source:** Own authorship.

The parameter  $d$  represents the fault location in relation to the local terminal, in percentage

of the line length, while  $R_F$  represents the fault resistance and the parameters  $F_L$  and  $F_R$  are the multiplier variables of Thévenin equivalents connected to the line terminals, which determine the strength of the local and remote sources, respectively. Hence, the higher the value of the multiplier parameter, the higher the equivalent impedance and the lower the short-circuit contribution current coming from that terminal.

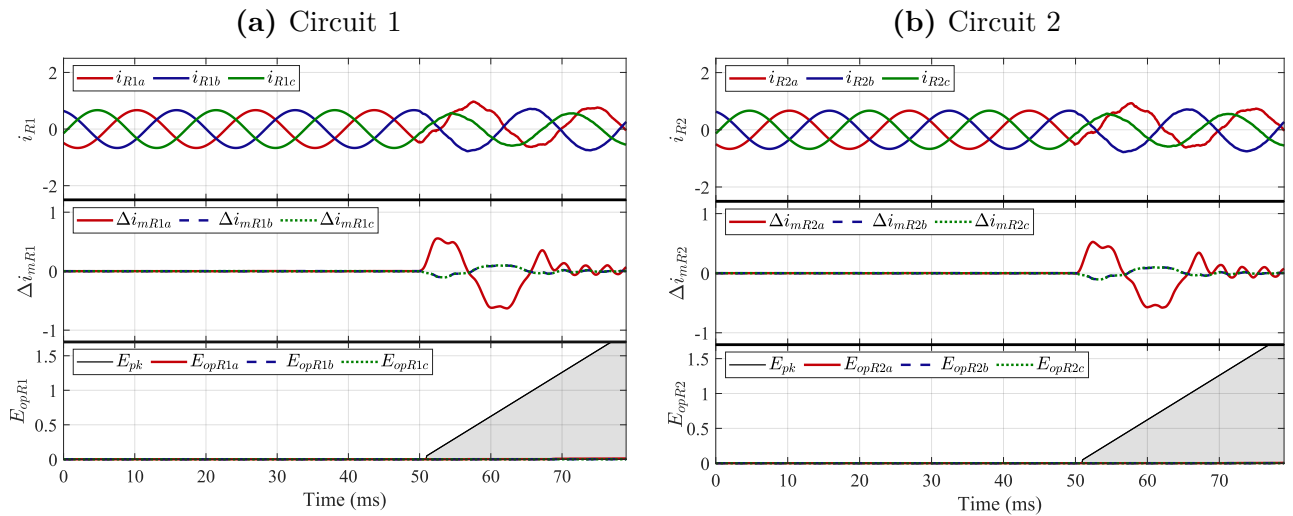
Results portrayed in Figures 5.3 and 5.4 illustrate the behavior of the proposed algorithm under normal operation. For each transmission line terminal, two figures are obtained, representing circuits 1 and 2. Both are composed of current signals read by the relay, incremental mimic currents supplied by the relay as well as operating coefficients and pickup values obtained from the algorithm.

**Figure 5.3.** Local terminal without CT saturation.



**Source:** Own authorship.

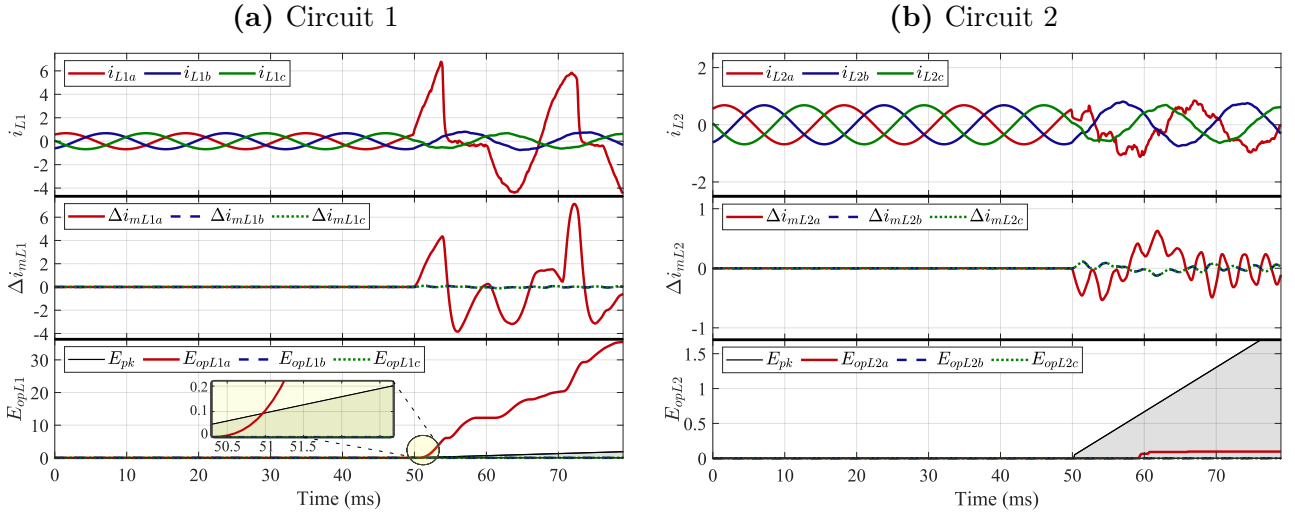
Analyzing Figures 5.3(a) and 5.3(b), which consider the local terminal of the double circuit transmission line, it is possible to notice that both circuits undergo changes in their current signals, as well as in their incremental replica currents. Phase segregated integrated operating conditions from each of the analyzed circuits are obtained, and through these elements analysis it can be seen that, for circuit 1, only phase A exceeds the predefined value of integrated pickup, ensuring the correct performance of the algorithm. Furthermore, for circuit 2, operating coefficient of phase A shows variation in its value, but it remains lower than pickup, ensuring security of the proposed algorithm.

**Figure 5.4.** Remote terminal without CT saturation.**Source:** Own authorship.

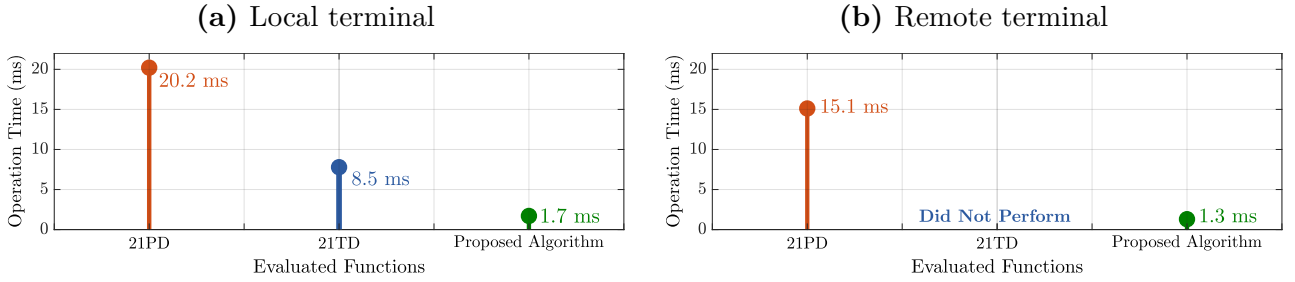
Comparatively, considering the remote terminal of the evaluated double circuit line, Figures 5.4(a) and 5.4(b) are obtained. Through its analysis it is observed that both circuits are affected during the short-circuit, but in this case the faulted circuit phase element is not affected. That is explained because the SLG fault was applied at 1% of the line, considering the local terminal as reference. So, the fault took place at 99% of the transmission line from the remote terminal standpoint. Additionally, the remote source is 2.5 times weaker than the local source, hence the short-circuit contribution provided from both circuits at the remote termination of the line are very similar.

In Case 02, the local terminal CT's burden was set higher than its adjustment for circuit 1 of the transmission line in order to evaluate the algorithm's performance during saturation. Both circuits of the transmission line considering its local terminal are presented in Figures 5.5(a) and 5.5(b) where it can be noted that the CT saturation does not play an influence on the correct performance of the proposed algorithm. It is clear that only the correct operating coefficient is affected. As expected, the remote terminal operation remains the same as previously shown in Figures 5.4(a) and 5.4(b).

The illustration of phasor and time domain distance protection functions transient response is not feasible, as the data needed to reproduce their representation plane is not provided by the relay. However, it is possible to analyze functions embedded in these devices operating times. Figure 5.6 exhibits the operation of the proposed algorithm, phasor and time domain distance

**Figure 5.5.** Remote terminal without CT saturation.**Source:** Own authorship.

protection functions considering a SLG fault at 30% of the transmission line and considering weak local source and strong remote source,  $F_L = 2.5$  and  $F_R = 1.0$ .

**Figure 5.6.** Operation time of evaluated functions in comparison with the proposed algorithm.**Source:** Own authorship.

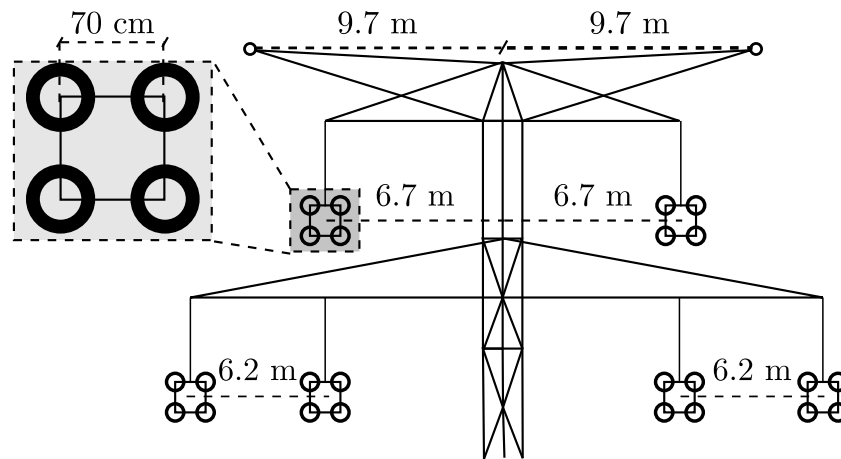
Note from Figure 5.6(a) that 21PD and the proposed algorithm exhibit good performance, operating at both line ends. It is possible to calculate a difference of 18.5 ms between their operation times at local terminal, and 13.8 ms at remote end. Furthermore, although the 21TD function has a shorter operating time than 21PD, it operates only at the local end of the transmission line. It can be concluded that the proposed algorithm could present itself as a companion function to be implemented with readily available protection functions in commercial relays.



### 5.4.2 Zero-sequence Mutual Coupling Variation Analysis

Considering the transmission tower geometry displayed in Figure 5.7, parameters related to the position of phase conductors and ground wires are inserted into the line constant module in ATP. The module calculates line parameters, including mutual coupling values, from the input of cables geometric arrangement and their electrical characteristics.

**Figure 5.7.** Position and distance between cables on the evaluated transmission tower.



**Source:** Own authorship.

In order to test the proposed algorithms performance under zero-sequence mutual coupling variation, transmission line parameters were purposely altered and varied from -15% to 15% of their original values. This variation considers specifically horizontally phase and ground cables geometry, essentially making both circuits closer or further apart.

The simulations performed to pursue this analysis considered two different fault locations, 50% and 70% of the transmission line, more specifically at circuit 1 of the double circuit line, four different fault types and fault resistances of 0  $\Omega$ , 25  $\Omega$  and 50  $\Omega$  and considering  $F_L = 1.5$  and  $F_R = 1.5$ , as described in Table 5.2.

#### 5.4.2.1 Mutual Coupling Variation for Faults in 50% of Circuit 1

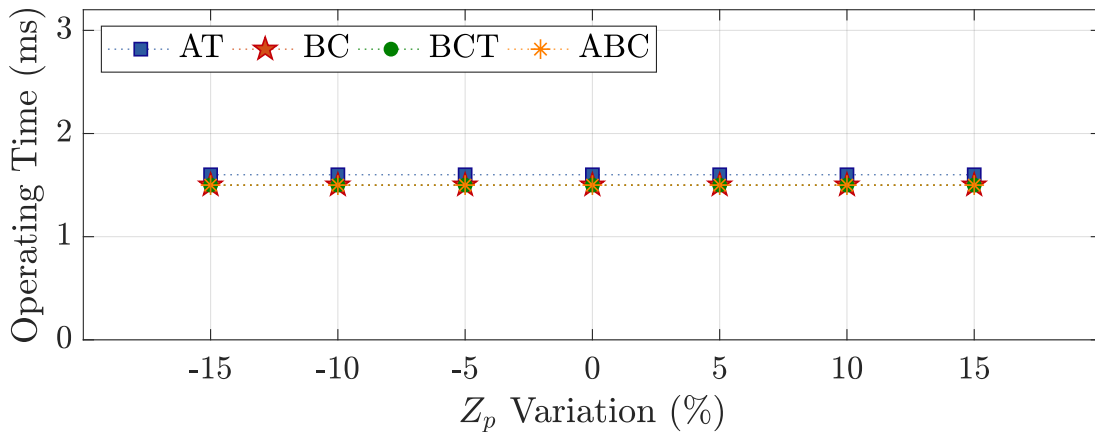
From Figures 5.8, 5.9 and 5.10 it is concluded that the performance of the proposed algorithm remains unaffected by variations in zero-sequence coupling. Its efficiency is consistent for the 30% range of variations, including when significant fault resistance values were

**Table 5.2.** Considered cases for the zero-sequence coupling variation analysis.

Case	Fault Type	$d$ (%)	$R_F$ ( $\Omega$ )	$F_L$	$F_R$
01	Fault Type	50	0.0	1.5	1.5
02	Fault Type	50	25.0	1.5	1.5
03	Fault Type	50	50.0	1.5	1.5
04	Fault Type	70	0.0	1.5	1.5
05	Fault Type	70	25.0	1.5	1.5
06	Fault Type	70	50.0	1.5	1.5

**Source:** Own authorship.

contemplated. Furthermore, operating time is stable and fast across all evaluated scenarios, maintaining operation under 3 ms.

**Figure 5.8.** Zero-sequence mutual coupling variation for solid faults on circuit 1 at 50% of the line.

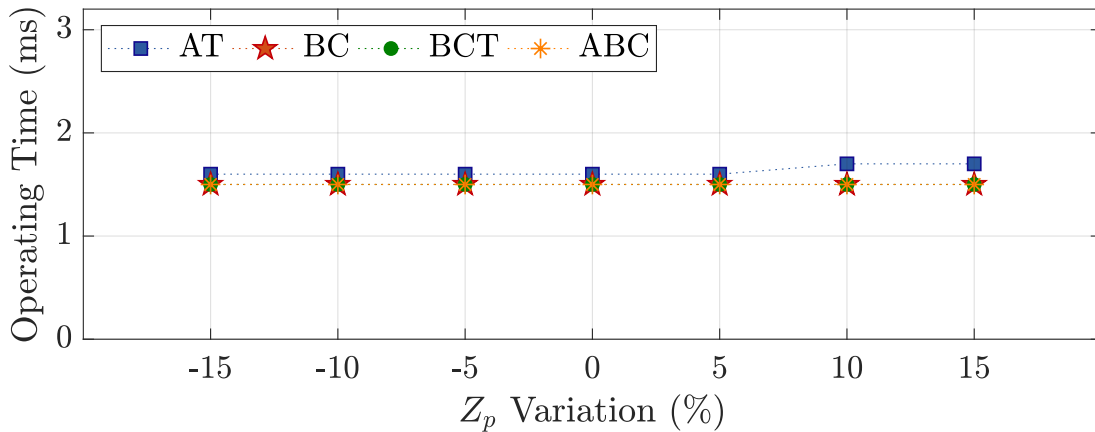
**Source:** Own authorship.

Considering the transient analysis disclosed in Figure 5.11, it can be detected from the positions of each plot line that operating time tends to decrease as variations lead to greater proximity between circuits. In contrast, when they are positioned farther apart, the proposed algorithm's operating time increases. Despite being small increments or decrements on the proposed algorithm's operating time, it is coherent with mutual coupling theory.

#### 5.4.2.2 Mutual Coupling Variation for Faults in 70% of Circuit 1

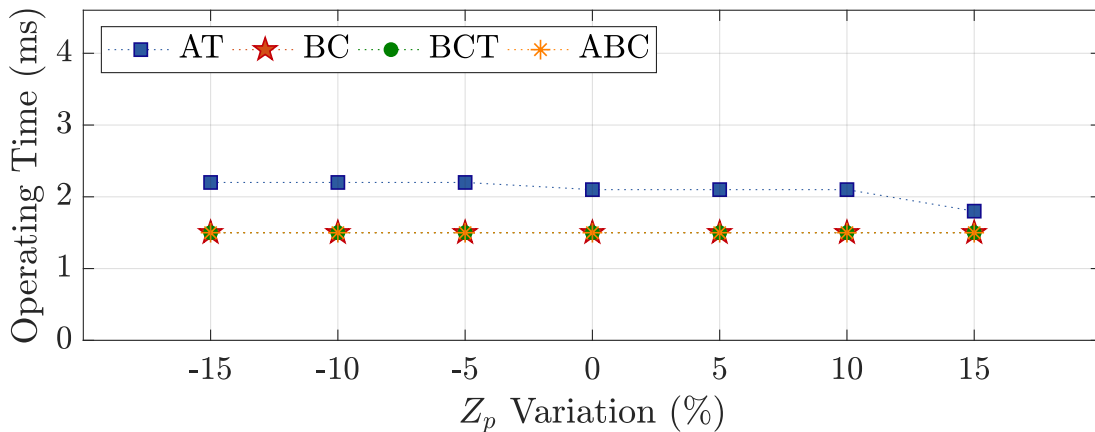
Figures 5.12, 5.13 and 5.14 present the proposed algorithms solid and quick response under four different fault types taking place at 70% of the transmission line, and considering three

**Figure 5.9.** Zero-sequence mutual coupling variation for faults on circuit 1 at 50% of the line, considering 25  $\Omega$  resistance.



**Source:** Own authorship.

**Figure 5.10.** Zero-sequence mutual coupling variation for faults on circuit 1 at 50% of the line, considering 50  $\Omega$  resistance.



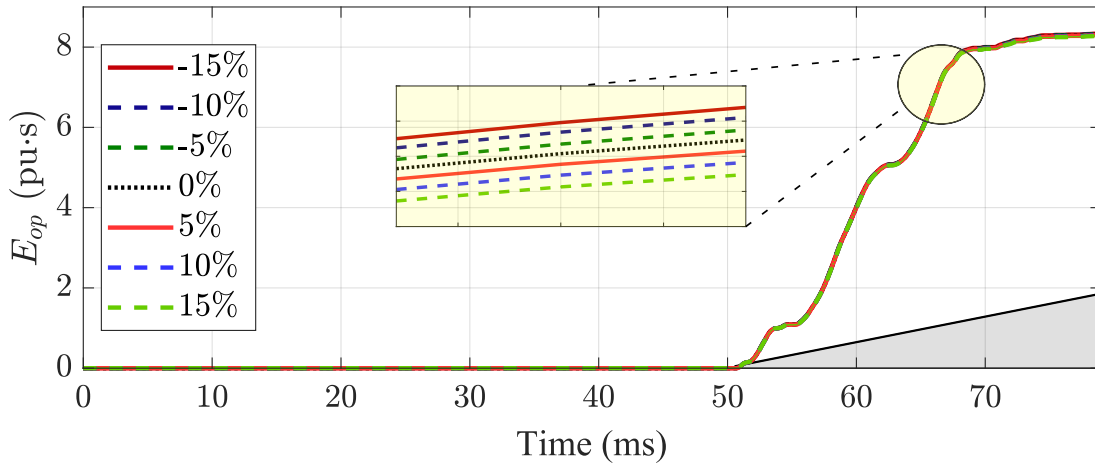
**Source:** Own authorship.

distinct fault resistance values. Also, strong local and remote source strengths are selected,  $F_L = 1.5$  and  $F_R = 1.5$ , respectively.

As evident, the sole difference from the previous analysis is the fault location. Consequently, the proposed algorithm's remained consistent performance under mutual coupling variation can be recognized. Operating time falls under 4 ms for all cases. From Figure 5.15, the exact same evaluations, expressed in the former investigation, can be made.

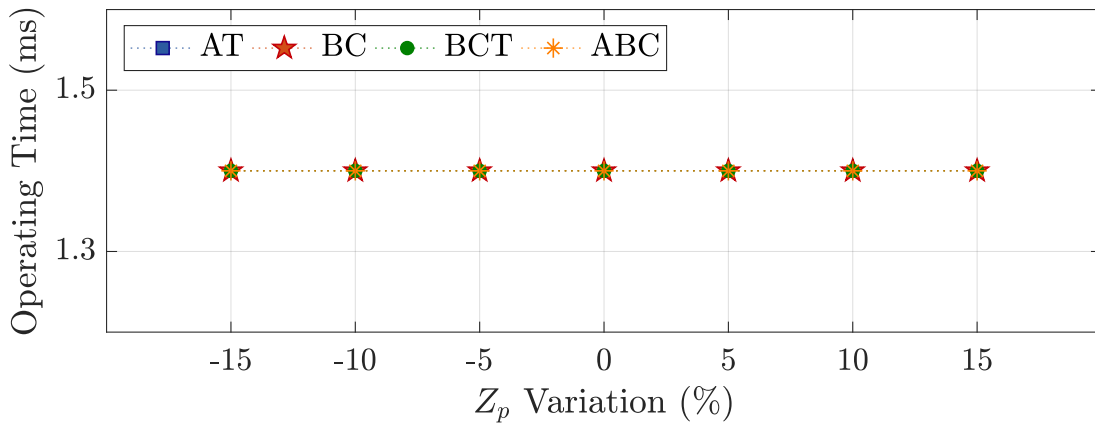
Considering the transient analysis disclosed in Figure 5.11, it can also be detected that, for variations resulting in greater circuits proximity, operating time is faster. And the further the circuits are from each other, the slower the proposed algorithm's operation is.

**Figure 5.11.** Transient analysis of SLG fault on circuit 1 at 50% of the line, considering 25  $\Omega$  resistance.



Source: Own authorship.

**Figure 5.12.** Zero-sequence mutual coupling variation for solid faults on circuit 1 at 70% of the line.

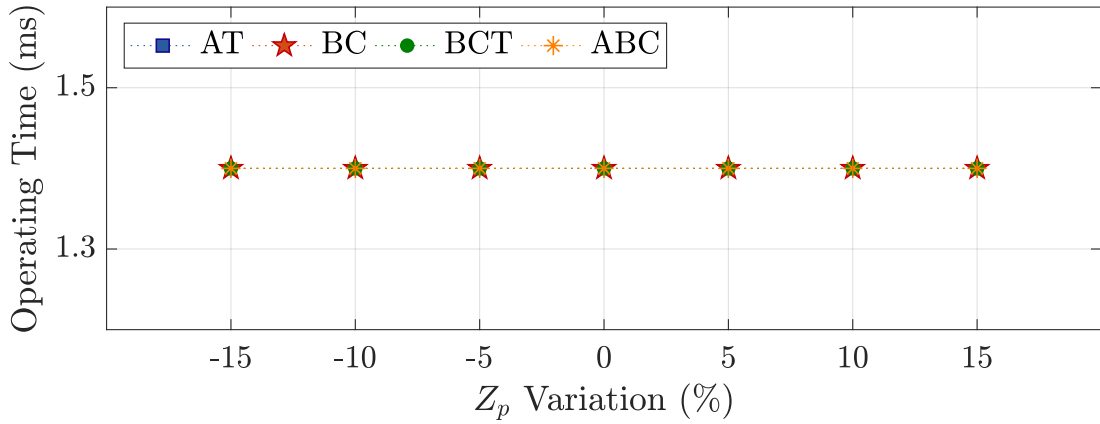


Source: Own authorship.

### 5.4.3 Parametric Sensitivity Fault Analysis

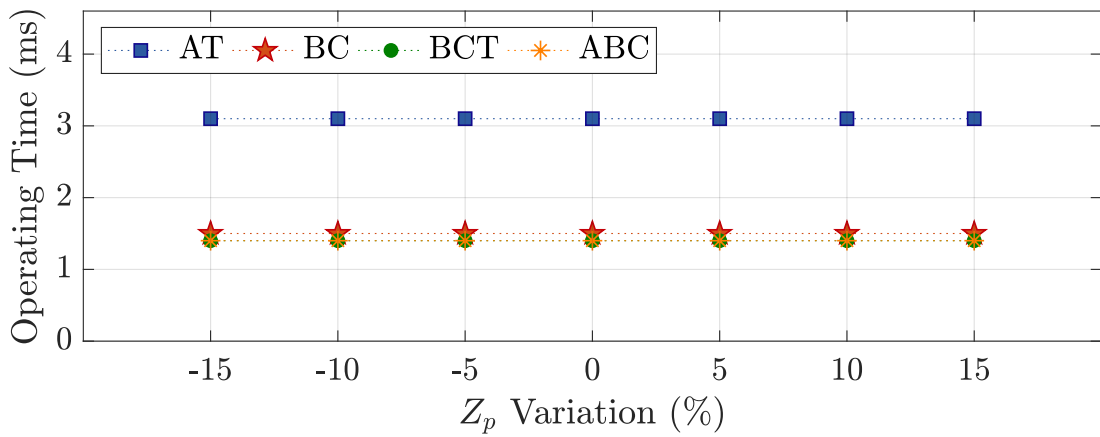
To evaluate the performance of the proposed algorithm and compare it with phasor and time-domain distance functions, parametric sensitivity analysis were performed. Parametric sensitivity analysis evaluate the protection functions performance during steady state fault condition considering the variation of specified parameters. In this thesis, cases of fault location and resistance variation were considered for the evaluated system, contemplating different sources strength scenarios, as shown in Table 5.3. Inception and load angle were kept at  $90^\circ$  and  $10^\circ$  for all evaluated cases, respectively.

**Figure 5.13.** Zero-sequence mutual coupling variation for faults on circuit 1 at 70% of the line, considering 25  $\Omega$  resistance.



Source: Own authorship.

**Figure 5.14.** Zero-sequence mutual coupling variation for faults on circuit 1 at 70% of the line, considering 50  $\Omega$  resistance.



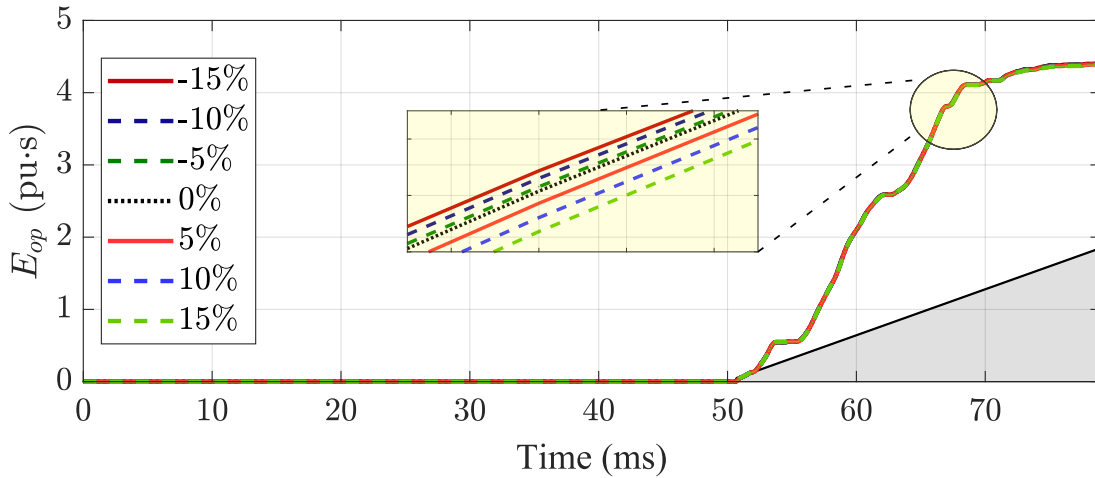
Source: Own authorship.

**Table 5.3.** Considered cases for the parametric sensitivity analysis evaluation.

Case	Fault Type	$d$ (%)	$R_F$ ( $\Omega$ )	$F_L$	$F_R$
01	SLG	$d$	0.0	1.0	2.5
02	SLG	$d$	0.0	1.0	5.0
03	SLG	$d$	0.0	1.5	1.5
04	SLG	$d$	50.0	1.5	1.5
05	SLG	1	$R_F$	1.5	1.5
06	SLG	50	$R_F$	1.0	5.0
07	SLG	30	$R_F$	1.5	1.5
08	SLG	30	$R_F$	1.0	5.0

Source: Own authorship.

**Figure 5.15.** Transient analysis of SLG fault on circuit 1 at 70% of the line, considering 25  $\Omega$  resistance.



**Source:** Own authorship.

For the results, only SLG faults were considered, since these correspond to 85% of short-circuits observed in transmission lines (PAITHANKAR; BHIDE, 2011).

#### 5.4.3.1 Case 01: Fault Location Variation - Considering Strong Local Source and Weak Remote Source

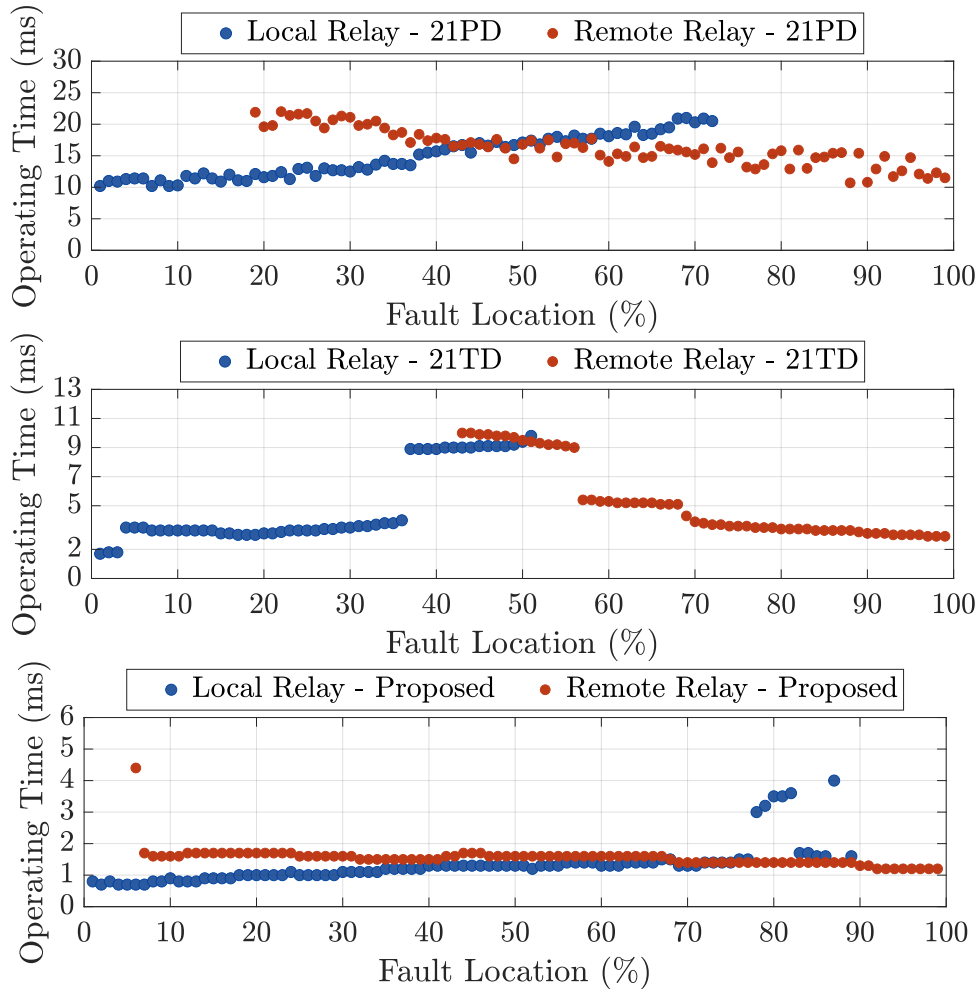
In Case 01, fault location variation of a SLG fault in circuit 1, involving phase A, is evaluated. The fault location parameter was varied from 1% to 99% in 1% steps considering strong local source and weak remote source,  $F_L = 1.0$  and  $F_R = 2.5$ .

Figure 5.16 depicts the performance of 21PD and 21TD functions as well as the proposed algorithm. Phasor-based distance elements provide line coverage of 72% and 81% for local and remote relays, respectively, resulting in 54% of the protected line coverage for instantaneous operation (i.e., when the zone 1 of both local and remote relays operates), and an average operating time of 16 ms.

Results from time-domain distance elements show local and remote coverage as 51% and 57%, respectively, leading to only 9% of instantaneous protection coverage and average operating time of 7.9 ms.

For the proposed algorithm, results portray a flat performance regarding operating time considering both local and remote relays, in addition to having a higher line coverage. As a

**Figure 5.16.** Case 01 - Fault location variation for a solid SLG fault on phase A of circuit 1, considering  $F_L = 1.0$  and  $F_R = 2.5$ .



**Source:** Own authorship.

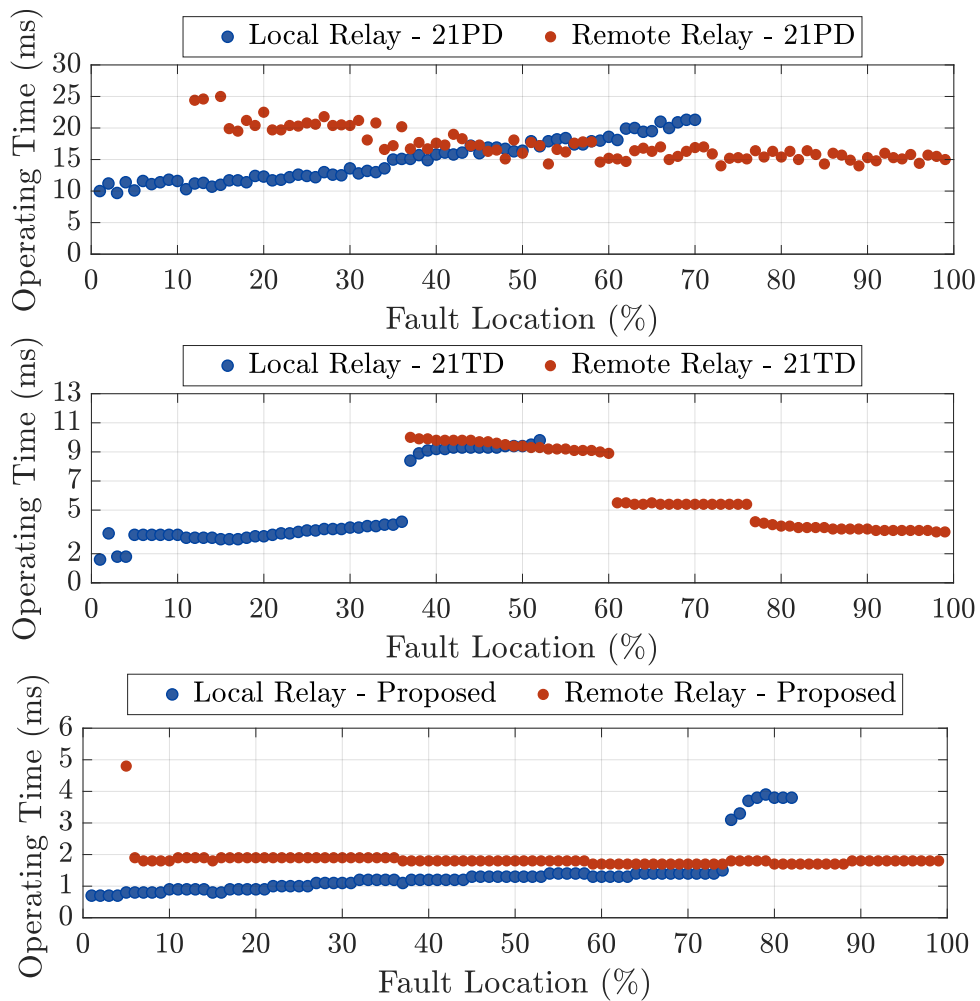
result, line coverages of 89% and 94% were obtained for local and remote terminals, respectively, resulting in a total instantaneous operation coverage of 84% of the transmission line and an average operating time of 1.6 ms.

Differences of 40% and 75% are detected for instantaneous coverage of the transmission line in which the proposed algorithm has an advantage in relation to 21PD and 21TD, respectively. Delays of 14.4 ms and 6.3 ms in the average operating time of functions 21PD and 21TD are also verified when compared with the proposed algorithm. Therefore, the proposed algorithm successfully accomplishes its intended objective of demonstrating fast performance and providing larger instantaneous protection coverage for transmission lines. In addition to validating its immunity to zero sequence mutual coupling effects on the protection function performance.

### 5.4.3.2 Case 02 - Fault Location Variation - Considering Strong Local Source and Weaker Remote Source

In Case 02, fault location variation of a SLG fault in circuit 1, involving phase A, is evaluated. The fault location parameter was also varied from 1% to 99% in 1% steps considering strong local source and a weaker remote source compared to Case 01,  $F_L = 1.0$  and  $F_R = 5.0$ .

**Figure 5.17.** Case 02 - Fault location variation for a solid SLG fault on phase A of circuit 1, considering  $F_L = 1.0$  and  $F_R = 5.0$ .



**Source:** Own authorship.

In Figure 5.17 the performance of the proposed algorithm was compared with the evaluated protection functions considering Case 02.

Phasor-based distance protection function operates for faults up to 70% and 87% of the line for local and remote relays, respectively. Which results in 53% of the line protected by the instantaneous mode (i.e, when the zone 1 of both local and remote relays operates), and



an average operating time of 15.9 ms. The remote relay presents a 7% overreach, since the distance element setting was at 80%. This can be explained by the remote source strength – a weak source.

Time-domain-based distance function reveals local and remote line coverage of 52% and 63%, respectively, issuing an instantaneous coverage of 16% and 7.6 ms average operating time.

The proposed algorithm presents 82% and 95% line coverage for local and remote terminals, respectively. As a result, 78% of the transmission line is instantaneously protected with an average operating time of 1.5 ms. Instantaneous coverage differences of 20% and 62%, in which the proposed algorithm has an advantage in relation to 21PD and 21TD, respectively, are identified. Delays of 14.4 ms and 6.3 ms in the average operating time of functions 21PD and 21TD are also verified when compared with the proposed algorithm.

#### 5.4.3.3 Case 03: Fault Location Variation - Considering Local and Remote Sources as Strong

The analysis of the fault location variation exhibited for the next two cases aims to evaluate and evidence the influence of fault resistance on instantaneous operation coverage along the transmission line. To do so, the fault location is varied in the range between 1% and 99% of the line, while a phase A SLG fault in circuit 1 is applied and both sources are considered strong,  $F_L = 1.5$  and  $F_R = 1.5$ .

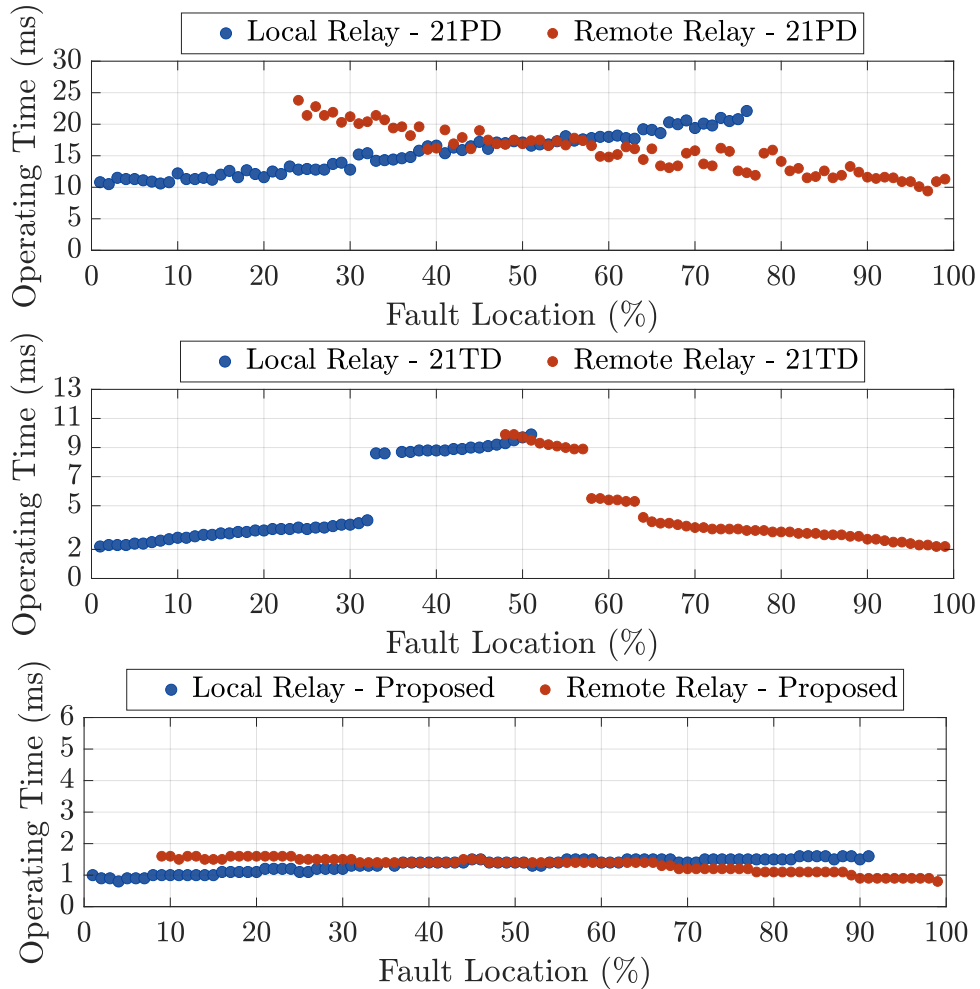
The results obtained for Case 03, in which a solid SLG fault is considered, are shown in Figure 5.18. In this way, the operating time for phasor and time-domain distance protection function and the proposed algorithm, are evaluated.

In accordance with the above, it can be seen that the instantaneous coverage of the transmission line, when using the 21PD protection function, is 53%. Local and remote coverage being both 76%. Also, the average operating time for these overlapped cases is 15.8 ms.

The performance of time-domain distance protection function observed, as the sources strengths are the same, both relays operate to very similar percentage of the line, 51% and 53%, respectively. This results in an instantaneous coverage of 4% with average time of 7.8 ms.

The proposed algorithm performance has instantaneous coverage of 83% of the protected

**Figure 5.18.** Case 03 - Fault location variation for a solid SLG fault on phase A of circuit 1, considering  $F_L = 1.5$  and  $F_R = 1.5$ .



Source: Own authorship.

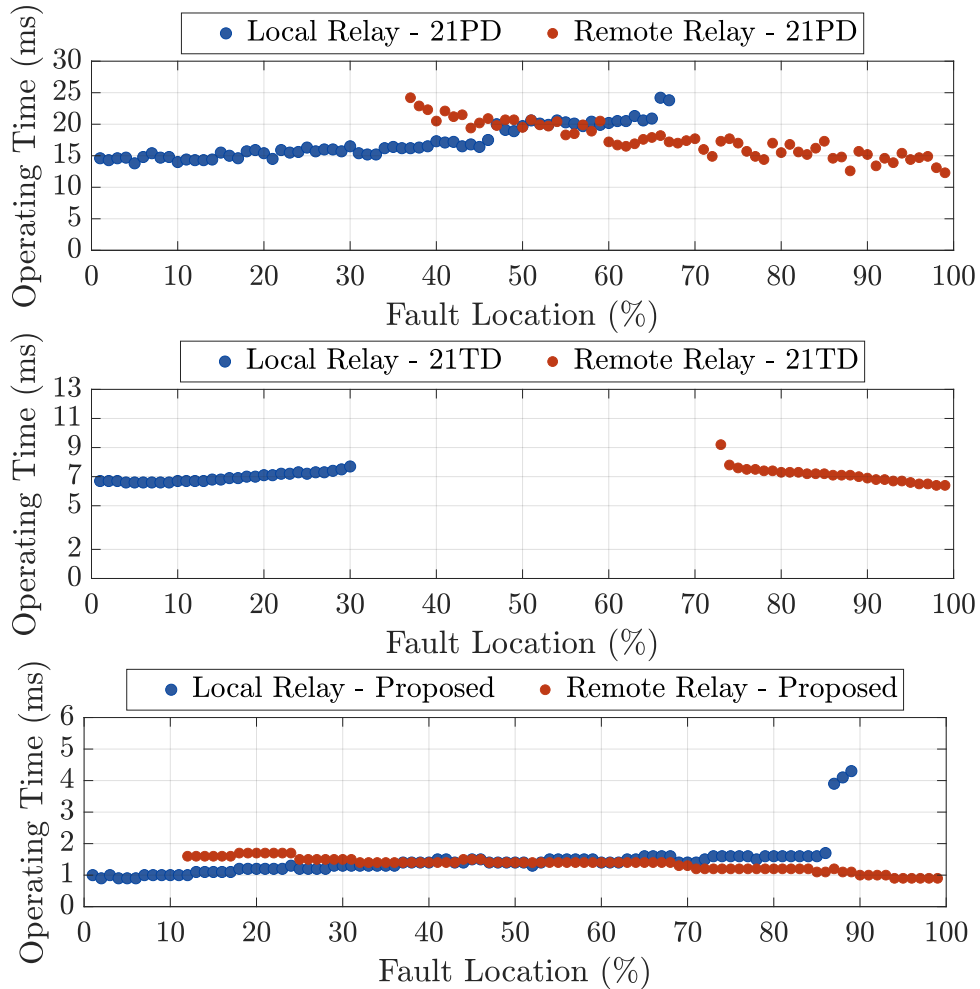
transmission line. Also, its average instantaneous operating time is 1.5 ms. Local and remote terminals display the same line protection reach of 91%.

#### 5.4.3.4 Case 04: Fault Location Variation - Considering Local and Remote Sources as Strong and Fault Resistance

For Case 04, source strengths remain the same as previous case,  $F_L = 1.5$  and  $F_R = 1.5$ , but the SLG short-circuit in phase A is no longer solid and presents a fault resistance of  $50 \Omega$ . Functions 21PD, 21TD and the proposed algorithm performance are shown in Figure 5.19.

It can be seen that the phasor distance element is strongly influenced by the fault resistance since the  $50 \Omega$  resulted in an instantaneous coverage of 31% of the protected line, a decrease of

**Figure 5.19.** Case 04 - Fault location variation for a SLG fault on phase A of circuit 1 with fault resistance of  $50 \Omega$ , considering  $F_L = 1.5$  and  $F_R = 1.5$ .



**Source:** Own authorship.

22% when compared to Case 02. Local and remote coverage being 67% and 63%. In addition, the average operating time is 18.4 ms, 2.6 ms slower than the previous evaluated case.

The time-domain distance protection function is most affected by the increase of fault resistance when SLG short circuit is applied, as shown in Figure 5.19. With local and remote operating ranges of 30% and 27% of the transmission line extension, provided outputs do not portray an overlap in the operating range, that is, the 21TD function underreached and there is no instantaneous coverage for the protected line. Hence, the average operating time for the 21TD is made not considering overlapped value, and results in 6.1 ms.

Figure 5.19 also shows the constant and flat behavior of the proposed algorithm, in which the range remains high even with the presence of a considerable fault resistance value. The

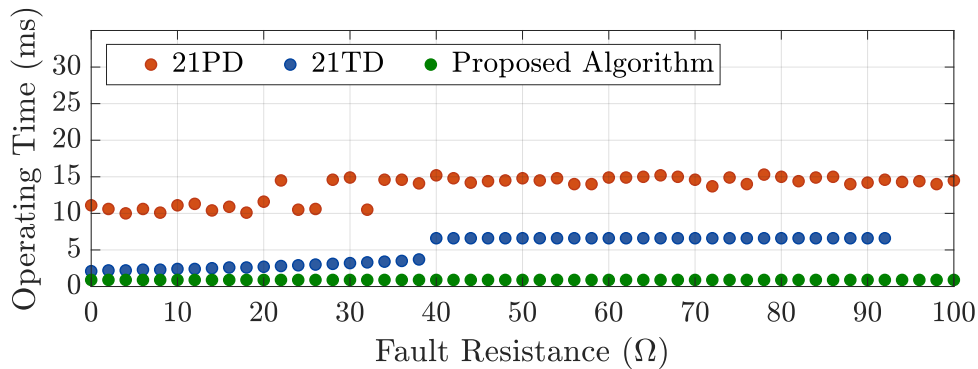
instantaneous coverage of the transmission line is little affected and represents 78% of the line, local and remote protection ranges of 89% and 88%, respectively. For overlapped outputs the average operating time of 1.6 ms.

#### 5.4.3.5 Case 05: Fault Resistance Variation - Solid SLG Phase A Fault in 1% of Circuit 1

It is observed through the comparison of the two behaviors evaluated with Cases 03 and 04, that the variation of the fault resistance practically does not interfere in the performance of the proposed algorithm. In order to prove this observation, Cases 05 to 08 aim to evaluate the influence of fault resistance in a SLG fault.

In Case 05,  $R_F$  is varied in the range of 0 to 100  $\Omega$  while a SLG fault in phase A is applied at 1% of the protected transmission line and both sources are considered strong:  $F_L = 1.5$  and  $F_R = 1.5$ . The performances of functions 21PD, 21TD and the proposed algorithm are shown in Figure 5.20, representing the local terminal viewpoint.

**Figure 5.20.** Case 05 - Fault resistance variation for a SLG fault on phase A of circuit 1 with fault location of 1%, considering  $F_L = 1.5$  and  $F_R = 1.5$  - Local terminal results.



**Source:** Own authorship.

From Figure 5.20 the dependability of inspected functions over severe fault condition, a short-circuit very close to a strong source, is recognized. All compared functions accommodated correct operation, for most cases, under a wide range of fault resistances.

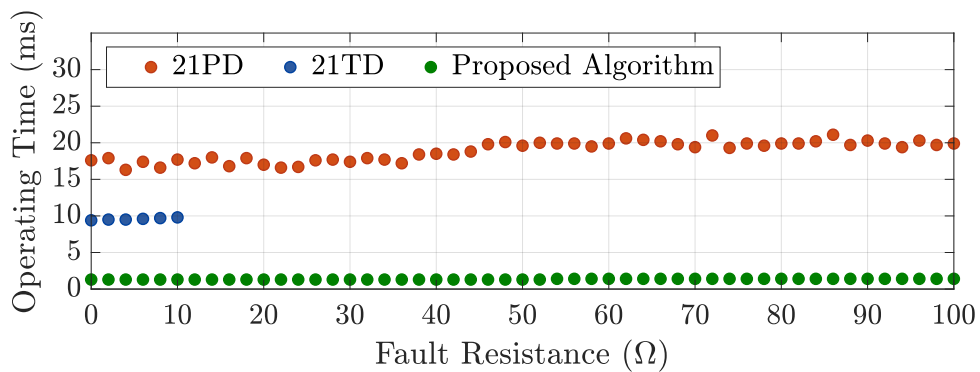
A fault taking place at 1% of the transmission line, considering local terminal as reference, means the fault would be taking place at 99% of the line from remote terminal point of view.

With that into account, the non operation of the analyzed functions is expected.

#### 5.4.3.6 Case 06: Fault Resistance Variation - Solid SLG Phase A Fault in 50% of Circuit 1

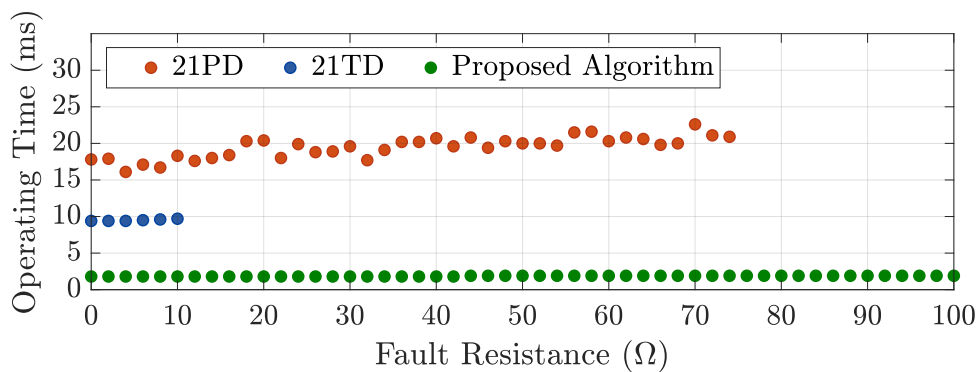
With Case 06, the same evaluation from the previous case is made, considering a fault at 50% of the transmission line. For Case 06,  $R_F$  varies in the range of 0 to 100  $\Omega$  for a phase A fault applied at 50% of the protected transmission line and local sources is considered strong,  $F_L = 1.0$ , while remote source is set to be weak,  $F_R = 5.0$ . The functions performance from local and remote terminal are shown in Figures 5.21 and 5.22.

**Figure 5.21.** Case 06 - Fault resistance variation for a SLG fault on phase A of circuit 1 with fault location of 50%, considering  $F_L = 1.0$  and  $F_R = 5.0$  - Local terminal results.



Source: Own authorship.

**Figure 5.22.** Case 06 - Fault resistance variation for a SLG fault on phase A of circuit 1 with fault location of 50%, considering  $F_L = 1.0$  and  $F_R = 5.0$  - Remote terminal results.



Source: Own authorship.

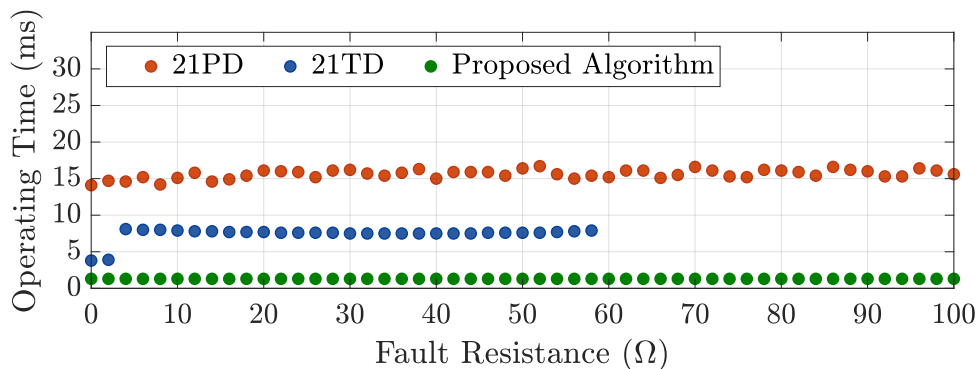
By evaluating the results, it can be seen that source strengths made a significant impact

for 21PD, phasor distance protection, 74  $\Omega$  remote reach, and not for its time domain function, with 21TD operating correctly up to 10  $\Omega$  for both local and remote viewpoint. As for the proposed algorithm, it can be seen that it operates regardless of the fault resistance employed.

#### 5.4.3.7 Case 07: Fault Resistance Variation - Solid SLG Phase A Fault in 30% of Circuit 1

For Cases 07 and 08, besides the evaluation of fault resistance influence during a SLG fault, it will be possible to examine how source strengths can affect the evaluated functions performance. Fault resistance  $R_F$  is varied in the range of 0 to 100  $\Omega$ , for Case 07, while a SLG fault in phase A is applied at 30% of the protected transmission line and both sources are considered strong:  $F_L = 1.5$  and  $F_R = 1.5$ .

**Figure 5.23.** Case 07 - Fault resistance variation for a SLG fault on phase A of circuit 1 with fault location of 30%, considering  $F_L = 1.5$  and  $F_R = 1.5$  - Local terminal results.

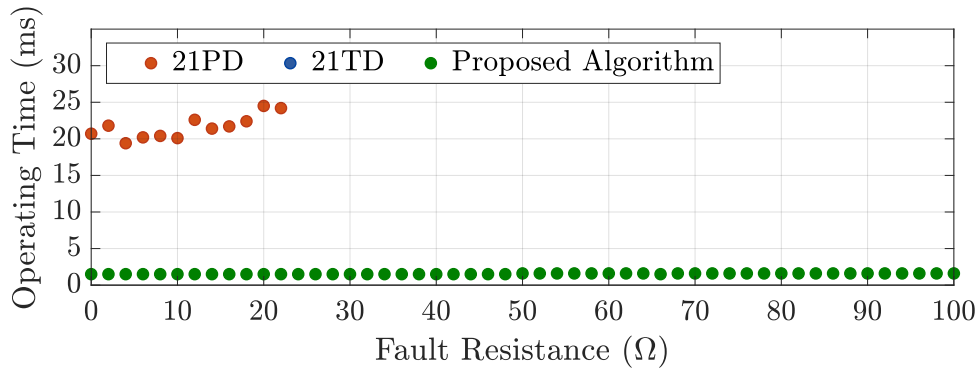


**Source:** Own authorship.

The results shown in Figures 5.23 and 5.24 display the performance of 21PD, 21TD and the proposed algorithm for local and remote terminals, respectively. Even though both sources are considered strong, different behavior is presented due to the fault location and how it is referenced to the local terminal. Thus, for Figure 5.24, the fault is actually taking place at 70% of the transmission line, which justifies distance protection functions operation.

Considering results obtained from the local terminal, phasor-based distance elements exhibit correct operation across all simulated fault resistance values, mirroring the behavior of the proposed algorithm. However, it is evident that time domain-based distance protection is highly influenced by variations in fault resistance, operating for SLG faults that consider

**Figure 5.24.** Case 07 - Fault resistance variation for a SLG fault on phase A of circuit 1 with fault location of 30%, considering  $F_L = 1.5$  and  $F_R = 1.5$  - Remote terminal results.



**Source:** Own authorship.

fault resistance values up to 58  $\Omega$ . This influence is more pronounced based on the fault location. For instance, in Figure 5.24, where the fault takes place at 70% of the transmission line, time domain-based distance elements do not operate for any simulated value. Moreover, phasor-based distance protection experiences a considerable reduction in its correct operation, triggering its element only until 22  $\Omega$ .

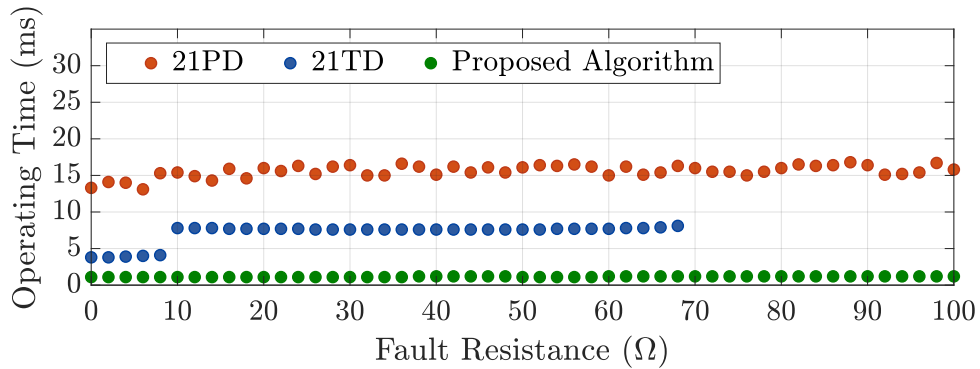
#### 5.4.3.8 Case 08: Fault Resistance Variation - Solid SLG Phase A Fault in 30% of Circuit 1

For Case 08,  $R_F$  continue to be varied in the range of 0 to 100  $\Omega$  while a SLG fault in phase A is applied at 30% of the protected transmission line. On the other hand, for this case source strengths are different. Local source is considered strong,  $F_L = 1.0$ , and remote source is weak,  $F_R = 5.0$ .

Figure 5.25 depicts local terminal performance and it can be seen that time-domain distance protection function operates correctly considering fault resistances up to 68  $\Omega$ , which represents a higher sensitivity when compared to Case 07. As for Figure 5.26, it discloses the lack of operation regards 21TD, which was expected considering the fault location of 70% from the remote viewpoint.

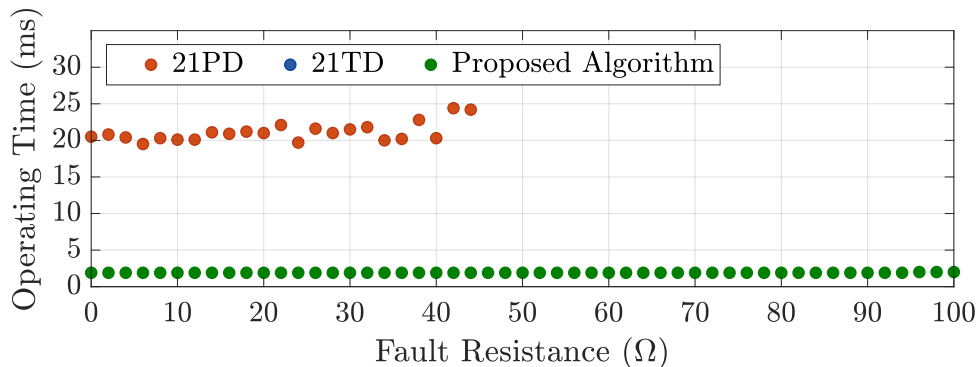
As shown, the proposed algorithm's performance is not affected by fault resistance variation when considering the evaluation range shown in this research. Function 21PD's operation

**Figure 5.25.** Case 08 - Fault resistance variation for a SLG fault on phase A of circuit 1 with fault location of 30%, considering  $F_L = 1.0$  and  $F_R = 5.0$  - Local terminal results.



**Source:** Own authorship.

**Figure 5.26.** Case 08 - Fault resistance variation for a SLG fault on phase A of circuit 1 with fault location of 30%, considering  $F_L = 1.0$  and  $F_R = 5.0$  - Remote terminal results.



**Source:** Own authorship.

depends on the fault location, but it operates correctly for the most part of evaluated  $R_F$  values examined. This behavior is justified by the fact that quadrilateral characteristic was adjusted in the relay alongside mho characteristic for ground elements. Hence, considering that in the  $R-X$  diagram quadrilateral characteristic covers a considerable part of the  $X$ -axis, higher fault resistance values can be accommodated. The 21TD protection function, has its operation limited and it is very dependent on the fault resistance value, since it was developed considering critical fault scenarios. The proposed algorithm operates for all values of  $R_F$  considered.



## 5.5 ADDITIONAL REMARKS

- The operating principle of cross-differential protection assumes the simultaneous operational condition from both circuits of the transmission line. Consequently, the implementation of the proposed algorithm cannot take place as a stand alone function, requiring a companion relay or protection function to be employed alongside it.
- The proposed algorithm was designed to operate exclusively in the instantaneous operating mode, due to the use of incremental quantities. Commercial relays often employ delta filters to compute incremental quantities, and such filters are affected by difficulties that could potentially compromise the security of operation in successive mode (BEN-MOUYAL; ROBERTS, 1999). This is another reason as to why it is imperative for this algorithm to operate in conjunction with a companion protection function to ensure reliable operation.
- A greater concentration of cables is required to measure currents from both circuits of the transmission line. Nonetheless, this does not suggest a technological limitation. For instance, this drawback can be entirely mitigated with the employment of digital substations.
- The potential application of the proposed algorithm might demand a relay capable of measuring four sets of three-phase currents, depending on the specific bus configuration, such as breaker and a half. Although not all commercially available relays are designed to measure more than two sets of currents, certain manufacturers offer the option to expand the number of current measurement sets. Meaning that different bus configurations also do not impose a technological limitation.
- Communication between relays was not considered during the comparison with 21PD and 21TD. Nonetheless, the proposed algorithm exhibited superior performance in range and in instantaneous coverage. Considering unit protection schemes, the proposed algorithm remains beneficial. If associated with a Direct Transfer Trip (DTT) scheme, the percentage of the line not protected by instantaneous coverage becomes instantaneously protected.

- Cross-differential protection function inherently provides security for external faults. However, in cases where the circuits do not share the same transmission tower and carry distinct parameters, there is a possibility of false trip commands being issued. To overcome this drawback, the equations (4.5) and (4.6) are proposed aiming to balance the currents of both circuits and avoid protection malfunctions.
- Moreover, from a practical viewpoint, the implementation of the proposed algorithm is simple as it relies on using already processed signals and quantities from commercially available relays.

# CONCLUSIONS AND FUTURE INVESTIGATIONS

In this thesis, a new time domain cross-differential protection algorithm for double circuit transmission lines was presented. The methodology calculates operating and restraining values using incremental replica currents from both circuits at a selected terminal of the transmission line. It is phase segregated, a single terminal based protection, it does not depend on communication channels, its differential nature makes it immune to the effects of zero-sequence coupling and, as time domain-based, it is not limited by inherent time delay regarding phasor estimation.

The proposed method operates without requiring a communication channel between the terminals of the transmission line. It relies solely on the measurement of currents at one of the line terminals. Consequently, data synchronization is also not necessary. Nevertheless, it is recommended to implement the algorithm alongside a companion protection function or relay. That is because cross-differential protection basic principle of operation assumes simultaneous operation of both circuits of the transmission line. Consequently, the proposed algorithm can not be implemented as a stand alone function.

The proposed method's evaluation was carried out through digital fault simulations via ATP/EMTP software, in which a double circuit transmission line modeled with parameters from real electrical systems was considered. Based on the results, the proposed algorithm reveals to be a promising solution for high-speed protection of double circuit transmission lines. It was also demonstrated that time domain cross-differential protection has a simple implementation, and the results demonstrate great benefit in an incorporation of the proposed algorithm within time domain-based protection devices commercially available. Moreover, the proposed algorithm is more robust to fault resistance than protection functions embedded in commercially available relays, and as it is based on incremental replica currents, it is little affected by system loading. The simulated tests conducted indicate that the proposed algorithm's performance remains

---

unaffected by variations in mutual coupling values. The behavior of the proposed algorithm remains minimally affected by fault location and source strength variations. Nevertheless, the algorithm consistently demonstrates superior performance in comparison to other evaluated functions, specifically in terms of operating time and instantaneous transmission line coverage.

Although the analyses presented in this thesis contemplate a diverse range of fault scenarios, proposals aiming to consolidate the proposed algorithm for future investigations and the continued advancement of the study are listed below.

- Develop a prototype of the time-domain cross-differential protection algorithm intended for hardware-in-the-loop testing via real-time simulation, aiming to conduct a comprehensive performance analysis of the proposed protection scheme and its interaction with the examined electrical power system.
- Evaluate the performance of the proposed algorithm within multi-circuit systems and investigate possible adjustments required for its correct operation. Analyze potentially incorporating current mapping strategies to develop an adaptive formulation, suitable for systems featuring multiple parallel lines.
- Conduct tests to ascertain the possibility of integrating the time-domain cross-differential protection algorithm into existing commercially available devices, and evaluate its behavior using real oscillographic records.
- Execute a thorough assessment to further solidify the robustness and adaptability of the performance of the proposed algorithm across a range of scenarios, including lines with diverse voltage levels and lengths, multiple terminals, and series compensation. Performing extensive computational and experimental tests, wherein parameters such as source strength, fault incidence angle, and fault location are systematically altered, and subsequently have their resulting behaviour compared with those of phasor cross-differential protection.

## BIBLIOGRAPHY

- AGENCIA NACIONAL DE ENERGIA ELÉTRICA. *Atlas de Energia Elétrica do Brasil*. Brasília, 2008. Available at <<http://www2.aneel.gov.br/arquivos/pdf/atlas3ed.pdf>>; Accessed in May 2022. Cited in page 1.
- ANDERSON, P. M. *Power System Protection*. Piscataway, New Jersey, EUA: John Wiley & Sons Inc., 1999. Cited in page 9.
- ANDERSON, P. M.; FOUAD, A. A. *Power system control and stability*. [S.l.]: John Wiley & Sons, 2008. Cited in page 3.
- APOSTOLOV, A.; THOLOMIER, D.; SAMBASIVAN, S.; RICHARDS, S. Protection of double circuit transmission lines. In: *2007 60th Annual Conference for Protective Relay Engineers*. [S.l.: s.n.], 2007. p. 85–101. Cited 5 times in pages 2, 7, 8, 10, and 11.
- BENMOUYAL, G.; ROBERTS, J. Superimposed quantities: Their true nature and application in relays. In: *Proceedings of the 26th Annual Western Protective Relay Conference, Spokane, WA*. [S.l.: s.n.], 1999. Cited in page 71.
- BO, Z. Q.; DONG, X. Z.; CAUNCE, B. R.; MILLAR, R. Adaptive noncommunication protection of double-circuit line systems. *IEEE transactions on power delivery*, IEEE, v. 18, n. 1, p. 43–49, 2003. Cited 2 times in pages 2 and 8.
- BOYLESTAD, R. L. *Electronic devices and circuit theory*. [S.l.]: Pearson Education India, 2009. Cited in page 23.
- BP ENERGY ECONOMICS. *Statistical Review of World Energy - 2021*. London - United Kingdom, 2021. Available at <<https://www.bp.com/statisticalreview>>; Accessed in May 2022. Cited in page 1.
- BP ENERGY ECONOMICS. *Energy Outlook - 2022 Edition*. London - United Kingdom, 2022. Available at <<https://www.bp.com/en/global/corporate/energy-economics/energy-outlook>>; Accessed in May 2022. Cited in page 1.
- CALERO, F. Mutual impedance in parallel lines–protective relaying and fault location considerations. *TP6283-01*, p. 1–15, 2007. Cited 3 times in pages 8, 9, and 10.
- CHAMIA, M.; LIBERMAN, S. Ultra high speed relay for ehv/uhv transmission lines – development, design and application. *IEEE Transactions on Power Apparatus and Systems*, PAS-97, n. 6, p. 2104–2116, 1978. Cited 3 times in pages 23, 35, and 38.
- COOK, V. *Analysis of distance protection*: Research studies press ltd. 1985. Cited 2 times in pages 28 and 29.
- COSTA, F. B.; MONTI, A.; LOPES, F. V.; SILVA, K. M.; JAMBORSALAMATI, P.; SADU, A. Two-terminal traveling-wave-based transmission-line protection. *IEEE Transactions on Power Delivery*, v. 32, n. 3, p. 1382–1393, 2017. Cited 2 times in pages 36 and 38.

- COSTA, F. B.; SOBRINHO, A. H. P.; ANSALDI, M.; ALMEIDA, M. A. D. The effects of the mother wavelet for transmission line fault detection and classification. In: *Proceedings of the 2011 3rd International Youth Conference on Energetics (IYCE)*. [S.l.: s.n.], 2011. p. 1–6. Cited in page 43.
- COSTA, F. B.; SOUZA, B. A.; BRITO, N. S. D. A wavelet-based algorithm to analyze oscillographic data with single and multiple disturbances. In: *2008 IEEE Power and Energy Society General Meeting - Conversion and Delivery of Electrical Energy in the 21st Century*. [S.l.: s.n.], 2008. p. 1–8. Cited in page 43.
- DANTAS, D. T.; PELLINI, E. L.; MANASSERO, G. Time-domain differential protection method applied to transmission lines. *IEEE Transactions on Power Delivery*, v. 33, n. 6, p. 2634–2642, 2018. Cited 2 times in pages 36 and 38.
- DOMMEL, H.; BHATTACHARYA, S. *EMTP Theory Book*. [S.l.]: Microtran Power System Analysis Corporation, 1992. Cited 2 times in pages 9 and 48.
- DOMMEL, H. W. High speed replying using traveling wave transient analysis. *IEEE Publications*, IEEE PES Winter Power Meeting, p. 1–7, 1978. Cited in page 23.
- DONG, X.; LUO, S.; SHI, S.; WANG, B.; WANG, S.; REN, L.; XU, F. Implementation and application of practical traveling-wave-based directional protection in uhv transmission lines. *IEEE Transactions on Power Delivery*, v. 31, n. 1, p. 294–302, 2016. Cited 2 times in pages 36 and 38.
- EASTVEDT, R. The need for ultra-fast fault clearing. In: *Third Annual Western Protective Relay Conference*. [S.l.: s.n.], 1976. Cited 2 times in pages 3 and 22.
- EMPRESA DE PESQUISA ENERGÉTICA. *Consumo Nacional de Energia Elétrica na Rede por Classe: 2013 - 2022*. Rio de Janeiro, 2023. Available at <<https://www.epe.gov.br/pt/publicacoes-dados-abertos/publicacoes/Consumo-Anual-de-Energia-Eletrica-por-classe-nacional>>; Accessed in July 2023. Cited in page 1.
- FRANCA, R. L. d. S.; JUNIOR, F. C. d. S.; HONORATO, T. R.; RIBEIRO, J. P. G.; COSTA, F. B.; LOPES, F. V.; STRUNZ, K. Traveling wave-based transmission line earth fault distance protection. *IEEE Transactions on Power Delivery*, v. 36, n. 2, p. 544–553, 2021. Cited in page 35.
- GILANY, M.; MALIK, O.; HOPE, G. A digital protection technique for parallel transmission lines using a single relay at each end. *IEEE transactions on power delivery*, IEEE, v. 7, n. 1, p. 118–125, 1992. Cited 2 times in pages 31 and 38.
- GOMES, M. F. B.; SILVA, K. M. Avaliação da proteção diferencial transversal aplicada às linhas de transmissão de circuito duplo. In: IEEE. *2014 Simpósio Brasileiro de Sistemas Elétricos (SBSE)*. [S.l.], 2014. p. 1–6. Cited 2 times in pages 33 and 38.
- GREENWOOD, A. *Electrical transients in power systems*. New York, NY (USA); John Wiley and Sons Inc., 1991. Cited in page 23.
- GUZMÁN, A.; MYNAM, M. V.; SKENDZIC, V.; ETERNOD, J. L.; MORALES, R. M. Directional elements-how fast can they be? In: *proceedings of the 44th Annual Western Protective Relay Conference*. [S.l.: s.n.], 2017. Cited 2 times in pages 36 and 38.

- GUZMÁN, A.; SMELICH, G.; SHEFFIELD, Z.; TAYLOR, D. Testing traveling-wave line protection and fault locators. In: *Proc. 14th Int. Conf. Develop. Power Syst. Protection*. [S.l.: s.n.], 2018. p. 1–7. Cited in page 50.
- HENSLER, T.; PRITCHARD, C.; FISCHER, N.; KASZTENNY, B. Testing superimposed-component and traveling-wave line protection. In: *proceedings of the 44th Annual Western Protective Relay Conference, Spokane, WA*. [S.l.: s.n.], 2017. Cited in page 24.
- HONORATO, T. R.; SERPA, V. R.; RIBEIRO, J. P. G.; CUSTÓDIO, E. A.; SILVA, K. M.; LOPES, F. V. On evaluating a time-domain distance element of a real relay for doublecircuit transmission line protection. In: *IET. 2020 15th Developments in Power System Protection*. [S.l.], 2020. Cited in page 11.
- HOROWITZ, S. H.; PHADKE, A. G. *Power system relaying*. [S.l.]: John Wiley & Sons, 2008. v. 22. Cited 2 times in pages 1 and 29.
- HU, Z.; LI, B.; ZHENG, Y.; WU, T.; HE, J.; YAO, B.; SHENG, Y.; DAI, W.; LI, X. Fast distance protection scheme for wind farm transmission lines considering r-l and bergeron models. *Journal of Modern Power Systems and Clean Energy*, v. 11, n. 3, p. 840–852, 2023. Cited 2 times in pages 37 and 38.
- HU, Z.; XU, Z.; FAN, J.; CHEN, M. Novel method of live line measuring the zero sequence parameters of transmission lines with mutual inductance. In: *2009 IEEE Power & Energy Society General Meeting*. [S.l.: s.n.], 2009. p. 1–4. Cited in page 7.
- IEEE. *EMTP Reference Models for Transmission Line Relay Testing*. 2004. Cited in page 47.
- IEEE. Ieee draft standard for common format for transient data exchange (comtrade) for power systems. *IEEE PC37.111/D4, January 2012 (IEC 60255-24 Ed.2)*, p. 1–72, 2012. Cited 2 times in pages 50 and 51.
- JONGEPIER, A.; SLUIS, L. Van der. Adaptive distance protection of a double-circuit line. *IEEE Transactions on power delivery*, IEEE, v. 9, n. 3, p. 1289–1297, 1994. Cited in page 11.
- KASZTENNY, B.; GUZMÁN, A.; FISCHER, N.; MYNAM, M. V.; TAYLOR, D. Practical setting considerations for protective relays that use incremental quantities and traveling waves. In: *43rd Annual Western Protective Relay Conference, Washington, USA*. [S.l.: s.n.], 2016. Cited in page 25.
- KASZTENNY, B.; VOLOH, I.; UDREN, E. A. Rebirth of the phase comparison line protection principle. In: *IEEE. 59th Annual Conference for Protective Relay Engineers, 2006*. [S.l.], 2006. p. 60–pp. Cited in page 35.
- LANZ, O.; HANGGLI, M.; BACCHINI, G.; ENGLER, F. Transient signals and their processing in an ultra high-speed directional relay for ehv/uhv transmission line protection. *IEEE Transactions on Power Apparatus and Systems*, IEEE, n. 6, p. 1463–1473, 1985. Cited 2 times in pages 35 and 38.
- LEUVEN, E. *Alternative Transients Program: Rule Book*. [S.l.]: EMTP Center, 1987. Cited 2 times in pages 48 and 49.
- LI, S.; CHEN, W.; YIN, X.; CHEN, D.; MALIK, O. P. Integrated transverse differential protection scheme for double-circuit lines on the same tower. *IEEE Transactions on Power Delivery*, IEEE, v. 33, n. 5, p. 2161–2169, 2017. Cited in page 14.

- LOPES, F. V.; FERNANDES, D.; NEVES, W. L. A. A traveling-wave detection method based on park's transformation for fault locators. *IEEE Transactions on Power Delivery*, v. 28, n. 3, p. 1626–1634, 2013. Cited in page 43.
- MCLAREN, P.; FERNANDO, I.; LIU, H.; DIRKS, E.; SWIFT, G.; STEELE, C. Enhanced double circuit line protection. *IEEE Transactions on Power Delivery*, v. 12, n. 3, p. 1100–1108, 1997. Cited in page 3.
- MOHANTY, R.; SAHU, N. K.; PRADHAN, A. K. Time-domain techniques for line protection using three-dimensional cartesian coordinates. *IEEE Transactions on Power Delivery*, v. 37, n. 5, p. 3740–3751, 2022. Cited 2 times in pages 37 and 38.
- MORAES, C. M. Masters Thesis, *Modal Parameters and Fault Transients in Double-Circuit Transmission Lines: On the Effects Of Conductor Transposition, Shield Wires, and Lossy Soil Modeling*. Brasília, DF: [s.n.], 2023. Cited 2 times in pages 48 and 49.
- NAIDU, O. D.; PRADHAN, A. K.; GEORGE, N. A hybrid time-domain protection scheme for series compensated transmission lines. *IEEE Transactions on Power Delivery*, v. 37, n. 3, p. 1823–1833, 2022. Cited 2 times in pages 37 and 38.
- NAMDARI, F.; SALEHI, M. High-speed protection scheme based on initial current traveling wave for transmission lines employing mathematical morphology. *IEEE Transactions on Power Delivery*, v. 32, n. 1, p. 246–253, 2017. Cited 2 times in pages 36 and 38.
- NEVES, E. T.; SILVA, K. M. Parametric sensitivity analysis of longitudinal and transverse differential protections applied to double circuit transmission lines. In: IEEE. *2018 Simpósio Brasileiro de Sistemas Elétricos (SBSE)*. [S.l.], 2018. p. 1–6. Cited 2 times in pages 33 and 38.
- OPERADOR NACIONAL DO SISTEMA. *Nota Técnica - 1a Revisão Quadrimestral das Projeções da demanda de energia elétrica: 2023 - 2027*. Rio de Janeiro, 2023. Available at <[https://www.ons.org.br/AcervoDigitalDocumentosEPublicacoes/NT\\_1RQ\\_2023\\_2027\\_Final.pdf](https://www.ons.org.br/AcervoDigitalDocumentosEPublicacoes/NT_1RQ_2023_2027_Final.pdf)>; Accessed in July 2023. Cited in page 1.
- PAITHANKAR, Y. G.; BHIDE, S. *Fundamentals of power system protection*. [S.l.]: PHI Learning Pvt. Ltd., 2011. Cited in page 60.
- PAJUELO, E.; RAMAKRISHNA, G.; SACHDEV, M. Phasor estimation technique to reduce the impact of coupling capacitor voltage transformer transients. *IET generation, transmission & distribution*, IET, v. 2, n. 4, p. 588–599, 2008. Cited in page 47.
- RIBEIRO, J. P. G. Masters Thesis, *Estudo e avaliação das funções de proteção de linhas de transmissão aplicadas no domínio do tempo disponíveis no relé SEL-T400L*. Brasília, DF: [s.n.], 2019. Cited in page 26.
- RIBEIRO, J. P. G.; LOPES, F. V.; JR, E. L. Influência da componente cc de decaimento exponencial sobre o desempenho de elementos direcionais aplicados no domínio do tempo. *Natal, Brasil: Simpósio Brasileiro de Sistemas Elétricos (VI SBSE)*, 2016. Cited in page 26.
- ROBERTS, J.; TZIOUVARAS, D.; BENMOUYAL, G.; ALTUVE, H. The effect of multiprinciple line protection on dependability and security. In: *54th Annual Conference for Protective Relay Engineers*. [S.l.: s.n.], 2001. p. 3–5. Cited 2 times in pages 3 and 12.



- SANAYE-PASAND, M.; JAFARIAN, P. Adaptive protection of parallel transmission lines using combined cross-differential and impedance-based techniques. *IEEE Transactions on Power Delivery*, v. 26, n. 3, p. 1829–1840, 2011. Cited 5 times in pages 1, 2, 8, 33, and 38.
- SANTOS, A. dos. Impact of double circuit lines operated in parallel on distance protection. IET, 2008. Cited 2 times in pages 2 and 8.
- SCHWEITZER, E. O.; KASZTENNY, B.; GUZMÁN, A.; SKENDZIC, V.; MYNAM, M. V. Speed of line protection-can we break free of phasor limitations? In: IEEE. *2015 68th Annual Conference for Protective Relay Engineers*. [S.l.], 2015. p. 448–461. Cited 10 times in pages 13, 23, 24, 25, 26, 27, 29, 30, 35, and 38.
- SCHWEITZER, E. O.; KASZTENNY, B.; MYNAM, M. V. Performance of time-domain line protection elements on real-world faults. In: IEEE. *2016 69th Annual Conference for Protective Relay Engineers (CPRE)*. [S.l.], 2016. p. 1–17. Cited 2 times in pages 36 and 39.
- SCHWEITZER ENGINEERING LABORATORIES. *Advanced Line Differential Protection, Automation, and Control System - Instruction Manual*. [S.l.], 2015. Cited 2 times in pages 2 and 44.
- SCHWEITZER ENGINEERING LABORATORIES. *Ultra-high-speed transmission line relay traveling-wave fault locator high-resolution event record - Instruction Manual*. [S.l.], 2019. Cited 6 times in pages 25, 26, 30, 35, 39, and 43.
- SERPA, V. R. Masters Thesis, *Avaliação das Proteções Diferencial Transversal e de Distância Aplicadas às Linhas de Transmissão de Circuito Duplo*. Brasília, DF: [s.n.], 2020. Cited 2 times in pages 15 and 39.
- SERPA, V. R.; HONORATO, T.; SILVA, K. M. Evaluation of cross-differential protection applied to double-circuit transmission lines under inter-circuit faults. In: IEEE. *2020 Simpósio Brasileiro de Sistemas Elétricos (SBSE)*. [S.l.], 2020. p. 1–6. Cited 2 times in pages 34 and 38.
- SERPA, V. R.; HONORATO, T. R.; SILVA, K. M.; NEVES, E. T. Avaliação experimental da função diferencial transversal aplicada na proteção de linhas de transmissão de circuito duplo. In: CIGRE. *XVIII Encontro Regional Ibero-Americano do Cigre (ERAC)*. [S.l.], 2019. p. 1–6. Cited 2 times in pages 34 and 38.
- SILVA, K. M. e. *Estimação de Fasores Baseada na Transformada Wavelet para Uso na Proteção de Distância de Linhas de Transmissão*. 203 f. Tese (Doutorado em Engenharia Elétrica) — Universidade de Campina Grande, Campina Grande, Paraíba, Brasil, abr. 2009. Cited in page 29.
- TANG, L.; DONG, X.; LUO, S.; SHI, S.; WANG, B. A new differential protection of transmission line based on equivalent travelling wave. *IEEE Transactions on Power Delivery*, v. 32, n. 3, p. 1359–1369, 2017. Cited 2 times in pages 36 and 38.
- TIFERES, R. R.; MANASSERO, G. Time-domain differential protection of transmission lines based on bayesian inference. *IEEE Transactions on Power Delivery*, v. 37, n. 3, p. 1569–1577, 2022. Cited 2 times in pages 37 and 38.
- TZIOUVARAS, D. A.; ALTUVE, H. J.; CALERO, F. Protecting mutually coupled transmission lines: Challenges and solutions. In: IEEE. *2014 67th Annual Conference for Protective Relay Engineers*. [S.l.], 2014. p. 30–49. Cited 4 times in pages 8, 9, 10, and 11.

- VITINS, M. A fundamental concept for high speed relaying. *IEEE Transactions on Power Apparatus and Systems*, PAS-100, n. 1, p. 163–173, 1981. Cited 2 times in pages 35 and 38.
- WANG, Q.; DONG, X.; BO, Z.; CAUNCE, B.; APOSTOLOV, A.; THOLOMIER, D. Cross differential protection of double lines based on supper-imposed current. In: *CIREN 2005 - 18th International Conference and Exhibition on Electricity Distribution*. [S.l.: s.n.], 2005. p. 1–4. Cited 3 times in pages 15, 32, and 38.
- WANG, Q. P.; DONG, X. Z.; BO, Z. Q.; CAUNCE, B. R. J.; APOSTOLOV, A. Application of percentage cross differential relay in ehv double lines. In: *2005 IEEE Russia Power Tech*. [S.l.: s.n.], 2005. p. 1–6. Cited 4 times in pages 12, 14, 31, and 38.
- WANG, Q. P.; DONG, X. Z.; BO, Z. Q.; CAUNCE, B. R. J.; THOLOMIER, D.; APOSTOLOV, A. Protection scheme of cross differential relay for double transmission lines. In: *IEEE Power Engineering Society General Meeting, 2005*. [S.l.: s.n.], 2005. p. 2697–2701 Vol. 3. Cited 6 times in pages 13, 14, 31, 38, 42, and 43.
- ZIEGLER, G. *Numerical distance protection: principles and applications*. [S.l.]: John Wiley & Sons, 2006. Cited 2 times in pages 2 and 28.
- ZIEGLER, G. *Numerical differential protection: principles and applications*. [S.l.]: John Wiley & Sons, 2012. Cited in page 1.